Master's thesis
Geography
Physical geography

METHANE FLUX CHANGES DURING IRRIGATION EXPERIMENT IN BOREAL UPLAND FOREST SOIL

Tiia Määttä

2020

Supervisors:
Associate professor Annalea Lohila (FMI)
Professor Miska Luoto

UNIVERSITY OF HELSINKI
FACULTY OF SCIENCE
DEPARTMENT OF GEOSCIENCES AND GEOGRAPHY
DIVISION OF GEOGRAPHY

PL 64 (Gustaf Hällströmin katu 2)
00014 Helsingin yliopisto

HELSINGIN YLIOPISTO
HELSINGFORS UNIVERSITET
UNIVERSITY OF HELSINKI

Tiedekunta/Osasto Fakultet/Sektion – Faculty Matemaattis-luonnontieteellinen tiedekunta	Laitos/Institution – Department Geotieteiden ja maantieteen laitos	
Tekijä/Författare – Author Tiia Määttä		
Työn nimi/Arbets titel – Title Metaanivuon muutokset kastelukokeen aikana boreaalisen lakimetsän maaperässä		
Oppiaine/Läroämne – Subject Luonnonmaantiede		
Työn laji/Arbetets art – Level Pro gradu	Aika/Datum – Month and year Toukokuu 2020	Sivumäärä/Sidoantal – Number of pages 81+17

Tiivistelmä/Referat – Abstract

Metaani (CH_4) on kasvihuonekaasu, jolla on merkittävä vaikutus globaaliin ilmastoon. Maaperässä sitä muodostuu hapettomissa ja kuluu hapellisissa oloissa mikrobitoiminnan tuloksena. Yhdessä erilaisten metaanin kulkeutumismuotojen kanssa metaanin tuotanto ja kulutus määräävät suoraan maaperän metaanivuota. Boreaalisten lakimetsien katsotaan yleisesti toimivan metaaninieluina korkean metaanin kulutuksen vuoksi. Joissakin tutkimuksissa on kuitenkin havaittu boreaalisen lakimetsän maaperän muuttuvan metaanin lähteeksi pitkäkestoisen ja runsaan sadannan jälkeen. Tämän tutkimuksen tavoitteena oli tarkastella maaperän kosteuden vaikutuksia metaanivuohon manipulatiivisesti kasvatetun sadannan seurauksena pohjoisboreaalisen lakimetsän maaperässä, ja sitä kuinka orgaanisen karikkeen lisäys sekä sen ja juurten eristys ja maaperän lämpötilan kasvu vaikuttavat vuon ajallisiin muutoksiin.

Tutkimus toteutettiin Kenttärovan metsässä Kittilässä, Suomessa kesällä 2018. Kokeessa käytettiin osaruutuasetelmaa, jossa maaperän kosteus oli pääruutumuuttuja ja maaperän lämmitys (T), orgaanisen karikkeen lisäys (A) sekä orgaanisen karikkeen ja juurten eristys (E) osaruutumuuttujia. Asetelmassa oli kaksi pääruutua: kastelu (I) ja kontrolli (C), joiden sisällä osaruutumuuttujat toistettiin kolme kertaa. Maaperän kosteuden vaikutuksen analysoimiseksi T, A ja E-käsittelyiden lisäksi kokeessa oli mukana osaruutumuuttuja, jossa ei ollut osaruututason käsittelyä (O) ja jolla oli neljä toistoa pääruutujen sisällä. Metaanivuo mitattiin vähintään kerran viikossa kammiomenetelmällä. Lisäksi maaperän kosteutta ja lämpötilaa mitattiin jatkuvatoimisesti. Käsittelyiden vaikutuksia analysoitiin sekä autoregressiivisillä että autoregressiivisillä heterogeenisillä kaksisuuntaisilla varianssianalyyseillä, TukeyHSD-menetelmällä, korrelaatioanalyyseillä ja yleistetyillä lineaarisilla malleilla.

Maaperä ei muuttunut metaanin lähteeksi mutta tulokset osoittivat merkitseviä eroja kastelun ja kontrollin välillä, mikä viittasi maaperän kosteuden voimakkaaseen metaaninielua pienentävään vaikutukseen kaikilla käsittelytasoilla. Kaikilla käsittelyryhmillä oli pienimmät nielut elokuussa mahdollisesti korkean maaperän kosteuden vuoksi. IA-ryhmä tuotti pienimmät nielut luultavasti kaasudiffuusion vähenemisen ansiosta. IE-ryhmän nielut kasvoivat kasvavan maaperän kosteuden myötä mutta E-käsittelyt tuottivat yleisesti ristiriitaisia ja epävarmoja tuloksia, ja syyt nielujen muutosten takana jäivät selvittämättömiksi. T-käsittelyllä ei ollut merkitseviä vaikutuksia nieluihin luultavasti lämpötilamanipulaation epäonnistumisen vuoksi, minkä takia maaperän kosteuden ja lämpötilan yhteisvaikutuksia ei voitu tutkia luotettavasti. Tulosten perusteella nielujen muutokset ovat todennäköisesti olleet riippuvaisempia metaanin kulutuksesta kuin tuotannosta. Lisää tutkimusta tarvitaan erityisesti karikkeen lisäyksen, maaperän kosteuden ja lämpötilan kasvun yhteisvaikutuksesta metaanivuohon ajallisia koetoistoja hyödyntäen.

Avainsanat – Nyckelord – Keywords
metsän metaanin tuotanto – metanogeneesi – metanotrofia – maaperän kosteus – osaruutukoe – monimuuttujakoe

Säilytyspaikka – Förvaringställe – Where to be deposited
E-thesis

Muita tietoja – Övriga uppgifter – Additional information

HELSINGIN YLIOPISTO
HELSINGFORS UNIVERSITET
UNIVERSITY OF HELSINKI

Tiedekunta/Osasto Fakultet/Sektion – Faculty	Laitos/Institution – Department	
Faculty of Science	Department of Geosciences and Geography	
Tekijä/Författare – Author Tiia Määttä		
Työn nimi/Arbets titel – Title Methane flux changes during irrigation experiment in boreal upland forest soil		
Oppiaine/Läroämne – Subject Physical geography		
Työn laji/Arbetets art – Level	Aika/Datum – Month and year	Sivumäärä/Sidoantal – Number of pages
Master's thesis	May 2020	81+17

Tiivistelmä/Referat – Abstract

Methane (CH_4) is a greenhouse gas with a great impact on global climate. In the soil, it is produced in anoxic and consumed in oxic conditions by microbes. Together with different methane transport mechanisms, methane production and consumption directly regulate the resulting soil methane flux. Boreal upland forests are generally considered to act as methane sinks due to high methane consumption. However, some studies have shown a boreal upland forest soil turning from a methane sink to a source after long-term abundant precipitation. This study aimed to examine the effects of soil moisture on CH_4 flux from simulated increase in rainfall in a northern boreal upland forest soil, and how simultaneous soil temperature increase, organic litter addition and organic litter and root exclusion affect the temporal changes in flux.

The study was conducted in Kenttärova forest in Kittilä, Finland in summer 2018. Split-plot design was used in the experiment with soil moisture being the main treatment variable and soil warming (T), organic litter addition (A) and organic litter and root exclusion (E) subtreatment variables. The design included two main plots: irrigation (I) and control (C), within which each subtreatment was replicated three times. In addition to the T, A and E manipulations, plots without additional manipulations (O) were included for the assessment of the effect of only soil moisture increase, and were replicated four times within both main plots. Methane flux was measured at least once a week using chamber method. Soil moisture and temperature were also continuously measured. The treatment effects were analysed using both autoregressive heterogeneous and autoregressive two-way analyses of variance, TukeyHSD method, variable correlations and Generalized Linear Models.

The soil did not turn into a methane source but the results showed significant differences between the irrigation and control site, indicating a strong decreasing effect of soil moisture on soil CH_4 sink in all treatment levels. All treatments had lowest uptake rates in August, possibly as a result from highest soil moisture levels. IA treatment was the most effective in producing low uptake rates possibly due to the reduction in gas diffusion. E treatments had contrasting results, IE showing increases in uptake rate by increases in soil moisture but the causes remained unsolved and the results were highly uncertain. T treatment had no effect on uptake likely due to a failure to create soil temperature differences and thus the interactions were not reliably analysed. The results suggest that the changes may have been more related to changes in methane consumption than production. Further research is needed especially for examining the combined effect of litter addition, soil moisture and soil temperature increase on methane flux with multiple temporal replications of the experiment.

Avainsanat – Nyckelord – Keywords
forest methane production – methanogenesis – methanotrophy – soil moisture – split-plot – multifactorial experiment

Säilytyspaikka – Förvaringställe – Where to be deposited
E-thesis

Muita tietoja – Övriga uppgifter – Additional information

Table of Contents

1 Introduction

Methane (CH_4) is an organic greenhouse gas that has a significant impact on the global climate. Due to its ability to absorb infrared radiation into the vibrations of its molecular carbon-hydrogen bonds, methane effectively traps heat energy within the atmosphere, increasing the global temperatures (Whalen 2005; Dlugokencky et al. 2011; Chai et al. 2016). Due to an increase in the emissions from anthropogenic sources, atmospheric methane concentrations have been notably increasing since the pre-industrial times (Wuebbles and Hayhoe 2002; Kirschke et al. 2013). In the soil, methane is primarily formed in biological anaerobic decomposition processes (Le Mer and Roger 2001; Wuebbles and Hayhoe 2002). Whether a soil is a source or a sink of methane depends on the ratio between methane production and consumption and its transport, all of which are further influenced by a large network of various intertwined abiotic and biotic variables. The variables contributing to the year-to-year fluctuations in global and regional CH_4 emissions are still largely unknown and contain significant uncertainties, and are thus essential for understanding the changing dynamics in the current and future CH_4 budgets (Bousquet et al. 2006; Fischer et al. 2008; Dlugokencky et al. 2011; Kirschke et al. 2013; Crill and Thornton 2017).

The boreal zone in the northern hemisphere continuously shows large methane emissions while counterbalanced by relatively low rates of consumption. Due to the abundance of anoxic wetlands in the region, the emissions are estimated to lie between 25 and 100 Tg yr^{-1} which together with subarctic tundra environments account for circa 3–10% of the global CH_4 emissions (Olefeldt et al. 2013). Boreal upland forests are generally considered methane sinks as a result of strongly oxic soils with high methane consumption rates carried out by certain methane oxidising bacteria (Yavitt et al. 1990; Whalen et al. 1991; Yavitt et al. 1995; Gulledge and Schimel 2000; Megonigal and Guenther 2008). Despite the abundance of oxygen in the soil, there are some indications of smaller-scale methane-producing areas, such as wet depressions, occurring in the boreal upland forest areas (Megonigal and Guenther 2008; Christiansen et al. 2012; Lohila et al. 2016). In addition, some studies have found that even larger areas of upland forest soils may become methane sources of varying significance due to a so-far unknown network of processes after long periods of heavy precipitation (Savage et al. 1997; Lohila et al. 2016). As a large portion of the boreal zone is occupied by upland forests, a more careful investigation of the complex dynamics behind the sink-source transitions of the forests is required particularly in the context of climate warming which is estimated to change global and regional precipitation and temperature patterns (e.g. Beier et al. 2012; Lehtonen et al. 2014; Lohila et al. 2016).

Experimental studies on soil methane fluxes are relatively few and most of them have been single-factor designs. Thus, the focus of the research has been mostly fixed on finding causal relationships between individual environmental variables, such as soil temperature and atmospheric CO_2 concentration, and soil methane flux emphasising soil oxidation rates

instead of assessing the complex interactions between those variables and methane production and consumption (Rustad and Fernandez 1998; Blankinship et al. 2010). It has especially been highlighted by multiple studies that there is a need for more multifactorial experiments studying the interactions between soil temperature, moisture and substrate availability that may strongly contribute in the spatiotemporal distribution of methane sinks and sources in situ, particularly with respect to the current and future climate warming (Rustad and Fernandez 1998; Blankinship et al. 2010; Wu et al. 2011; Beier et al. 2012). Boreal forests in particular have not yet been adequately examined as sources or sinks of CH_4 via soil temperature and moisture manipulations and even the few studies focusing on boreal forests assessed soil CO_2 fluxes (Billings et al. 2000; Niinistö et al. 2004; Allison and Treseder 2008; Wu et al. 2011). It has also been recommended that more focus is put into experiments that manipulate precipitation either by drying or wetting and establishing those experiments more in forest ecosystems which are relatively underrepresented (Wu et al. 2011).

In this study, the effect of increased rainfall via changes in soil moisture on CH_4 flux is assessed with an irrigation experiment during the growing period in a boreal upland forest in Kenttärova in northern Finland. Kenttärova was chosen as the study site due to significant soil CH_4 emissions that were detected there after long period of abundant precipitation in 2011 by Lohila et al. (2016). Additional variables considered in the research are soil temperature and organic litter accumulation and roots of the vegetation as they are found to affect the methane production and consumption processes in the soil. The study is based on the following research questions:

1. Does a period of high irrigation and increase in soil moisture turn an upland mineral soil from a CH_4 sink into a CH_4 source?

2. Do soil warming and organic litter and root manipulations change the soil CH_4 flux during a period of high irrigation?

The consistently high precipitation rate, as manipulated with irrigation, and the subsequent increase in soil moisture was expected to turn the forest soil from a CH_4 sink into a CH_4 source in late summer or early autumn, approximately around August when the growing period was ending. The increase in soil moisture in the experimental site was expected to lead to the partial or full saturation of the soil pores in the whole soil profile or its parts, resulting in fully or partially anoxic conditions and, eventually, higher methane production and a switch to a methane source. Similar response to heightened precipitation in a natural environment has recently been observed for example by Lohila et al. (2016) in the same catchment area as that of the study site.

Manipulating soil temperature increase, and the amount of soil organic litter, was expected to affect the timing of the switch between a sink and a source. Increases in the soil temperature were expected to enhance the rate of methane production especially when combined with

higher soil moisture in the experimental site because the warming increases microbial activity and decomposition rates (Christensen et al. 1995; Wu et al. 2011). Organic litter and root removal, on the other hand, would likely decrease the methane production rate due to lower organic substrate availability for methanogenic microbes (e.g. Schlesinger and Bernhardt 2013; Serrano-Silva et al. 2014), but also possibly methane consumption by simultaneously decreasing the amount of produced methane within the soil layers, as suggested by Yavitt et al. (1990) and Kähkönen et al. (2002). Similarly, organic litter additions were likely to enhance the methane producing processes (e.g. Brumme and Borken 1999; Xu et al. 2013; Serrano-Silva et al. 2014).

The experiment was made in collaboration with the Finnish Meteorological Institute, Natural Resources Institute of Finland and University of Helsinki as a part of UPFORMET (Role of upland forest soils in regional methane balance: from catchment to global scales) project.

2 Theoretical background

2.1 Methane

Methane is an organic gas that consists of one carbon and four hydrogen atoms that are combined together by carbon-hydrogen bonding. The vibration of the carbon-hydrogen bonds absorbs long-wave infrared radiation coming from the Earth's surface which prevents the radiation from proceeding further to space and increases the temperatures of the Earth's surface (Chai et al. 2016). Thus, methane is considered a strong greenhouse gas significantly contributing to the global direct radiative forcing which marks the difference between incoming radiation absorbed by the Earth's surface and outgoing radiation from the Earth's surface (Dlugokencky et al. 2011; Chai et al. 2016). Methane is also the most common organic trace gas in the global atmosphere (Wuebbles and Hayhoe 2002; Keppler et al. 2006).

The Global Warming Potential (GWP) of methane varies according to the temporal scale used due to the relatively rapid degradation of the methane molecule into carbon dioxide (CO_2) and water (H_2O) in the atmosphere. GWP refers to the effectiveness of a greenhouse gas to absorb heat energy in a certain time scale in relation to CO_2 (Chai et al. 2016). In the atmosphere with an abundance of nitrogen oxides (NO_x), CH_4 reacts with two hydroxyl radicals (OH) in photochemical reactions which results in CO_2, formaldehyde (CH_2O), carbon monoxide (CO) and ozone (O_3) and, in a longer time scale, decrease in available OH radicals and following increase in CH_4 in the atmosphere (Wuebbles and Hayhoe 2002; Conrad 2009; Dlugokencky et al. 2011; Chai et al. 2016). The reactions between atmospheric methane and OH radicals creates the largest consumption of methane in the global methane budget by over 80% of the whole consumption but it is still associated with an uncertainty varying

between 10 and 20% (Conrad 2009). The lifespan of a methane molecule in the atmosphere is shorter than that of CO_2: in general, the time for atmospheric molecular degradation is considered to be 8–9 years or between 12 and 14.4 years in perturbation calculations, depending on the model used in the different studies (Dlugokencky et al. 2011; Chai et al. 2016). As a molecule, however, methane is often considered a 3-22 times stronger greenhouse gas than CO_2 especially due to the absorption of infrared radiation (Megonigal and Guenther 2008).

2.1.1 Methane production and consumption

Methane formation can occur biogenically in microbial processes, thermogenically in long-term geological processes and pyrogenically in incomplete combustion reactions in wildfires and burning of anthropogenic biofuels and fossil fuels (Neef et al. 2010; Kirschke et al. 2013; Chai et al. 2016). Biogenic sources generally include wetlands, termites, oceans and ruminant animals, each one's emissions varying both temporally and spatially (Dlugokencky et al. 2011). The biological formation of methane occurs in methanogenesis which is carried out by anaerobic microbes called methanogens. The diverse group of single-celled methanogens belongs in the *Archaea* taxon and includes genera such as *Methanosarcina* and *Methanosaeta*, both of which decompose carbon compounds strictly in anoxic conditions but differ in their specialisation on specific substrates used in their metabolism (Megonigal et al. 2003; Chai et al. 2016). The mineralization of large carbon compounds as a whole is divided into multiple steps carried out by a variety of different anaerobic microbes due to their highly specialised substrate requirements. Methanogenesis itself is the final step of anaerobic decomposition of organic matter (Garcia et al. 2000). This dependence on other anaerobic organisms in metabolism forms a mutualistic ecological relationship called syntrophy between the different species which is common for all anaerobic organisms. Due to the multistep organization of the mineralization, the microbes are able to conserve more energy for their metabolism (Garcia et al. 2000; Megonigal et al. 2003).

Prior to the biological processes of methanogenesis, the complex carbon compounds are converted to more simplified forms in steps by a number of various microorganisms. First, the compounds are hydrolysed from carbohydrates, proteins and lipids to sugars, peptides, amino acids and fatty acids by specified species ranging from strictly anaerobic to aerobic microbes, after which the resulting products go through either facultatively or strictly anaerobic acidogenesis or acetogenesis, both of which are forms of fermentation. In the acidogenic fermentation processes the compounds are converted to volatile fatty acids, alcohols, ammonia (NH_3), CO_2 and H_2 while acetogenesis results in acetate (Le Mer and Roger 2001; Megonigal et al. 2003; Chai et al. 2016). Using the products of the fermentation processes, methanogens subsequently start the final methanogenic reduction reactions which produce methane as a waste product (Chai et al. 2016). The reduction can occur in three different

ways: methanogens either directly reduce CO_2 and H_2 to CH_4 and water in a chemical reduction process called hydrogenotrophic methanogenesis, demethylate the methyl groups from acidogenesis producing CH_4 and water in methylotrophic methanogenesis or further convert the acetate products to CO_2 and CH_4 in degradative acetogenetic pathways in acetotrophic methanogenesis (Megonigal et al. 2003; Chai et al. 2016). Due to the higher energy gain from directly reducing CO_2 and H_2 to CH_4 and water, hydrogenotrophic methanogenesis is more common among methanogens than methylotrophic and acetotrophic methanogenesis that produce less energy. As a consequence, natural selection in the evolution of methanogens has led to higher numbers of hydrogenotrophic methanogens (Garcia et al. 2000; Megonigal et al. 2003). The ratio between the three different pathways differs spatially and temporally depending on the underlying environmental factors (Megonigal et al. 2003).

The counter effect of methanogenesis is methanotrophy which occurs in oxic conditions with adequate supplies of oxygen. The consumption of methane is carried out by specialised aerobic bacteria that oxidise methane either through high or low affinity oxidation. High affinity oxidation occurs in environments where the concentration of CH_4 is close to the corresponding atmospheric value (less than 12 ppm) due to the high mixing ratio of CH_4 whereas low affinity oxidation takes place at over 40 ppm concentrations resulting from low CH_4 mixing ratio (Bender and Conrad 1992; Le Mer and Roger 2001). The bacteria that account for low affinity oxidation of CH_4 in their metabolism are called methanotrophs and consist of various genera such as *Methylomonas*, *Methylocystis* and *Methylosinus* that belong in the physiological group of methylotrophic bacteria (Hanson and Hanson 1996; Le Mer and Roger 2001; Megonigal and Guenther 2008; Jones et al. 2010). The high affinity bacteria, on the other hand, are mostly unknown but still often considered as part of the group of methanotrophs (Bender and Conrad 1992). Since the concentration of methane in the atmosphere is lower than in the soil in general, high affinity methanotrophs with their powerful enzymes are required for the oxidation of atmospheric methane (Conrad 2009). Methanotrophy as a process includes multiple steps in which oxygen is reduced, water and methanol (CH_3OH) are formed, followed by oxidation sequences of methanol, formaldehyde (CH_2O) and formate (HCO_2^-), ultimately resulting in CO_2 and water (Hanson and Hanson 1996; Megonigal et al. 2003). In contrast to methanogens, methanotrophs use methane as their sole carbon and energy source (Hanson and Hanson 1996; Le Mer and Roger 2001; Megonigal et al. 2003).

Environmental factors controlling both methanogenesis and methanotrophy in the process-level include oxygen concentration and reduction-oxidation potential (redox potential, E_h), pH, temperature, salinity, organic substrates used in microbial metabolism and nutrient availability (Megonigal et al. 2003; Olefeldt et al. 2013; Chai et al. 2016, figure 2). Since oxygen is directly toxic for most methanogens, increases in oxygen concentrations may effectively inhibit methanogenesis (Megonigal et al. 2003; Megonigal and Guenther 2008; Chai et al.

2016). In addition, since methanogens are not able to consume acetate and H_2 as effectively as many other reducing microorganisms, the competitors often decrease the methanogenic activity by reducing nitrogen (N), iron (Fe) and sulfate (SO_4^{2-}) while simultaneously oxidising acetate and H_2. Therefore, the presence of oxygen may indirectly also lead to higher rate of oxidation of nitrogen, iron and sulfur (S) which increases the support for the competing microorganisms and further decreases methanogenic activity (Megonigal and Guenther 2008). Furthermore, oxygen depletion leads to reducing conditions where a sequence of reduction reactions of certain chemical compounds occur which gradually lowers the reduction-oxidation potential and increases the pH in a soil environment (McBride 1994; Schlesinger and Bernhardt 2013). The redox potential itself measures the intensity of the redox reactions in the soil solution (McBride 1994). The E_h required for methanogenesis is less than -200 mV which marks extreme reducing conditions in the soil (McBride 1994; Le Mer and Roger 2001). In contrast, since methanotrophs are aerobic bacteria, methanotrophy is effectively inhibited by oxygen depletion and vice versa. Most of the variations in the efficiency of methanotrophic activity in an oxic environment are caused by competition between other heterotrophic bacteria that use oxygen in their respiration (Megonigal et al. 2003).

Methanogenesis is affected by changes in pH directly due to methanogens' limited ability to adapt to pH values outside the optimum range. The optimum pH conditions of the environment for methanogens is considered to be around 6–8, but some methanogens are found to survive in pH conditions as low as 5.6. So far, however, there are no studies proposing any methanogens growing and producing methane under pH 4.7 (Garcia et al. 2000; Le Mer and Roger 2001). In contrast, pH and its changes do not have a significant effect on methanotrophic activity as long as the values do not decrease under pH 5 which is the minimum value for the growth of methanotrophs (Hanson and Hanson 1996; Megonigal et al. 2003). In addition, micronutrients, such as nickel (Ni), cobalt (Co), iron and sodium (Na), are required for methanogenesis so decreases or increases in their availability affect methane production significantly. Depending on the microbial environment, especially nickel that catalyses the methanogenic reduction reactions and iron are found to stimulate methanogenesis (Garcia et al. 2000; Megonigal et al. 2003). Nitrogen is the most important nutrient regulating methanotrophy because it acts as an inhibitor in enzymatic reactions in methanotrophic metabolism and, thus, prevents the consumption of methane. Some nitrogen compounds, such as ammonia (NH_3) and nitrite (NO_2^-) are toxic for methanotrophs, the presence of which decreases the efficiency of methanotrophy (Hanson and Hanson 1996; Megonigal et al. 2003). The influence of nitrogen toxicity and inhibition is often minor in anoxic environments in practice, however, due to the lower oxygen concentration and nitrification efficiency (Megonigal et al. 2003).

Methanogenic activity is prevalent within a relatively large temperature range from 4 to 110°C (Garcia et al. 2000). However, the optimal temperatures for most methanogens are

30–40°C (Le Mer and Roger 2001). Temperature influences both the methanogens and other syntrophic microbes contributing in the methanogenic processes by decreasing their activity (Le Mer and Roger 2001). The temperature sensitivity of methanogenesis is generally higher than other biological processes in terms of the rate in which its activity increases with a 10°C increase (Q_{10}) in temperature. For example, generally biological processes may double in a 10°C increase (Q_{10}=2) but methane production has been found to reach Q_{10} values of 4.1 in incubation experiments (Le Mer and Roger 2001; Megonigal et al. 2003). Methanotrophic oxidation, on the other hand, is not affected as significantly by temperature changes. For example, the Q_{10} values often reach only 1.9 for the methanotrophic activity in wetland environments and approximately Q_{10} value of 2 in general, showing a significant difference to the methanogenic counterpart (Le Mer and Roger 2001; Megonigal et al. 2003; Smith et al. 2003). The microbial growth of most methanotrophs is maintained under 50°C while the optimal temperature for methanotrophy seems to be around 25°C, depending on the species and their ability to adapt to lower temperatures (Hanson and Hanson 1996).

Organic substrates used in the metabolism of methanogens include a variety of carbon compounds, the molecular structure and composition of which are a major control of those processes. In methanogenesis, carbon compounds can act as sources of electrons or their acceptors in the redox reactions or, alternatively, they can be converted to inorganic compounds that are toxic to methanogens by non-methanogenic decomposition or support the competing microorganisms with electron acceptors not used by methanogens, both of which decrease the rate of methanogenesis (Megonigal et al. 2003). The chemical structure of the organic carbon compounds influences especially the fermentation processes of methanogenesis and notably dissolved labile carbon has been found to stimulate the methanogenic processes (Megonigal et al. 2003). Since methanotrophs use only CH_4 as a substrate for metabolism and its concentration affects methanotrophic efficiency, carbon in soil organic matter is not a primary environmental variable in methanotrophy (e.g. Hanson and Hanson 1996; Gulledge et al. 1998; Le Mer and Roger 2001; Megonigal et al. 2003).

Salinity is also an important factor controlling methanogenesis and its tolerance among methanogens vary largely according to their osmotic adaptability (Garcia et al. 2000). In general, however, it has been suggested that higher amounts of sodium chloride (NaCl) in the microbial environment decrease methanogenic activity and growth of methanogens (van den Gon and Neue 1995). For methanotrophic bacteria the amount of salt in the microbial environment to inhibit methane oxidation is approximately 40 mM and some studies suggest that methanotrophy is more influenced by variations in salinity in relation to methanogenesis (Le Mer and Roger 2001; Megonigal et al. 2003).

2.1.2 Sinks and sources in the soil

The quantity, spatial distribution and temporal variation of methane emissions from the soil in larger scale depend on the ratio between methanogenesis and methanotrophy which occur simultaneously in soils, and methane transport from the soil into the atmosphere (e.g. Whalen 2005; Lai 2009). Methane emissions and uptake are often measured as vertical fluxes which calculate the amount of emitted methane per unit area per unit time, often expressed as $\mu g\ m^{-2}h^{-1}$ or $mg\ m^{-2}d^{-1}$ in chamber measurements (e.g. Pihlatie et al. 2008, 2013; Lohila et al. 2016; Korkiakoski et al. 2017). A flux is an average of flux density over a specific area, while flux density marks the amount of mass, energy or momentum that passes a plane of unit area per unit time (Vesala et al. 2008). In this study, when methane flux of the studied area is positive, the soil is considered to produce more methane and result in a methane source whereas negative flux values indicate higher consumption rate of methane and thus a methane sink. The relation between sinks and sources determine the amount of methane in the atmosphere in different spatial and temporal scales (e.g. Bousquet et al. 2006; Conrad 2009). In this study, methane sink and uptake rates are used to refer to the rates of methane uptake and source rates to the emission of the soil for the clarity of the direction of the flux in question. The temporal variation in the sink-source dynamics of methane is often studied by interannual, seasonal and daily variations. For example, wetlands show the highest variation in methane fluxes interannually when compared to other methane-producing processes including anthropogenic sources (Kirschke et al. 2013).

Methane transport in and between soil and the atmosphere is carried out through molecular gas diffusion, ebullition and transpirational pathways of plants (Lai 2009; Xu et al. 2016, figure 1). In the soil, methane diffuses passively from high CH_4 concentrations to lower within soil pores that are either completely or partly saturated with water, ultimately reaching the atmosphere which has a lower CH_4 concentration in relation to the soil pores. Ebullition takes place in aquatic soils where CH_4 proceeds in bubbles without oxidising as a result from the partial pressure of CH_4 in the production site reaching a certain threshold and the site being saturated with CH_4 (Lai 2009; Xu et al. 2016). Methane emissions by ebullition are often large due to the rapid formation of the gas in supersaturated conditions (Megonigal et al. 2003; Lai 2009; Xu et al. 2016). In addition, some plants are able to transfer CH_4 from the anoxic layers of the soil into the atmosphere in molecular diffusion or bulk flow through aerenchyma (Bartlett and Harriss 1993; Megonigal et al. 2003; Lai 2009). Aerenchyma is a transpirational pathway within a plant's structure which carries oxygen from the leaves into different parts of the plant, including roots that are often located in the anoxic soil layers (Ström et al. 2005; Moor et al. 2017). Methane-carrying aerenchymal species can mostly be found in the family *Cyperaceae* which mostly consists of wetland sedges (Ström et al. 2005). Aerenchymal transport of methane is very efficient and accounts for most of the positive methane fluxes in aquatic soils, such as rice paddies and wetlands (e.g. Le Mer and Roger

2001; Whalen 2005; Serrano-Silva et al. 2014).

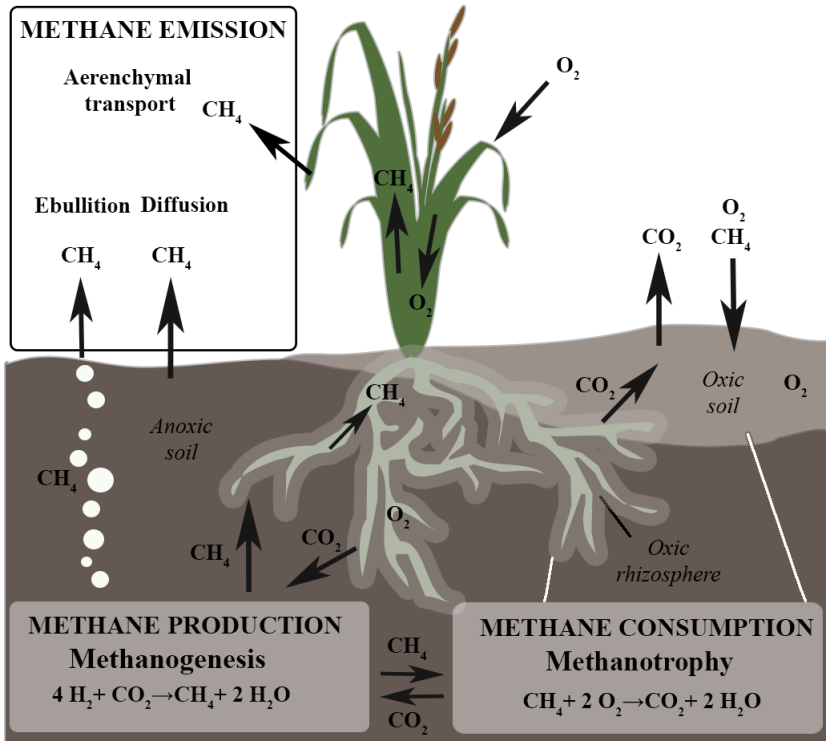

Figure 1: The three main processes affecting methane emissions in an example wetland soil with both anoxic and oxic soil layers. Methanogenesis occurs primarily in the anoxic soil layers with a limited amount of oxygen (O_2) and reduced conditions and is carried out by methanogenic archaea. The chemical formula represents hydrogenotrophic methanogenesis. Methanotrophy is mostly located in the oxic layers and rhizosphere with adequate amount of oxygen for the oxidation processes by methanotrophic bacteria. Methane transport occurs via diffusion, ebullition and transpiration pathways of aerenchymal vegetation. Both methane production and consumption occur simultaneously in soils and, together with methane transport processes, strongly affect the resulting soil methane emissions. The figure includes only processes relevant to methanotrophic and methanogenic activities and thus does not include all possible processes in carbon cycle occurring in wetlands. The figure was made following Le Mer and Roger (2001), Jones et al. (2010), and Schlesinger and Bernhardt (2013).

In the soil, the spatiotemporal variation of the ratio between methane production and consumption and its transport depend on a network of a number of biological and physical variables affecting those processes (figure 2). Many of the factors are those that directly affect methanogenesis and methanotrophy, such as soil temperature, CH_4 concentration and carbon substrate availability. Soil moisture is one of the most important factors governing the emissions in the soil scale. According to multiple studies by e.g. Arnold et al. (2005), Whalen (2005), Ström and Christensen (2007), Lai (2009), and von Fischer et al. (2010), water table level is a major factor influencing soil moisture and methane flux in the soils. Higher water table level leads to larger anoxic and narrower oxic layers in the soil causing higher methane production and lower methane consumption. Methanotrophic activity maintains its efficiency up to the point where soil moisture reaches the field capacity, after which oxygen depletion inhibits methane oxidation more effectively (Le Mer and Roger 2001). However, variations in the water table depth may cause significant lagging fluctuations in

the methane flux in temporal scale (Kettunen et al. 1996). Despite the anoxic conditions, a soil with high moisture content can hold a high potential for methanotrophic activity due to the ability of methanotrophs to stay viable in anoxic conditions especially with low carbon availability (Le Mer et al. 1996; Le Mer and Roger 2001; Megonigal et al. 2003). Similarly, it has been suggested that methanogens are able to remain in the soil in oxic conditions when located within the anoxic centres of soil aggregates, increasing the potential of the soil to start producing methane in higher soil moisture (Megonigal and Guenther 2008). Soil temperature does not have a direct impact on methane transport except in wetlands where higher temperatures increase methane source rate by increasing ebullition and amount of methane bubbles (Lai 2009).

Vegetation composition affects both methane production and consumption and its transport. Vegetation composition in part affects soil organic matter quality and methane flux by producing species-specific carbon compounds that ultimately end up in the soil carbon pool via plant decay or plant roots as root exudates. Ultimately, methanogens obtain the carbon substrates from the soil solution or plant hair roots which enhances their methanogenic metabolism (Ström et al. 2005). In addition, especially deep-rooted vegetation consisting of aerenchymal species enables the produced methane to pass through the oxic zones within the soil and, consequently, enhances methane transport and methane emissions (Whalen 2005; Ström and Christensen 2007; Lai 2009). For example, Ström and Christensen (2007) found that a dominance of *Carex* species in soils ranging from dry to wet led to a significant increase in methane source rate. However, vegetation can also cause a counteracting phenomenon where the oxygen obtained from the atmosphere is transported to the rhizosphere and subsequently methanotrophs are able to oxidise methane before it reaches the aerenchyma or atmosphere by diffusion, preventing methane transport and decreasing methane source rate (Megonigal et al. 2003; Ström et al. 2005, figure 1). In addition, some tree species alter the soil moisture content by taking up water in their transpiration and, as a consequence, indirectly influence methane production and consumption by creating variations in the oxygen concentrations (Megonigal and Guenther 2008).

Another factor influencing soil methane flux is soil texture. Soil texture is the distribution of different particle sizes within a soil which directly affects the aeration of the soil (e.g. Boeckx et al. 1997; Smith et al. 2003; Simojoki et al. 2008a). Coarse-textured sandy soils have been found to have higher methane oxidation rates than fine-textured clayey soils which results from the larger soil pore spaces that allow a more efficient oxygen and methane diffusion for the sandy soils (Boeckx et al. 1997; Regina et al. 2007). However, it has been proposed that the type of the clay mineral may affect methane fluxes due to the fact that some clays store organic matter in their crystal structures, preventing it being used in the methanogenic mineralization (Le Mer and Roger 2001). In addition, clayey soil and its small pore spaces may trap some of the methane bubbles formed in ebullition which further decreases soil

methane source rate (Le Mer and Roger 2001). Since negatively charged clay particles can form complex aggregates with organic matter and silt, their anoxic centres are favourable habitats for methanogens. Therefore, the finer-textured the soil is, the more there may be anoxic sites for methanogens and the higher the potential for methane emission (Wagner et al. 1999). The bulk density, which means the mass of a unit volume of dry soil, or in other words the degree of compaction of the soil, directly controls the diffusion of gases within the soil. Thus, high bulk densities may lead to higher CH_4 uptake rates by decreasing the diffusion of CH_4 (Ball et al. 1997; Serrano-Silva et al. 2014).

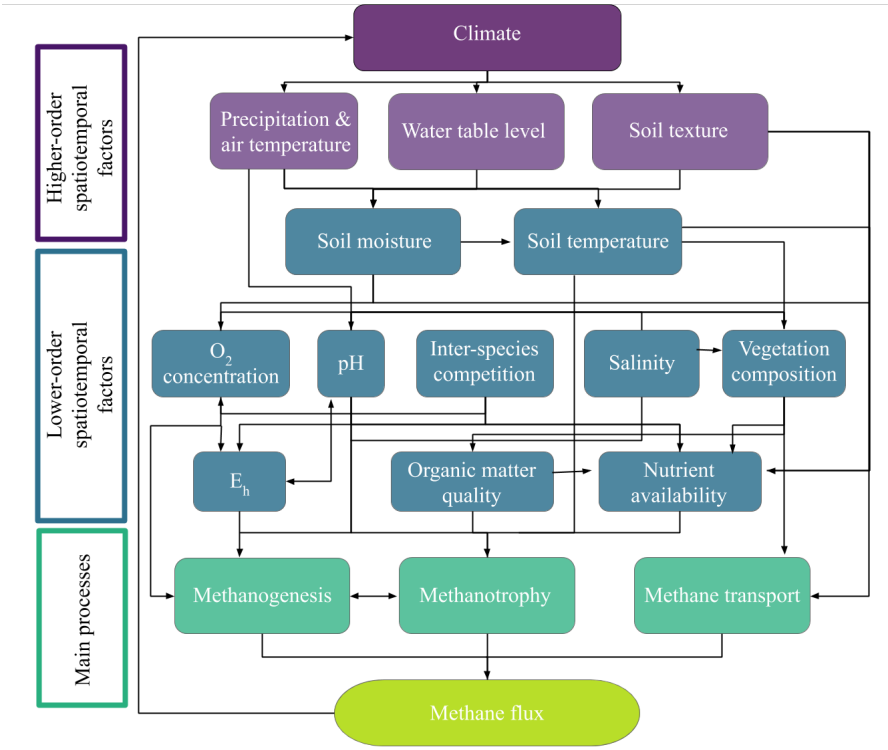

Figure 2: A conceptual model of the various factors influencing methane production, consumption and transport and ultimately soil methane flux. Higher-order spatiotemporal factors influence the network in larger spatial scale and change slowly over time. Lower-order factors have much higher spatiotemporal variability and are connected to each other in multiple ways and have both direct and secondary or tertiary effects on the main processes behind soil methane fluxes. Soil methane flux itself has a significant impact on climate in a positive feedback loop. Factors affecting inter-species competition are not included in the model due to their complexity and relative irrelevance in the context of this study. The figure was made based on multiple studies such as McBride (1994), Hanson and Hanson (1996), Garcia et al. (2000), Le Mer and Roger (2001), Megonigal et al. (2003), Smith et al. (2003), Ström et al. (2005), Ström and Christensen (2007), Lai (2009), Olefeldt et al. (2013), Schlesinger and Bernhardt (2013), and Serrano-Silva et al. (2014).

2.2 Methane fluxes in boreal environments

In this study, the term boreal environment is used to cover the terrestrial deciduous-coniferous biome that ranges across the northern hemisphere including northern parts of North America, Fennoscandia and Russian Siberia (figure 3). Being the largest biome in the world, the climatic conditions of the boreal zone vary widely between its regions with temperatures ranging from 0°C to -50°C in winter and 10°C–22°C in Siberia in summer. The soil

temperatures in general are relatively low in the boreal environments due to low average air temperatures (Jögiste et al. 2008). Precipitation patterns and amounts vary relatively strongly as well, annual precipitation amounts varying between 300 and 600 mm (Jögiste et al. 2008). The soil texture in the boreal zone in general is relatively coarse, often including gravel and larger stones mixed with some finer textural classes which together form glacial till (Simojoki et al. 2008a). The biodiversity of boreal forests is relatively low: most of the vegetation in a boreal forest consists of coniferous *Abies*, *Picea* and *Pinus* tree genera and wide populations of mosses and lichens and more sparse ones of shrubs on the ground layer (Jögiste et al. 2008). Boreal wetlands include ombrotrophic bogs and minerotrophic fens in particular, the vegetation of which consists primarily of grasses and sedges, shrubs and some trees (Bartlett and Harriss 1993). Boreal soils are dominated by organic histosols with thick peat layers, permafrost-containing gelisols and podzols, the latter of which consists of characteristic organic (O), eluviation (E, translocation of iron and aluminum oxides and clays) and illuviation (B, accumulation of the translocated particles) horizons (Simojoki et al. 2008b).

Strong accumulation of organic matter in boreal soils increase both methanogenic and methanotrophic potentials and, consequently, influences soil methane fluxes. Especially in low temperatures the rate of the growth of biomass and its decomposition in microbial processes decrease significantly, leading to the accumulation of incompletely decomposed humus particles and increase in the soil carbon pool which accounts for approximately 13% of the accumulated carbon in the global biosphere (Post et al. 1985; Simojoki et al. 2008b, figure 3). Organic matter decomposition occurs and accumulates in the top O and A horizons as lignins, proteins, and humus with a soil residence time reaching a millennia (Hari et al. 2008; Simojoki et al. 2008b). The highest accumulation of organic matter in the boreal zone occurs in wetlands, however, with approximately 43–144 $kg\ m^{-2}$ of organic carbon content (Jones et al. 2010), forest soils containing approximately 88–159 Pg in carbon pool with or without including living biomass (Gorham 1991). Boreal and subarctic wetlands together may have a carbon pool as large as 455 Pg which increases the significance of the high-latitude and boreal regions in global carbon cycle and methane emissions (Gorham 1991). Due to the large carbon pool of the boreal soils, changes in climatic variables, such as temperature and precipitation, may have significant influences to the soil methane fluxes in the region (e.g. Gorham 1991; Whalen et al. 1991; Minkkinen et al. 2002).

In general, boreal forests are considered methane sinks, and wetlands considered sources, due to the relatively clear difference in the oxygen concentration of the soils. The combination of high soil moisture content and anoxic conditions of wetlands and cool temperatures leads to remarkably high methane emissions with an estimated rate of 23 $g\ CH_4\ m^{-2}yr^{-1}$ for wetlands within boreal forest areas and high CO_2 consumption, in other words, a CO_2 sink (Aurela et al. 2004; Zhuang et al. 2004; Ström et al. 2005). The estimations of the

rate of methane consumption in boreal forests vary strongly both spatially and temporally and between different studies with the estimated rate ranging from 0 to 15 Tg CH_4 yr^{-1} (Zhuang et al. 2004). Boreal forests are estimated to account for approximately 8% of the global terrestrial CO_2 exchange which is calculated as the ratio between net primary production, decomposition of organic matter and CO_2 released in wildfires (McGuire et al. 2009). While methanotrophic consumption is high in boreal forests, the wetland emissions exceed the consumption rate of forests, leading to a positive flux of methane in the larger scale of the whole boreal region (Whalen et al. 1991).

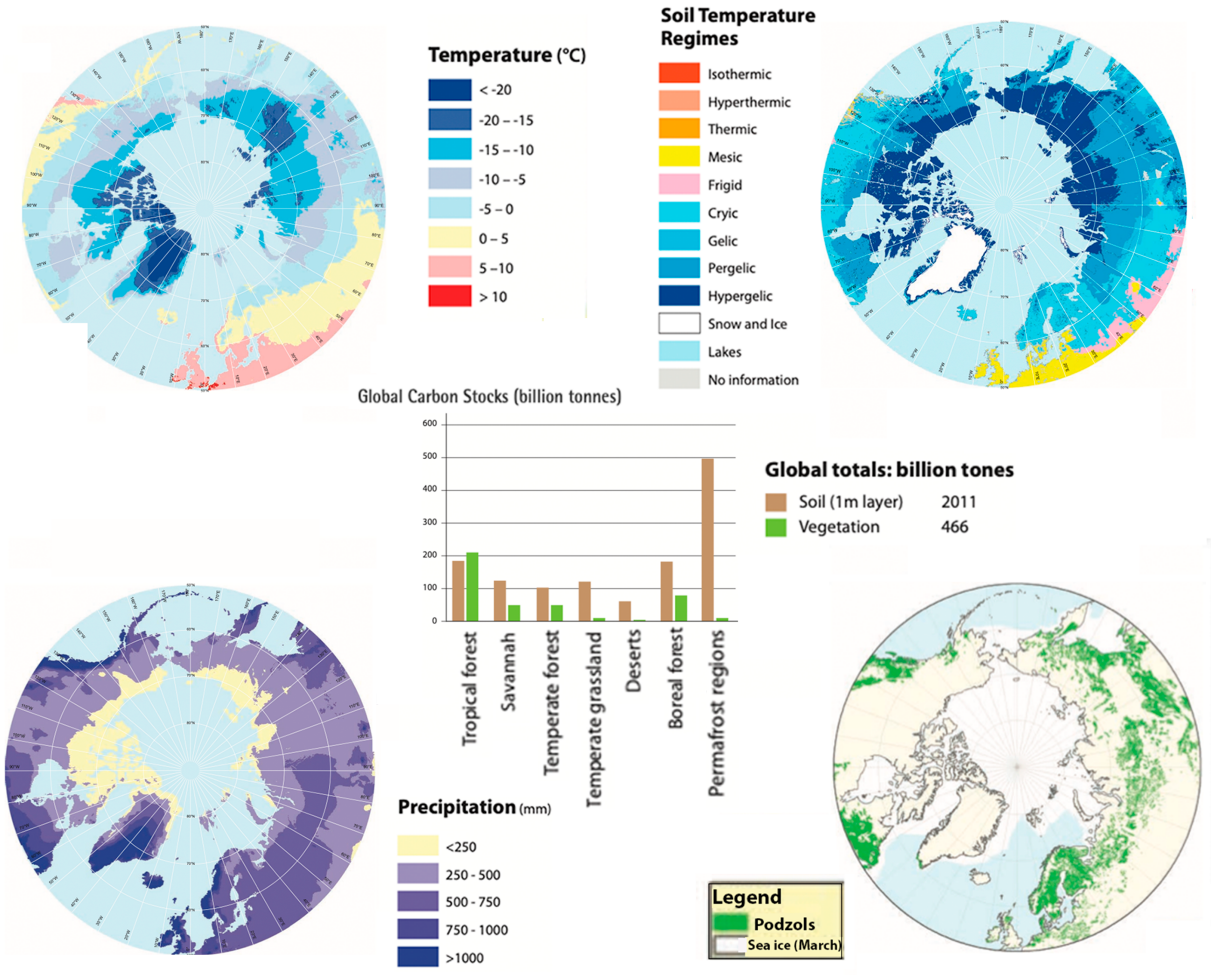

Figure 3: General climatic and soil characteristics of circumpolar boreal zone. Cool air temperatures have led to low mean soil temperatures especially in the northern boreal areas (cryic and gelic), which together with relatively high precipitation enhance organic matter accumulation in boreal soils. Cryic soil temperature regime refers to soils without permafrost whereas gelic soils are affected by permafrost. Podzols and histosols are the most common soil types in the region, the former of which is shown in the map. The borders of the boreal zone generally follow podzol distribution and thus the climate maps do not represent only boreal region but also other arctic environments. The figures were obtained from Jones et al. (2010).

2.3 Methane fluxes in upland forest soil

By upland soil, this study refers to those soil types that, due to higher topographical elevations, have soil volume consisting of up to 25% air-filled pore space, and are characterised by high air diffusivity, efficient drainage of water, and a relatively low water table (Schlesinger and Bernhardt 2013). Upland soils are often located adjacent to soils with higher water saturation due to the drainage of nutrient-rich water from uplands, resulting in wetlands that, in mostly waterlogged conditions, have 50% solid soil particles and another 50% water-filled pore space of the whole soil volume on average (Schlesinger and Bernhardt 2013). In general, microorganisms in upland forest soils are more efficient in decomposing soil organic matter than those in carbon-accumulating wetlands, which is indicated by the thinner organic horizons of the upland soils (Schlesinger and Bernhardt 2013). The microbial biomass of upland soils consists primarily of fungi instead of bacteria but still reaching high microbial biomass values in relation to lowland soils, for example (Anderson and Domsch 1980; Schlesinger and Bernhardt 2013).

Since upland forest soils have relatively low soil moisture, the resulting oxic conditions are favourable for methanotrophic bacteria and methane consumption (figure 4). The consumption is estimated to reach approximately 30 Tg yr^{-1} globally and change along the seasons, peak values occurring often in summer (Potter et al. 1996; Schlesinger and Bernhardt 2013). The efficiency of methane consumption in those soils is the result of generally coarse or highly mixed texture, low bulk density, high microbial biomass, and subsequent activity, and high soil organic matter content (Whalen et al. 1991; Dutaur and Verchot 2007; Regina et al. 2007). Especially the coarse texture and low bulk density leading to high porosity with greater amount of macropores increases methane diffusion from the atmosphere to the soil and methanotrophs (Ball et al. 1997; Dutaur and Verchot 2007; Regina et al. 2007). However, the significance of coarse texture for oxidation is less studied and possibly more varying in boreal upland forest soils (Dutaur and Verchot 2007). It has been estimated that methane oxidation in a very dry soil is primarily controlled by soil moisture, followed by oxygen concentration (Whalen and Reeburgh 1996; Saari et al. 1998). In boreal upland forest soils, however, soil moisture rarely decreases to as low levels as required for the significant decrease in methanotrophy, the optimal soil moisture content for methanotrophy being approximately 20%–35% of water holding capacity (WHC) of the soil (Saari et al. 1998; Pihlatie et al. 2008). Water holding capacity is a term used for the amount of water a soil in question can hold (Pihlatie et al. 2008).

Despite the overall strong diffusivity of methane from the atmosphere, the most efficient methane oxidation in boreal upland forest soils occurs in the layers below organic horizons. Depending on the study, the approximate depths of highest oxidation vary between 0–5 cm and 7–12 cm from the uppermost edge of the mineral soil through all seasons with a tendency for maximum oxidation in the illuvial horizons (Saari et al. 1997, 1998; Kähkönen

et al. 2002; Pihlatie et al. 2008). In the primarily oxic upland soils, the organic horizons (O in particular) can turn to sources of methane instead of their sinks (Saari et al. 1997). High methane concentrations within the soil are also located near the water table level, creating two maxima of methane production in the deeper and uppermost layers of the soil and a minimum with methanotrophic oxidation in between in the mineral soil (Megonigal and Guenther 2008). It has also been proposed that, the thicker the litter and organic layer, the higher the decrease in methane diffusivity from the atmosphere to the upper methanotrophic layers of the soil and the higher the nitrogen toxicity in the litter layer for methanotrophs (Kähkönen et al. 2002; Pihlatie et al. 2008). Especially boreal upland forest soils have relatively thin litter layers consisting mostly of needles, which results in higher diffusivity of methane and, consequently, higher methane oxidation rate than in deciduous forests, the litter of which consists mostly of broad leaves preventing the diffusion of methane from the atmosphere (Ball et al. 1997; Brumme and Borken 1999).

Since some methanogens are able to adapt to conditions with high oxygen concentration, mostly oxic upland forest soils may harbor a large potential for methanogenic activity. Methanogens have been found to survive for unexpectedly long times in relatively dry and oxic soils with some methane-producing activity (e.g. Ueki et al. 1997; Megonigal et al. 2003; Megonigal and Guenther 2008). The viable populations of methanogens in such dry soils may be protected from methanotrophic oxidation by being located within the anoxic centres of soil aggregates or by so-far unknown protective mechanisms of certain soil minerals such as pyrite (FeS_2) (Fetzer et al. 1993; Megonigal et al. 2003). While methane consumption and production may occur ubiquitously in upland soils, some studies suggest that both processes together may result in an almost net zero flux of methane (von Fischer and Hedin 2002). The production of methane in the anoxic aggregate structures within the oxic soils may in some cases enhance the methanotrophic oxidation further by generating more substrates for methanotrophy (Chan and Parkin 2001).

With high methanogenic potential, oxic upland soils may become methane sources after being exposed to higher soil moisture and anoxic conditions (figure 4). According to results from incubation experiments done by Wang and Bettany (1997), a decrease in E_h to below -200 mV in the originally well-drained oxic soils is one of the primary factors leading to the soil becoming a net source of methane. In addition, Wang and Bettany (1997) found that oxic soils in situ began producing methane after snowmelt and heavy summer precipitation events which was also connected to lower E_h and higher soil moisture content. The effect of precipitation on soil methane fluxes has been studied also by Savage et al. (1997) and more recently by Lohila et al. (2016), both finding positive correlations between heavy precipitation periods and positive methane fluxes in upland forest soils. For example, Lohila et al. (2016) found that a northern boreal upland forest soil turned from a methane sink to a significant and long-lasting source in autumn after an abnormally wet summer while the source rates

of the adjacent wetlands did not significantly change when upscaled to ecosystem-level. Boreal upland forest soils specifically include significant hot spots of methane production in areas with high water table level and water saturation, such as floodplains and sporadic formation of wet depressions, which may alter the local sink-source dynamics both spatially and temporally (Whalen et al. 1991; Gulledge and Schimel 2000; Christiansen et al. 2012). Furthermore, Keppler et al. (2006) have found that trees of boreal forests are able to emit significant amounts of methane via a so-far unknown aerobic mechanism but according to Kirschbaum et al. (2006) and Ferretti et al. (2007) the plant-originating emissions are not as significant and lower in amount in the global scale.

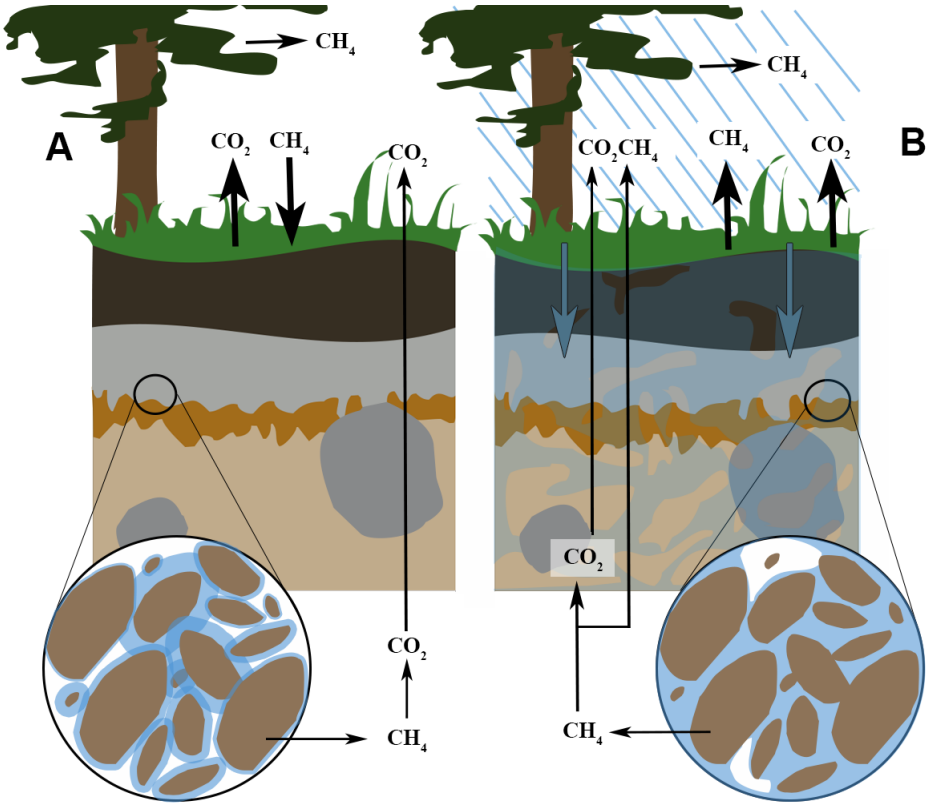

Figure 4: Methane production and consumption in a boreal upland forest soil. Normally soil pores are mostly filled with air, resulting in oxic conditions favourable for methanotrophic bacteria and methane consumption (A). However, soil aggregates within the soil structure contain anoxic centers in which methanogenic activity and thus methane production remain prevalent. In oxic conditions, the produced methane is effectively oxidised into carbon dioxide (CO_2). After heavy rainfall events or snowmelt upland forest soil can turn into a methane source when precipitation water infiltrates into the soil and soil pores fill with water (B). When soil moisture increases, oxygen is depleted and anoxic conditions dominate which increase methane production by methanogenic archaea. The produced methane diffuses into atmosphere or is oxidised in oxic soil layers. Trees are also found to emit methane in varying amounts in boreal forests. The figure includes only processes relevant to methanotrophic and methanogenic activities and thus does not include all possible processes generating carbon dioxide, such as soil respiration. The figure was made by combining studies by Le Mer and Roger (2001), Megonigal and Guenther (2008), Jones et al. (2010), Seneviratne et al. (2010), and Schlesinger and Bernhardt (2013).

3 Study area

The study site is located at the Kenttärova forest (67°59.237'N, 24°14.579'E) in the Kittilä municipality in Finnish Lapland near the border between the northern-boreal and subarctic zones. The site lies on a hilltop plateau with the approximate elevation of 347 m above sea level and 60 m above the surrounding plains (Aurela et al. 2015; Lohila et al. 2015a). The forest is one of the upland areas within the Pallaslompolo catchment (105.2 m^2) consisting of fells reaching elevations above the treeline, wetlands and the lake Pallasjärvi (Aurela et al. 2015; Lohila et al. 2015b). Due to its higher elevation in relation to the adjacent wetlands and plains, the direction of water drainage is to the adjacent Lompolojänkkä wetland, ultimately discharging to the lake Pallasjärvi (Aurela et al. 2015; Lohila et al. 2015a; Finnish Meteorological Institute 2018a). The area of the experimental site itself is approximately 436 m^2 including the control and experimental sectors.

The climatic and vegetational characteristics of the study site are typical for a northern-boreal environment. The mean annual temperature and precipitation sum of the catchment area reach circa -1.4°C and 484 mm, with long-term averages of January and July being -14°C and +14°C (Aurela et al. 2015; Lohila et al. 2015a). The median end date of snowmelt is May 14th and snow cover start date October 24th, respectively (Aurela et al. 2015; Lohila et al. 2015a; Finnish Meteorological Institute 2018a). Typical for a northern-boreal environment in northern Fennoscandia, the forest is defined as *Hylocomium-Myrtillus* type (HMT), dominant tree species being *Picea abies* with a variety of some deciduous species such as *Betula pubescens*, *Populus tremula* and *Salix caprea* (Cajander 1926). The vegetation on the forest floor includes woody shrubs, such as *Vaccinium myrtillus*, *Empetrum nigrum* and *Vaccinium vitis-idaea*, and an abundance of feather mosses including *Pleurozium schreberi*, *Hylocomium splendens* and *Dicranum polysetum* and only sparse occurrences of lichens, herbs and grasses (Cajander 1926; Ylläsjärvi and Kuuluvainen 2009; Aurela et al. 2015). The soil type is podzol with glacial till as soil parent material (Aurela et al. 2015). The vegetation height in general reaches circa 13 m and tree age varies between 70 and 240 years. The forest has experienced some forest management with the logging of birches in the 1960s but since then has been allowed to grow naturally (Aurela et al. 2015; Finnish Meteorological Institute 2018a).

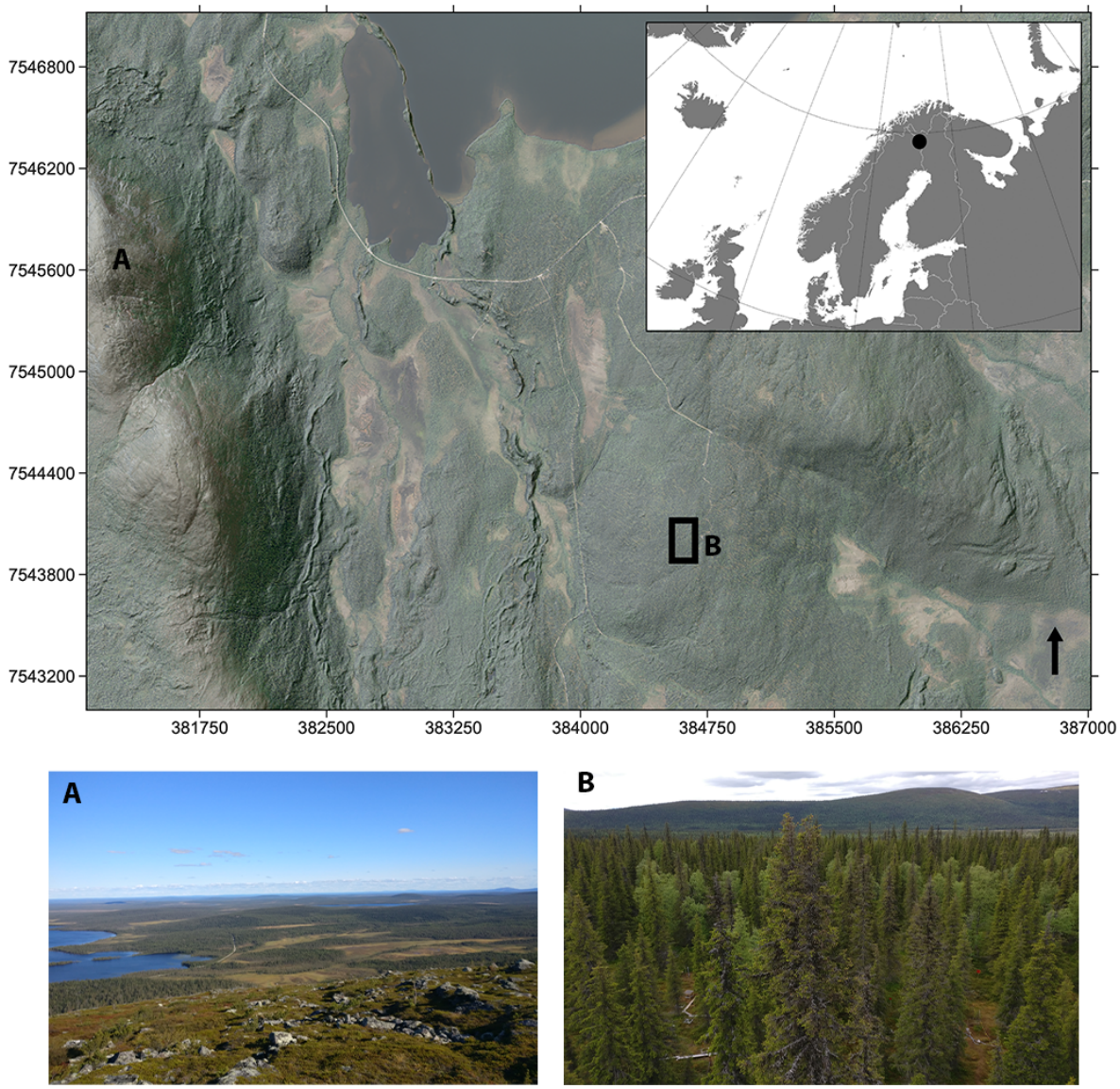

Figure 5: Location of the study site. The map is shown in ETRS-TM35FIN coordinate reference system. The map combines hillshade for displaying elevational differences and orthoimages for a general view of land cover. Image A was taken from the nearby Lommoltunturi fell toward east and image B from the Kenttärova station toward west. Figure was created using Quantum GIS software (GIS data: National Land Survey of Finland 2020).

4 Field data collection

Field data were collected from the end of May to the beginning of September in 2018. The study period was chosen to include the end of snowmelt, start and peak of growing season and start of wilting season in autumn. All the raw data collected from the field were processed using Python 3.7.3 (Python Core Team 2019) and RStudio software (R Core Team 2019) before moving on to the statistical analyses. See a list of the used Python and R packages in Appendix J.

4.1 Experimental design

For examining causal relationships between methane flux and chosen variables, the study was conducted as an unbalanced split-plot design which included two main plots: irrigation (I=irrigation) and control without irrigation treatment (C=control). The control was established in order to compare the results of the experimental irrigation site with the naturally occurring precipitation rate that served as a simultaneous baseline for the experiment. The areas of the sites reached approximately 281.25 m^2 in the control site and 118 m^2 in the irrigation site. Both main plots included 13 subplots with specific subtreatments. Subplots were assigned randomly in both sites and to the specific subtreatments and set to represent as similar vegetational, topographical and sun aspect characteristics as possible. Split-plot design was chosen due to its convenience in terms of the irrigation implementation for one larger area instead of multiple smaller individual plots. Since soil moisture was the main factor of interest with main effect on CH_4 flux, and the other independent variables were considered having interaction effects with soil moisture on CH_4 flux, its use was best argued in this study.

The design included four subplots without additional manipulation treatments per site (abbreviated as IO1, IO2, IO3 and IO4 in the irrigation site and CO1, CO2, CO3 and CO4 in the control site; O=original). The collars were installed in the ground in 15.6.2016. The O subplots were used for the assessment of the effect of soil moisture on CH_4 flux without additional interactions. Other subplots included were 3 + 3 plots with root and litter exclusion (IE1, IE2, IE3 and CE1, CE2, CE3; E=exclusion), litter addition (IA1, IA2, IA3 and CA1, CA2, CA3; A=addition) and temperature manipulation (IT1, IT2, IT3 and CT1, CT2 and CT3; T=temperature, figure 6). The collars of the manipulated subplots were installed in the ground from the end of May to beginning of June 2018. Both the control and irrigation areas and subplots within them were connected with wooden boardwalks in order to minimise soil and vegetation disturbance from trampling. Since the experiment was set in heterogeneous forest environment, the experimental design included at least three replications of each treatment in order to reduce the experimental error. Experimental error is caused by confounding factors not measured in the study and may result in bias, which in this context refers to strongly distorted results into a specific direction, or error covariance which causes variation in the results which is not accounted by the measured variables (Kirk 2013). The amount of subplot replications in E, A and T plots were fewer than for O plots due to insufficient space around the boardwalks for fitting another three subplots as fourth replications.

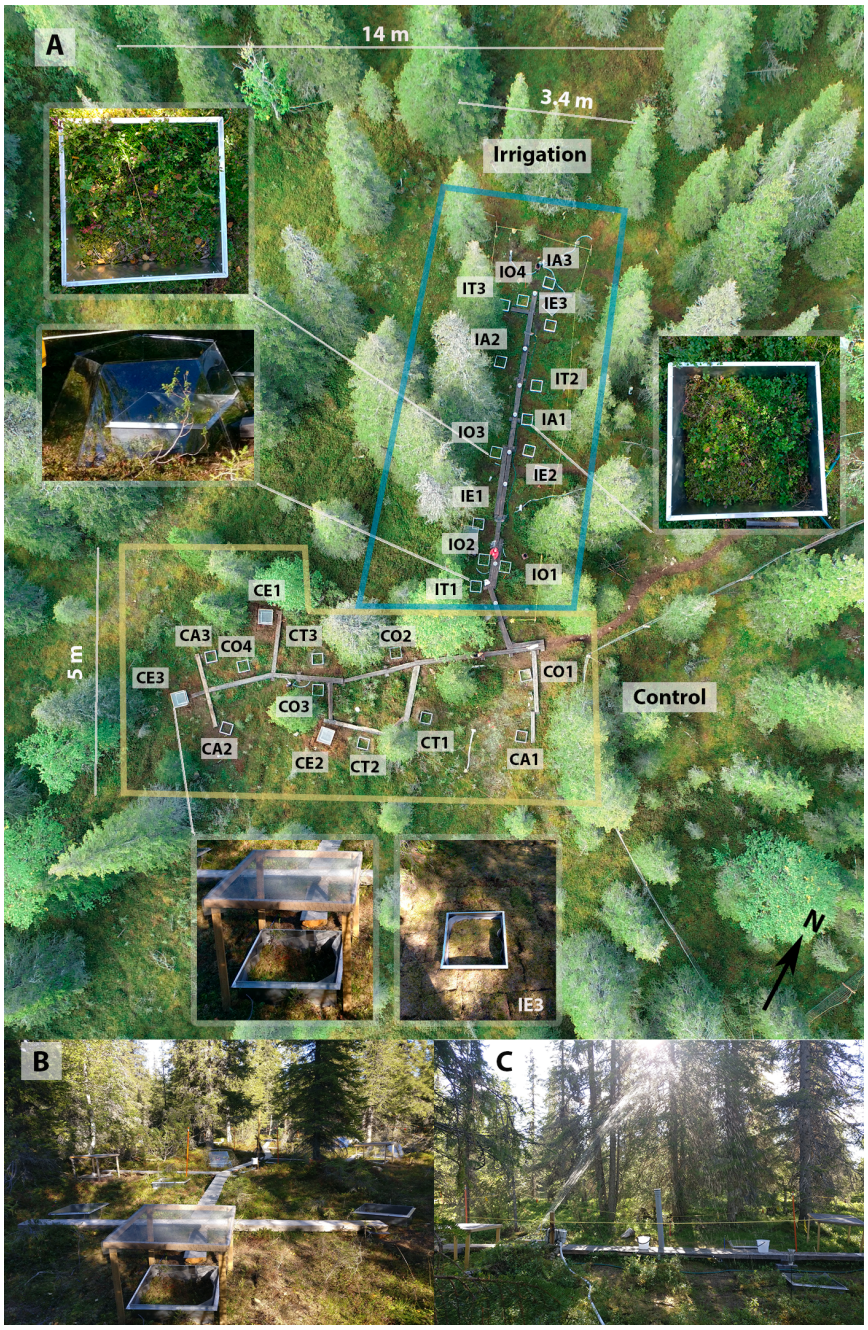

Figure 6: The experimental design and locations of irrigation and control sites, subtreatments and subplots within them (A). An example of each subtreatment is shown from selected subplots. Image B represents the control site toward east while image C shows the middle part of irrigation site toward west during irrigation. The lengths of the dimensions are approximations of the true distances between the site edges and especially the irrigated area experienced high spatiotemporal variation. Aerial image: Dr. Bastian Steinhoff-Knopp (Leibniz Universität Hannover, September 2018).

4.2 Organic litter and root manipulations

The organic litter and root manipulations included litter and root exclusion (CE and IE) and litter addition (CA and IA). Root exclusion was carried out by digging an extraction pit with an iron shovel below average root depth (ca. 27 cm) to approximately 32 cm depth with circa 25 cm margin space around the collar. The plot excavations were carried out

during 21.—25.5.2018. In addition, the top organic layer was separated from the mineral soil by cutting into approximately 6 cm depth. All the dug exclusion surfaces were covered with a polypropylene fabric (pore size 80 µm) that would prevent most of the roots from entering deeper in the soil, growing outward from the plot area and providing substrates for the microbes within the plot soil. Similar fabric and trenching exclusion technique has been used for instance by Vincent et al. (2010). For further details on the extraction measures, see Appendix A. The organic litter from vegetation above was excluded using litter collection nets (85 cm x 81 cm) 70 cm above the exclusion plots with collar in the centre (figure 6). The old accumulated litter from previous years was also removed by hand. The litter exclusion was executed in order to decrease decomposition of soil organic matter following the same method used in studies by Minkkinen et al. (2007) and Mäkiranta et al. (2010).

Litter addition was executed using the collection nets above litter exclusion plots and combining the collected litter together per site and then weighing it separately, after which all the collected litter from both sites was combined and mixed together. A litter sample equalling 10% of the whole amount of litter was taken for further composition analysis which will not be part of this thesis. The weighed and mixed litter was then divided evenly on all the six addition plots (CA and IA) within the collars. Litter weighing and addition was executed once a week. The litter additions were started 28.6.2018. The old litter from previous years that was collected from the exclusion plots was also weighed separately for each plot, mixed together and divided evenly on the addition plots in 5.7.2018. See Appendix B for further details of litter additions.

4.3 Soil temperature manipulation and measurements

Soil temperature was manipulated passively using 2.5 mm thick polycarbonate Open Top Chambers (OTC) in six subplots (CT and IT, figure 6). Each CT and IT subplot had one OTC around the collar, following the instructions of the ITEX Manual by Marion (1996) with the exception of their regular pentagonal shape. The choice of replacing hexagons with pentagons was made due to practical difficulties of removing larger hexagonal OTCs from the plots while measuring the fluxes and executing irrigations by one field worker. The length of one side's lower edge was 88 cm, side edge 60 cm and upper edge 53.5 cm resulting in 1.33 m^2 internal area and approximately 55–65 cm height depending on the ground depressions. The chambers were attached to the ground from three sides with iron spikes. The OTCs' sides were inclined inward in order to retain more heat within the plot (Marion 1996).

Soil temperature was measured using ten Soil Scout online sensors (Soil Scout Ltd, Helsinki, Finland) and six Stevens HydraProbe Soil Sensor Analog sensors (Stevens Water Monitoring Systems Inc, Portland, USA) that were installed in the ground inside the OTC coverage area. In addition, 13 HOBO U30 Station sensors (Model number: U30-NRC-000-10-S100-000, Onset Computer Corporation, Massachusetts, USA) were set in the soil to measure

soil temperature. All the sensors were set 5 cm below the soil surface in the mineral soil layer next to the collar and covered carefully with soil. The installment was executed during 23.5.—6.6.2018, which resulted in different start dates for temperature logging for different sensors (see Appendix C). The temperature data sets were set to begin 7.6.2018 and end 12.9.2018. After the experimental period in 2018, the HOBO temperature sensor for CT2 subplot was found to have malfunctioned during the whole measuring period and did not produce any data for analysis. The time intervals for soil temperature logging was 20 minutes for Soil Scouts and 30 minutes for Stevens HydraProbe and HOBO sensors. Since there was a different number of each sensor type, they were divided so that each plot in both control and irrigation sites had one or two sensors that together measured both the soil temperature and moisture.

4.4 Soil moisture manipulation and measurements

Soil moisture effect was examined in both main (I and C) and subtreatment level (IO and CO, figure 6). Soil moisture was manipulated by irrigating the experimental site with two water sprinklers. The irrigation period as a whole lasted from 28.5.2018 to 7.9.2018. The sprinklers were set in the site so that each subplot would be evenly reached by the irrigated water. The ultimate irrigated area in practice reached approximately 118 m^2 with 3–5.5 m width and 10–21 m length, strongly depending on the wind conditions. Before each irrigation, the litter collection nets from IE subplots and OTCs from IT subplots were moved aside in order to distribute the precipitation more evenly between all the subplots.

The amount of irrigated water was 2 x 1000 l a week during 28.5.—1.6.2018, after which the amount was increased to 3 x 1000 l a week in 7.—18.6.2018 and eventually to 5 x 2000 l a week starting from 20.6.2018 and ending at the beginning of autumn in 7.9.2018. The amount of irrigation water was sometimes less due to logistical problems with carrying the water. The goal was to keep a constantly high precipitation frequency within the irrigation site in order to increase soil moisture. However, the irrigated water was not enough for exceeding the long-term average in the area (table 1). The spatial distribution of irrigation during the study period was examined with rain gauges (unit: mm) and larger buckets. The collected water amount of each bucket was later proportioned to the rain gauges in mm based on their dimensions. The precipitated water was measured after each irrigation from the end of May to mid-June to ensure the relatively even distribution of water on the area. For the rest of the season the irrigated water was measured only when the weather was notably windy and/or natural rainfall occurred during the irrigation. See Appendix D for further details of the irrigation amounts.

As with the CT and IT subplots, the same ten Soil Scout online sensors and six Stevens HydraProbe sensors were installed in the ground to measure soil moisture every 20 (Soil Scout) and 30 (Stevens HydraProbe) minutes from end of May to the beginning of September. Ad-

Table 1: Summary of the irrigation measures and their relation to long-term precipitation averages. Hypothetical measurements refer to the hypothetical situation where all the irrigated water (1000–2000 l) is spread evenly over the approximately 118 m^2 area of the irrigation site (water amount in mm=$V_{water}/A_{irrigationsite}$, where V=volume in litres and A=area in m^2). Gauge measurements were actual measurements taken from the rain gauges and buckets distributed around the irrigation site (in mm) and were averaged to form a spatial mean of each irrigation occasion. The sums and means of the gauge measurements are thus based on the spatial means. Natural + hypothetical refers to the naturally-occurring precipitation amount (28.5—12.9.2018) to which the litre-based irrigation amounts were added by date of irrigation. Negative values of percentage change (% change = ($prec_{irrigated}$ - $prec_{long-term}$)/|$prec_{long-term}$|*100, where $prec$=precipitation) indicate a percentage decrease in precipitation in relation to the long-term average. Long-term averages were based on measurements taken in the weather station of Alamuonio (Pirinen et al. 2012). Precipitation amounts during 28.5—12.9.2018 in Kenttärova were obtained from Finnish Meteorological Institute (2018a). See a more detailed report of the irrigation manipulation in Appendix D.

measurement	time	sum (mm)	mean (mm)	change (%)
Hypothetical	whole period	879.3	14.9	-76.7
	May-June	184.3	12.3	-79.2
	July	336.7	16.0	-78.7
	August	282.8	15.7	-78.8
	September	75.8	15.2	-68.3
Natural + hypothetical	whole period	1085.8	10.5	-83.6
	May-June	236.5	7.0	-79.2
	July	364.1	11.7	-78.7
	August	407.7	13.2	-78.8
	September	77.5	11.1	-68.3
Gauges	whole period	486.9	18.0	-71.9
	May-June	130.2	13.0	-78.0
	July	142.3	20.3	-72.9
	August	169.2	21.2	-71.4
	September	45.2	22.6	-52.9

ditionally, 11 HOBO sensors (Model number: U30-NRC-000-10-S100-000, Onset Computer Corporation, Massachusetts, USA) were set in the soil to measure soil moisture through the same period with 30-minute logging intervals. Similar to the temperature manipulation plots, all the sensors were set 5 cm below the soil surface in the mineral soil layer next to the collar. All the sensors measured soil moisture as volumetric water content (VWC, θ_v) which is calculated by the volume of water divided by volume of dry soil (Seneviratne et al. 2010). As the data collected by Stevens HydraProbe and HOBO sensors measured the soil moisture in m^3/m^3 while Soil Scouts expressed it in percentages, the soil moisture values in Stevens and HOBO data files were multiplied by 100 for making the data sets comparable. In addition, all soil moisture data was set to begin on 7.6.2018 and end on 12.9.2018, similar to the soil temperature data. See further details of subplot-specific sensors and installment dates in Appendix C.

4.5 Methane flux measurements

Methane flux was measured from each subplot at least once a week from 15.6.2018 to 11.9.2018. However, the methane flux measurements were started already on 29.5.2018, followed by 7.6.2018 and 8.6.2018, all of which lacked flux information from some plots which led to the decision of including data starting from 15.6.2018 for the further data analysis. Some

exceptions to the measuring frequency were made with three measurement campaigns during one week in July (23., 25. and 26.7.2018). The total amount of measurement campaigns used in the data analysis was 16, ranging over 14 weeks in total.

Each measurement was 5 minutes long at minimum for ensuring more accurate estimations of the flux when calculating it using linear regression (e.g. Korkiakoski et al. 2017). The measurements were executed using 0.6 m x 0.6 m x 0.2 m and 0.6 m x 0.6 m x 0.3 m metal chambers with an air-mixing fan and a tube with circa 15–25 m length and a filter leading to the gas analyzer located in a cabin with an approximately 20 metres' distance from the study site. The methane and water vapour concentrations were measured by Picarro Gas Concentration Analyzer (Picarro Inc, California, USA) which uses cavity ring-down spectroscopy in concentration analyses and measures the gas and water vapor concentrations in circa four-second intervals. Due to the breakdown of the Picarro (CFADS2135, model: G2301) at the end of June, it was changed to an older version (CFDDS101, model: G1301-m) for the rest of the study period. After and before each measurement the chamber and the connecting tubes were exposed to the atmospheric air for some minutes in order to stabilise the gas ratios measured by Picarro.

Each subplot had one metal collar (58 x 58 cm, figure 6) installed in the soil. The collar leakage was prevented by the foam layer at the bottom of the chamber edges and by carefully cutting the collars into the soil with approximately 1–2 cm depth depending on the local coarseness of the soil, using a knife and covering some occurring holes with sand and checking the airproof condition prior to flux measurements. In the case of IE and CE subplots with separated organic layers, the flux was first measured from the whole plot with the organic layer, after which the organic layer was manually carefully removed with minimal disturbance and measured again without the organic layer. Therefore, the exclusion plots were measured twice per each measurement campaign. This was done in order to receive more information about the influence of organic and mineral layers to the CH_4 flux.

5 Statistical analysis and modelling methods

The statistical analyses in this study included both exploratory and confirmatory analyses of the treatment effects. Exploratory data analysis was carried out producing box plots, scatter plots, frequency histograms and descriptive statistics of the data. Confirmatory analysis included analysis of variance, TukeyHSD, correlations and regression modelling (figure 7). All statistical analyses were executed using RStudio software (R Core Team 2019) with the exception of the flux calculations which were carried out using Python (Python Core Team 2019) by the Finnish Meteorological Institute. See the full list of used R and Python packages in Appendix J.

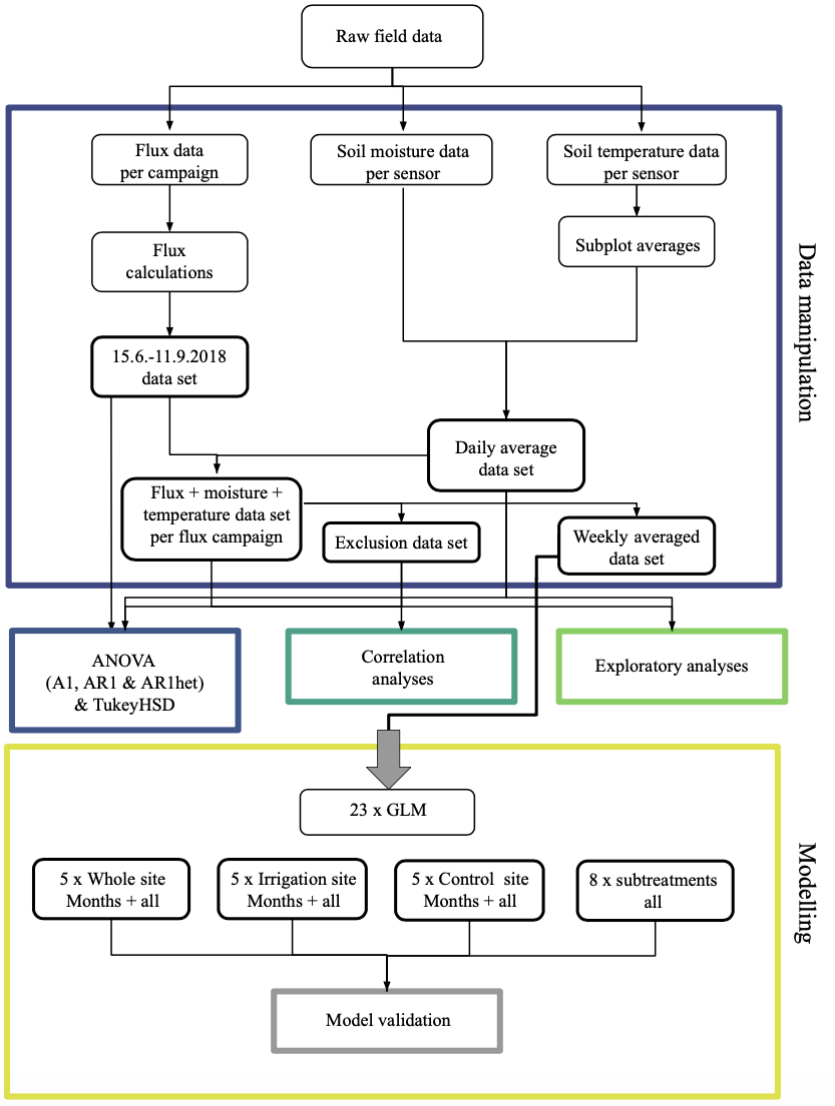

Figure 7: The workflow of this study. The first step contained data processing and flux calculations with Python and R, which resulted in five different data sets: flux data per each flux measurement date, a combined data set with flux, soil moisture and soil temperature set to flux measurement dates, exclusion manipulation data set containing separate fluxes for organic and mineral layers together with soil moisture and temperature for CE and IE subplots, daily soil temperature and soil moisture data set and a weekly data set with weekly averages of all the measured variables. Each data set was used in exploratory, ANOVA, TukeyHSD and correlation analyses, with the exception of combination data set which was only used for two- and three-way ANOVAs, and weekly data set which was used in the GLMs. 23 GLMs were built based on treatment levels and months (all=whole study period). All models were validated using model fit statistics and cross-validation methods.

5.1 Flux calculations

The methane fluxes for each subplot per weekly campaigns were calculated as $\mu g\ CH_4\ m^{-2}\ h^{-1}$, following similar steps to Korkiakoski et al. (2017). Due to the breakdown of Picarro CFADS2135 and the resulting switch to the older Picarro CFDDS101, dilution corrections were carried out for all the CH_4 and CO_2 data reported by CFDDS101 which did not do it automatically. Dilution corrections were made in order to achieve more accurate estimates of the changes in gas concentrations by correcting the changes in atmospheric water vapour.

Without the corrections, water vapour causes significant changes in the mole fractions of CH_4 and CO_2 which results in smaller estimates of the fluxes (Korkiakoski 2014). In this study, the dilution corrections of the concentrations into dry mole fractions were done using the following formula:

$$CH_{4_{dry}} = \frac{CH_{4_{wet}}}{(1 + z_1 H_{rep} + z_2 H_{rep}^2)}, \tag{1}$$

where $CH_{4,dry}$ is the dilution-corrected CH_4 concentration and $CH_{4,wet}$ is the mole fraction of the gas in question as humid gas. H_{rep} is the water vapour mole fraction which was measured by the instrument while z_1 and z_2 refer to the instrument-specific first and second order correction coefficients for the water vapour correction.

In addition, the dilution-corrected flux data was fitted with linear regression which describes the change in CH_4 concentration in unit time. The linear regression fitting was executed with the following formula, also used by Korkiakoski et al. (2017):

$$C(t) = a_{lin} + b_{lin} t, \tag{2}$$

where C equals to change in the CH_4 concentration, a_{lin} and $b_{lin}t$ to used parameters, the slope of the latter showing the change in CH_4 concentration, and t to the time starting from the chamber closure.

Finally, the CH_4 flux calculations were executed following the same formula as the one used by Korkiakoski et al. (2017):

$$F = \left(\frac{dC(t)}{Dt}\right)_{t=0} \frac{MPV}{RTA} 3600 \frac{s}{h}, \tag{3}$$

where F is the CH_4 flux in $\mu g\ m^{-2}\ h^{-1}$, $\left(\frac{dC(t)}{Dt}\right)_{t=0}$ is the time derivative (ppm s^{-1}) of the linear regression (b_{lin}) at the beginning of the chamber closure, M is the molecular mass of methane (16.042 $g\ mol^{-1}$), P is air pressure (Pa), R is the universal gas constant (8.31446 $J\ mol^{-1}\ K^{-1}$), T is the temperature within the chamber space during the closure, V is the volume (m^3) of the space inside the chamber (height of chamber either 20 or 30 cm + the mean height of the collar multiplied by the area of the chamber base) and A is the area of the chamber base, i.e. the area of the collar. In the lack of a temperature measurement within the chamber, the T in the calculation in this study was the atmospheric air temperature of the day of measurement, obtained from the Kenttärova measuring station of the Finnish Meteorological Institute. The values resulting from the used formula are either negative which marks for CH_4 uptake by the soil whereas positive values indicate CH_4 emission to the atmosphere.

5.2 Analyses of variance and covariance

Effects of main- and subtreatments with months or weeks on soil CH_4 flux was estimated using two-way analysis of variance (ANOVA), often used in split-plot analyses of main effects and some repeated measures analyses (Tabachnick 2014; Altman and Krzywinski 2015). Same method was used for the analysis of effects of treatments to soil temperature and soil moisture, the latter of which were response variables. In addition, more complex three-way ANOVAs with three independent variables were used for estimating the effects of treatment levels, soil moisture and/or soil temperature and/or months on CH_4 flux. One-way ANOVAs were used for the estimation of sensor-specific effects. The significance of treatment effects was estimated with probability values (p-values) with the following statistical significance levels: $p<0.001$ *** (high significance), $p<0.01$ **, $p\leq0.05$ * and $p>0.05$ ns (no significance). After constructing ANOVAs, multiple pairwise comparisons of treatment means were executed using Tukey's Honestly Significant Difference (TukeyHSD) test. In TukeyHSD, the variables found significant in ANOVA are further examined by comparing the means of the different categories of the variables in multiple pairs (Sjögersten and Wookey 2002; Tabachnick 2014). The treatment groups, months and weeks were categorical variables and CH_4 flux, soil moisture and soil temperature were continuous numerical variables.

The three different sensors showed significant differences in measured soil temperature and moisture over the whole study period. The HydraProbe sensors systematically showed significantly higher soil temperatures with approximately +5°C difference to the other sensors in same subplots (***). Thus, in the further analyses, the soil temperature in IO2, IO3 and IE2 subplots was calculated as the mean of the measured temperature by HOBO and HydraProbe sensors. If the temperatures measured by HydraProbe sensors in IO2, IO3 and IE2 were to be deleted and only the HOBO temperatures were left for those subplots, there would have still been three error-prone HydraProbe sensors left in IO1, IE1 and IT1 subplots as the sole temperature sensors and the measurement error would still have been present in the temperature data. Despite the high differences between soil moisture sensors caused by HOBO, all soil moisture data was decided to be kept in the data sets unchanged because each subplot had just one sensor measuring soil moisture and their removal would have decreased the statistical power and the differences may also have been partly caused by the experimental manipulations themselves. See Appendix G for further details of the sensor differences.

Because the measurements of soil moisture, soil temperature and soil CH_4 flux were taken repeatedly multiple times from the same subplots over 14 weeks, the assumption of independency of predictor variables was violated which may lead to errors in the results (Littell et al. 2000; Barnett et al. 2010; Logan 2010). Here, the analysis of repeated measures was carried out in two ways: two-way ANOVAs without assumptions of variance-covariance structures (hereby referred to as A1) and those with a set fit to such a structure. Two-way ANOVAs

without variance-covariance structure assumption included either month or week as the time variable and the treatment variable (main treatment or subtreatment), and if statistically significant, their interactions. If the interaction terms were insignificant, they were removed from the model. Based on the results of the A1, TukeyHSD tests were executed for the pairwise comparisons between the variables for finding significant spatial and temporal differences between the treatments (Sjögersten and Wookey 2002; Tabachnick 2014).

In addition to ANOVAs without specific assumptions of data variance-covariance structures, autoregressive correlation structure (hereby referred to as AR1) was used in the ANOVAs. In ANOVAs with soil temperature and soil moisture as response variables the used structure was autoregressive correlation with heterogeneous variances (hereby referred to as AR1het). Autoregressive correlation assumes that correlations between observations in June and July are higher than between June and September, for example, and that variances between months are equal (Littell et al. 2000; Logan 2010). Autoregressive correlation with heterogeneous variances, on the other hand, is otherwise similar but assumes unequal variances between months (Logan 2010). Their fit for the data was tested by fitting them into Generalized Least Squares models (GLS) along with other different correlation structures (compound symmetry, AR1, unstructured and AR1het) and comparing them in both main plot and subtreatment levels in ANOVA according to Akaike Information Criterion (AIC) values (see Littell et al. (2000) and Barnett et al. (2010)). In the flux data, the differences between both autoregressive models were not very large but autoregressive structure with equal variances had lowest AIC value, thus being the best fit for the GLS models. In both soil temperature and soil moisture data, AR1het had significantly lowest AIC values and the differences to all other structures were significant. After finding the best structure for each data set, the ANOVAs were computed based on GLS models that included the desired predictor terms to be examined and the variance-covariance structure. The data used in structure-specific ANOVAs with CH_4 flux as the response variable included day averages of soil temperature and soil moisture from the same dates as the CH_4 flux measurements. In other ANOVAs with soil moisture and soil temperature as response variables the used data was based on the daily averages from 7.6—12.9.2018.

Both spatial and temporal correlation analyses were carried out using Pearson's correlation coefficient due to the normal distributions of the data. Pearson's correlation coefficient (r) measures the association between two normally distributed variables and gets values between -1 and 1, 0 being mark of no correlation and ± 1 meaning strong relationship (Logan 2010; Tabachnick 2014; Bakdash and Marusich 2017). All correlation analyses were calculated based on a combined data set containing all CH_4 flux measurements and soil temperature and soil moisture as daily averages from the flux measurement dates. In this data set, separate flux measurements from the CE and IE groups were averaged into one per subplot. For the separate correlation analysis of the exclusion soil layers, an additional data set containing

only CE and IE soil layer flux data was created and applied along with the corresponding daily averages of soil temperature and soil moisture for those subplots.

5.3 Regression modelling and model validation

The effect of soil moisture and soil temperature on soil CH_4 flux within the different treatment groups over months was further examined using Generalized Linear Models (GLM). Soil temperature was included in the models as a second predictor because it may have been a confounding factor in the experiment and therefore may have influenced the effect of soil moisture on CH_4 flux (Christensen et al. 1995). By including known and measured confounding factors in the models, the causality of their effect on the studied relationships can be estimated more reliably (Rutherford 2001; Kirk 2012). Altogether, 23 models were built in this study due to the repeated and hierarchical nature of the design, as suggested by e.g. Logan (2010). For the modelling, the data was averaged by week and then divided into four separate monthly data sets and one data set including all months (June, July, August, September and whole period). The soil layer-specific flux data from the CE and IE groups were also averaged to subplot level and all rows containing NAs in soil temperature and CH_4 flux columns were omitted. The monthly data sets were further divided into irrigation, control and whole site groups. The models based on subtreatment groups included only the data from the whole study period and were not divided into monthly data sets. This was done in order to ensure an adequate amount of observations for the models and ensure higher reliability (n_{min}=4 observations in monthly subtreatment group data sets after omitting NAs). In addition, all data sets included subplot-specific (e.g. IA1, IA2 and IA3) measurements for preventing the models being based on overly influential observations which result from too small a number of observations in the data (Harrell 2015).

GLM was chosen as the model for it is often used for the estimations of the experimental effects and their significance on the studied response variable (Rutherford 2001; Logan 2010). Gaussian distribution family with identity link function was used in the models because the data contained negative values and were normally distributed. Each model was built first with second-order polynomials and an interaction term. Third-order polynomials were not used for reducing the possible over-fitting of the model caused by fit to the noise of the data (Harrell 2015). The models were fit by following the principle of parsimony, according to which the preferred model is as simple as possible for ensuring a better fit and generalisation to other environments and data sets. The model terms were selected with backward stepwise variable selection method where the least statistically significant terms were omitted from the model one by one and the model was re-run until there were only significant terms left ($p \leq 0.05$) (Guisan and Zimmermann 2000; Harrell 2015). The significance of the effect of the predictors on the response variable (CH_4 flux) and the goodness-of-fit statistics were tested using ANOVA with both type I (*anova()* in R) and type III-tests (*Anova()* in

R). The type III test was run due to the experimental design being unbalanced, although there is some dispute on which type to apply in ANOVA hypothesis testing of unbalanced designs (Langsrud 2003). Both ANOVAs included F-tests for the estimation of the statistical significance of the terms.

The fit of the models was estimated by calculating the explained deviance (D^2, formula: (null deviance - residual deviance)/null deviance), which tells how large amount of deviance the model explains with larger values marking better fit (Guisan and Zimmermann 2000). In addition to model fit estimation, the predictive performance of all models was assessed using leave-one-out cross-validation (LOOCV) method. In LOOCV, the data is divided into evaluation and calibration data by leaving one observation out in the calibration data and building the model based on it, and then predicting values of the response variable based on the built model and using the evaluation data that contains all observations. The method was repeated for the whole data so that every observation had a corresponding predicted value which could then be compared. Based on LOOCV, three different validation parameters were calculated, namely mean absolute error (MAE), root mean squared error (RMSE) and Pearson's correlation coefficient between the observed and predicted values. In this study, LOOCV was the preferred method of model validation because the data sets were too small ($n_{min} = 24$ observations in monthly main plot group data sets, $n_{max} = 341$ observations in whole site data sets containing all months) for dividing them into two separate evaluation and calibration data sets and the response variable was continuous (see Guisan and Zimmermann (2000)).

6 Results

6.1 Variation in soil moisture and soil temperature

Weather in Kenttärova was generally warmer and drier during the study period than the long-term monthly averages measured in the nearby weather station of Alamuonio (67°58'N, 23°41'E, circa 35 km from Pallas area, Pirinen et al. (2012) and Aurela et al. (2015)). In June, the air temperature was 1.2°C lower than the long-term average, after which the temperatures were approximately 4.9°C, 0.8°C and 4.7°C higher in July, August and September, respectively (Pirinen et al. 2012). The maximum daily air temperature was observed in July (25.1°C, 18.7.2018) and minimum in June (4.3°C, 7.6.2018). The precipitation amounts in Kenttärova were much lower than the long-term average, with differences of -57.1 mm, -74.1 mm, -70.0 mm and -46.9 mm in June, July, August and September, respectively (Pirinen et al. 2012). Days with no rain were observed every month and maximum precipitation amount of 30.4 mm was reached in August (3.8.2018, figure 8).

Over the whole measurement period from 7.6.—12.9.2018, soil temperature followed the

general changes in air temperature. Soil temperature varied between 4.21 (8.6.2018, CO3) and 21.76°C (1.8.2018, IO1) in the whole study site with a median of 11.60°C, mean of 11.96°C and standard deviation of 3.37. In the whole study site, the most common soil temperature value was 9.08°C (frequency n=220), while in the control site the value was the same but with frequency n=131 and in the irrigation site 14.52°C (frequency n=91, see histograms in Appendix F). Based on ANOVAs, changes in soil temperature were significantly affected by both main plots (A1: ***, AR1het: **) and subtreatments (A1: ***, AR1het: ns). In the irrigation site, the mean of the whole study period was 13.2°C ± 3.52 while that of control site was 10.7°C ± 2.62, indicating a 24% higher soil temperature in the irrigation site in relation

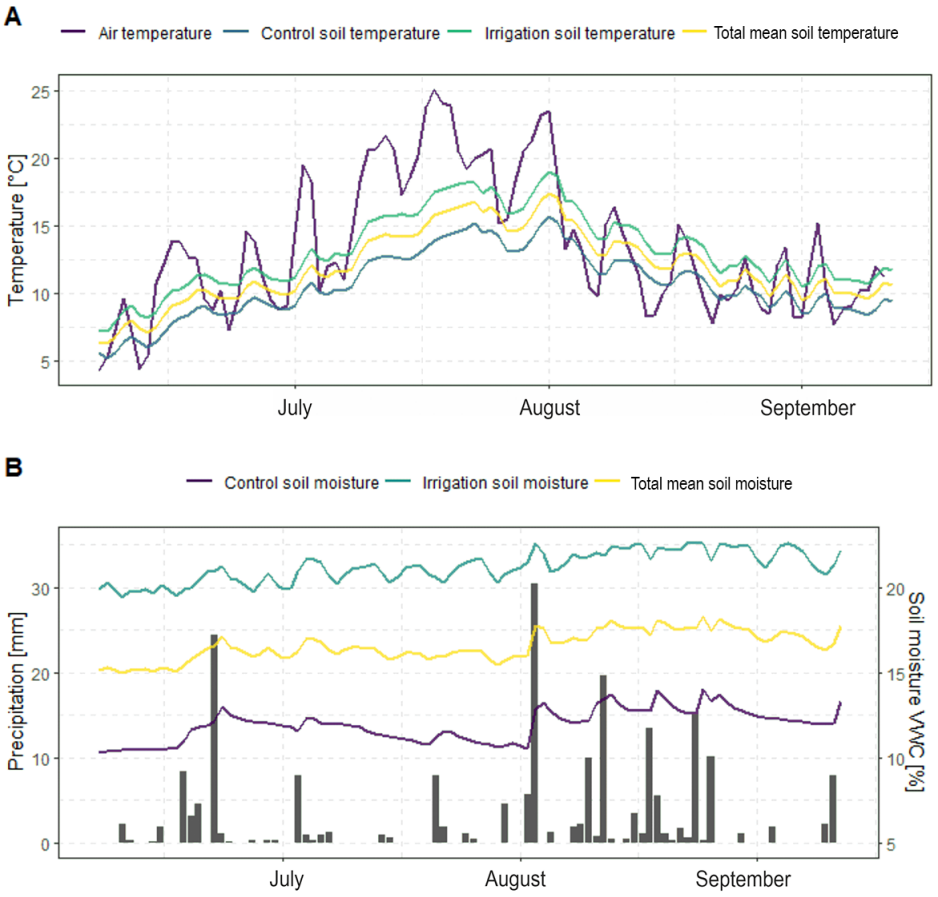

Figure 8: Variation in air and soil temperature and natural precipitation and soil moisture conditions during the study period. A: Daily mean air temperature (°C, purple) measured in the Kenttärova weather station (Finnish Meteorological Institute 2018b) and soil temperature averaged for the whole study site ("total mean soil temperature", yellow, plot n=25), control (blue, plot n=12) and irrigation (green, plot n=13) sites. Soil temperatures followed changes in air temperatures with a few days' lag. The highest temperatures in both air and soil were reached in July (air: 25.1°C 18.7.2018, soil: 21.2°C 31.7.2018) and the beginning of August (air: 23.5°C 1.8.2018, soil: 21.8°C 1.8.2018) while the lowest temperatures were observed in June (air: 4.3°C 7.6.2018, soil: 4.2°C 8.6.2018) and September (air: 7.7°C 3.9.2018, soil: 7.6°C 1.9.2018). Irrigation site consistently reached higher soil temperatures than the control site. B: Variation in daily mean natural precipitation (mm) and soil moisture (%VWC) averaged for the whole study site ("total mean soil moisture", yellow, plot n=26), control (purple, plot n=13) and irrigation (green, plot n=13) sites. Soil moisture followed changes in natural precipitation, especially during and after high precipitation events in June (24.4 mm, 22.6.2018) and August (30.4 mm, 3.8.2018). The highest soil moisture values were consistently observed in the irrigation site (whole period maximum irrigation: 44.3% 3.8.2018, control: 33.3% 19.8.2018).

to control site (table 2). In the subtreatment level, IO subplots had higher temperatures (***, IO-IE ns) in all pairwise comparisons. In addition, soil temperature was significantly higher in the irrigation site in all subtreatment comparisons (***), with the exceptions of comparisons between IA and CA and IA and CT groups ($p>0.05$). Within control site there were no significant differences in soil temperature between subtreatments, whereas within irrigation site significant differences were observed in all pairwise comparisons except that between IO and IE subplots.

Soil temperature varied significantly between months (***) in all experimental scales, the warmest month being July and coolest June. In the whole study site, the highest mean soil temperature was 14.22°C in July and lowest 8.9°C in June, with corresponding values being 15.64°C ± 2.88 and 10.01°C ± 2.47 in irrigation site, and 12.69°C ± 2.07 and 7.80°C ± 1.60 in control site. The differences between monthly soil temperatures were highly significant in the main plot level both between and within the main plots (table 2). However, according to ANOVA (AR1het), the effect of the treatments on soil temperature did not change signifi-

Table 2: Differences in soil temperature between paired treatment groups (I=irrigation, C=control, A=litter addition, E=litter and root exclusion, O=no additional manipulation and T=soil warming). Positive difference (diff.) values between the groups (diff = $temperature_{Imean}$ - $temperature_{Cmean}$), result from greater temperatures in irrigation site and vice versa. Positive values in percentage change (% change = ($temperature_{Imean}$ - $temperature_{Cmean}$)/|$temperature_{Cmean}$| *100) indicate a relative increase in soil temperature in the irrigation site as compared with control site. The significance of differences were determined with TukeyHSD multiple pairwise comparisons (see further details in Appendices E and G).

Time	**Whole period**		**June**		**July**		**August**		**September**	
Treatment	I	C	I	C	I	C	I	C	I	C
Mean	13.17	10.65	10.01	7.80	15.64	12.69	13.91	11.46	11.26	9.02
Median	13.22	10.32	9.54	8.07	15.71	12.80	13.49	11.21	10.13	8.98
Diff.	2.52		2.20		2.95		2.45		2.24	
% change	23.69		28.26		23.23		21.38		24.85	
Signif.	***		***		***		***		***	
Treatment	IA	CA	IA	CA	IA	CA	IA	CA	IA	CA
Mean	11.31	10.81	8.22	8.28	13.86	12.85	12.03	11.56	9.08	8.82
Median	10.72	10.47	8.74	8.38	14.31	12.78	11.99	11.34	9.09	8.73
Diff.	0.50		-0.01		1.00		0.47		0.26	
% change	4.60		-0.11		7.80		4.11		2.99	
Signif.	ns		ns		ns		ns		ns	
Treatment	IE	CE	IE	CE	IE	CE	IE	CE	IE	CE
Mean	13.90	10.41	10.69	7.48	16.33	12.57	14.69	11.21	12.12	8.72
Median	14.05	10.08	10.89	8.02	16.46	12.86	15.00	11.10	12.30	8.75
Diff.	3.49		3.21		3.76		3.48		3.40	
% change	33.55		42.97		29.91		31.06		38.98	
Signif.	***		***		***		***		***	
Treatment	IO	CO	IO	CO	IO	CO	IO	CO	IO	CO
Mean	14.17	10.66	11.08	7.68	16.74	12.65	14.79	11.55	12.19	9.26
Median	14.08	10.41	11.37	7.72	16.77	12.63	14.60	11.19	12.32	9.17
Diff.	3.51		3.40		4.09		3.24		2.93	
% change	32.95		44.28		32.36		28.03		31.61	
Signif.	***		***		***		***		***	
Treatment	IT	CT	IT	CT	IT	CT	IT	CT	IT	CT
Mean	12.95	10.72	9.68	7.90	15.27	12.72	13.83	11.50	11.31	9.25
Median	13.23	10.34	9.27	8.33	15.37	13.06	13.31	11.25	10.00	9.08
Diff.	2.23		1.78		2.55		2.33		2.06	
% change	20.80		22.59		20.03		20.22		24.55	
Signif.	***		**		***		***		ns	

cantly over months (interaction: ns). The soil temperature difference between the main plots was also clear in the subtreatment level in each month (***, figures 8 and 9 and table 2). The only exception was IA-CA comparison which did not show any significant differences in all months. In addition, soil temperature in the irrigation site was a little lower only in IA in comparison with CA in June. The largest variation in the monthly means was in IT, followed by IE and IO, all three of which had a standard deviation greater than 2.0 throughout the whole summer. For further details of descriptive statistics and pairwise comparisons of soil temperature, see Appendices E and G.

Soil moisture varied strongly between treatments. The range of soil moisture through the whole study period was 1.57–44.29%, the minimum occurring in 20.7.2018 (CO2) and max-

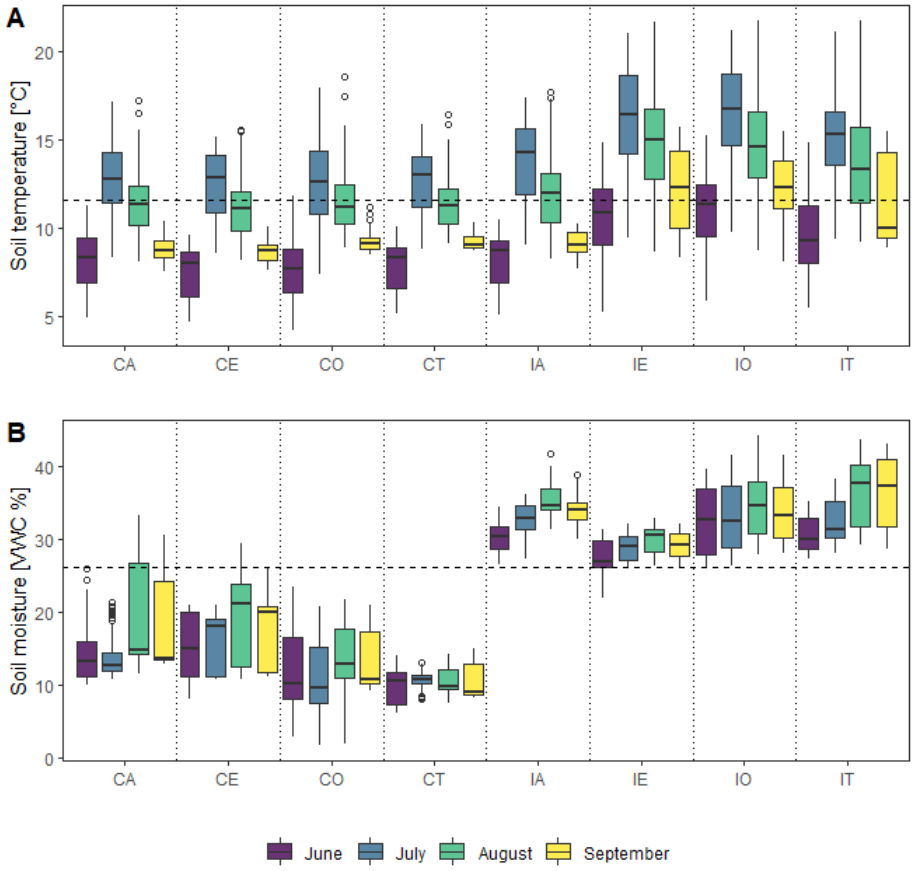

Figure 9: Soil temperature (A) and soil moisture (B) by month divided into subtreatment groups. Horizontal dashed lines represent the medians of the overall data in the whole study period over the whole study site (soil temperature: 11.6°C, soil moisture: 26.3%). Soil temperature varied along months and it was generally lower in both main plots in June and September, lower values reached more often in the control site. In terms of soil temperature, there was not very large variation between subtreatment groups within the control site per month. Larger variation among subtreatment groups occurred in the irrigation site along months, IA group having generally the lowest soil temperatures every month. Soil moisture was by far higher in the irrigation site, with all its subtreatment groups having most values above the overall median. IA consistently had highest values with small ranges, while the lowest soil moisture was observed in CT and CO, respectively. There was not much variation in soil moisture between months in all subtreatment groups, with the exception of IA, CA and IT which had varying ranges and medians along months. See details of the descriptive statistics of the variables in Appendix E.

imum 3.8.2018 (IO4) in the whole study site (figure 8). The most common values of soil moisture from the whole study period were 10.31% (frequency n=230) and 30.94% (frequency n=216), former also representing the most common value of control site and the latter of that of the irrigation site. The overall mean from the period was 23.15% ± 10.53. In the control site, soil moisture varied between 1.57 (20.7.2018, CO2) and 33.3% (19.8.2018, CA1) with 13.8% mean over the whole study period. The range in the irrigation site, on the other hand, was 22.0 (7.6.2018, IE3)–44.3% (3.8.2018, IO4) with 21.5% mean. According to ANOVAs and TukeyHSD, changes in soil moisture were significantly affected by main plots and the differences between them were highly significant (***) with approximately 18.6% VWC difference in the irrigation site. Thus, based on the overall means, soil moisture in the irrigation site was 134.5% higher than in the control site during the whole study period (figures 8 and 9 and table 3). In addition, subtreatments had significant effects and differences with each other in terms of their soil moisture means both within and between main plots. All differences between irrigation and control subtreatment groups were highly significant (***, table 3). Between treatment pairs, the lowest difference of 11.6% VWC was observed between IE and CE and highest between IT and CT with 23.4% VWC difference. Within irrigation site, IT had highest soil moisture mean, while IE had lower values in all pairwise comparisons (***). Moisture differences were significantly high within the control site between all subtreatment groups, highest moisture values occurring in CE, followed by CA.

Monthly changes in soil moisture were significant in all experimental levels (***). In the whole study site, monthly means reached their highest in August (24.90% ± 10.73) and lowest in June (21.48% ± 9.96). Monthly means of the irrigation site were consistently significantly higher than those of control site (***, figure 9 and table 3). According to ANOVAs, soil moisture in main plots did not vary very significantly according to months (interaction A1: *, AR1het: ns). The highest means were reached in August (I: 34.20% ± 4.33, C: 15.58% ± 6.17) and lowest in June (I: 30.35% ± 3.83, C: 12.60% ± 5.11, figures 8 and 9). Variation in soil moisture was higher in the control site which reached standard deviations greater than 4.45 every month while those of irrigation site had a maximum SD of 4.40 in September. High monthly soil moisture differences were consistently evident also in the subtreatment level, ANOVAs showing differing significance of both month and month-subtreatment interaction effects (A1: ***, AR1het: ns). Differences between the subtreatment pairs were highly significant every month (***, table 3). Groups in the control site experienced generally more fluctuations in soil moisture than those in the irrigation site, the latter of which showed a more consistent trend in increasing moisture until August, after which all except IT had a slight decrease. Similar to main plots, the highest soil moisture means in all subtreatments were generally observed in August while the range was large (figure 9). The largest variation in the monthly means were in IT, followed by IA and IO, all three of which had a standard deviation greater than 2.0 throughout the whole summer. The

lowest variation occurred in CT and IE over the summer with maximum SDs and ranges in June. For further details of the descriptive statistics and pairwise comparisons of soil moisture, see Appendices E and G.

Table 3: Differences in soil moisture between paired treatment groups. The difference (diff.) and percentage change (% change) between the groups were calculated with similar logic as with soil temperature (diff = $moisture_{Imean}$ - $moisture_{Cmean}$; % change = ($moisture_{Imean}$ - $moisture_{Cmean}$)/|$moisture_{Cmean}$| *100). The significance of differences were determined with TukeyHSD multiple pairwise comparisons (see further details in Appendices E and G).

Time	**Whole period**		**June**		**July**		**August**		**September**	
Treatment	I	C	I	C	I	C	I	C	I	C
Mean	32.45	13.84	30.35	12.61	31.91	12.78	34.21	15.58	33.51	14.53
Median	31.42	12.32	29.71	11.69	30.91	11.36	33.50	13.56	32.21	12.98
Diff.	18.61		17.74		19.13		18.63		18.99	
% change	134.49		140.73		149.61		119.56		130.69	
Signif.	***		***		***		***		***	
Treatment	IA	CA	IA	CA	IA	CA	IA	CA	IA	CA
Mean	33.21	15.96	30.07	14.47	32.92	13.64	35.36	18.83	34.11	17.51
Median	33.40	13.89	30.45	13.26	32.97	12.70	34.71	14.84	34.07	13.63
Diff.	17.26		15.91		19.28		16.53		16.60	
% change	108.14		109.97		141.33		87.80		94.80	
Signif.	***		***		***		***		***	
Treatment	IE	CE	IE	CE	IE	CE	IE	CE	IE	CE
Mean	28.81	17.22	27.10	15.26	28.86	16.29	29.94	19.45	29.22	17.79
Median	29.10	18.71	26.96	15.00	29.06	18.00	30.51	21.17	29.32	20.00
Diff.	11.59		11.84		12.57		10.49		11.43	
% change	67.31		77.62		77.13		53.91		64.25	
Signif.	***		***		***		***		***	
Treatment	IO	CO	IO	CO	IO	CO	IO	CO	IO	CO
Mean	33.61	12.30	32.52	11.29	33.16	11.13	34.77	13.94	33.94	13.10
Median	34.04	10.94	32.76	10.18	32.46	9.57	34.69	12.85	33.25	10.71
Diff.	21.31		21.23		22.03		20.83		20.85	
% change	173.32		188.03		198.01		149.48		159.29	
Signif.	***		***		***		***		***	
Treatment	IT	CT	IT	CT	IT	CT	IT	CT	IT	CT
Mean	33.78	10.40	30.67	9.85	32.29	10.63	36.58	10.66	36.65	10.21
Median	32.16	10.41	30.02	10.60	31.45	10.72	37.64	9.81	37.29	8.92
Diff.	23.39		20.82		21.66		25.92		26.45	
% change	224.99		211.39		203.71		243.30		259.16	
Signif.	***		***		***		***		***	

6.2 Variation in methane flux

During the whole study period, CH_4 flux remained negative, ranging from -643.89 (25.7.2018, CO1) to -38.55 $\mu g\ m^{-2}\ h^{-1}$ (8.8.2018, IT3) with a mean of -202.89 $\mu g\ m^{-2}\ h^{-1}$ and median of -185.76 $\mu g\ m^{-2}\ h^{-1}$ in the whole study site. The flux data were normally distributed and mostly skewed to left, most common value being -146.12 $\mu g\ m^{-2}\ h^{-1}$ (frequency n=57) in the whole study site and -271.36 $\mu g\ m^{-2}\ h^{-1}$ (n=25) in the control site and -146.12 $\mu g\ m^{-2}\ h^{-1}$ (n=34) in the irrigation site. The CH_4 flux in the irrigation site ranged between -328.76 (28.6.2018, IE2) and -38.55 $\mu g\ m^{-2}\ h^{-1}$ (8.8.2018, IT3) with -146.50 $\mu g\ m^{-2}\ h^{-1}$ mean and -145.08 $\mu g\ m^{-2}\ h^{-1}$ median while the uptake in the control site generally was significantly higher (i.e. fluxes were lower) with a range of -643.89 (25.7.2018, CO1) – -101.06 $\mu g\ m^{-2}\ h^{-1}$ (21.6.2018, CE3), -256.63 $\mu g\ m^{-2}\ h^{-1}$ mean and -241.41 $\mu g\ m^{-2}\ h^{-1}$ median (***, figure

10 and table 4). As with the main plots, the effect of subtreatment groups on CH_4 flux was highly significant (***) and the uptake rates were significantly lower (i.e. fluxes were higher) in all irrigation subtreatment groups (***).

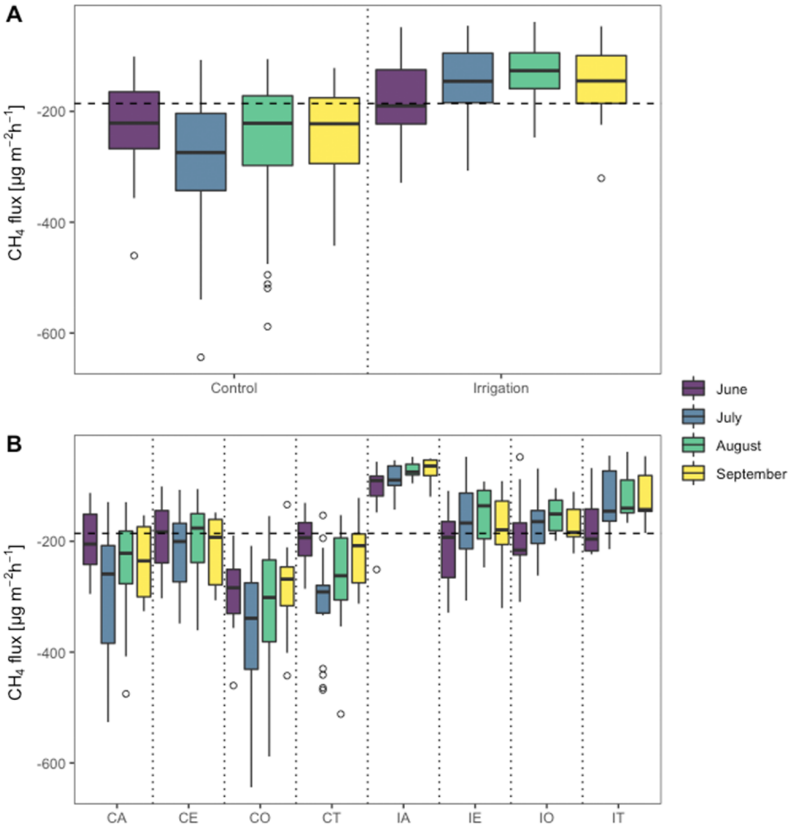

Figure 10: Variation in CH_4 flux between main plots (A) and subtreatment groups (B) by month. Fluxes were negative, indicating uptake of CH_4 from the atmosphere into the soil, through the whole study period and did not have large changes between months. In control site and its subtreatments, the lowest uptake rates were in June and highest in July, the latter of which had a larger range. In irrigation site and its subtreatments, sink decreased gradually from June to August, after which it slightly increased. Fluxes in irrigation site were higher than the overall median (-185.76 $\mu g\ m^{-2}\ h^{-1}$) from June to September while those of control site were consistently lower with some values reaching above the median. IA clearly had the lowest uptake rates which further decreased in September. Sink in CO, on the other hand, reached the highest values in July and August with large ranges. Most outliers were observed in the control site in CO and CT. See more details of the descriptive statistics of CH_4 flux in Appendix F.

Temporal changes in uptake rate varied according to treatment levels. In the scale of the whole study site, there was not high variation between the monthly means, and the differences between months and its effect were only of low significance or insignificant (A1: *, AR1: ns). The lowest mean uptake rate in the whole study site was in August with -190.31 $\mu g\ m^{-2}\ h^{-1}$ $\pm$ 101.26 and highest in July with -218.21 $\mu g\ m^{-2}\ h^{-1}$ $\pm$ 115.62. However, the month effect was stronger in the main plot level (ANOVA interactions between main plots and months ***), uptake rates being generally significantly lower in the irrigation site in comparison with the control site (table 4). The differences between monthly uptake rates within main plots were generally lower than between them (ns). In the irrigation site, the lowest uptake rates

were observed in August and highest in June, whereas in control site lowest uptake rates occurred in June and highest in July (table 4 and figure 10). The trend of lower uptake rates in the irrigation site was clear also in the subtreatment level every month (***) with the exception of CE which had lower mean uptake rate (-195.50 $\mu g\ m^{-2}\ h^{-1} \pm 61.57$) than IE (-207.80 $\mu g\ m^{-2}\ h^{-1} \pm 65.57$) in June, after which IE continued having significantly lower uptake rates for the rest of the study period (***, table 4). The effect of month varied according to ANOVA (A1: **, AR1: ns) but monthly changes in uptake rates varied significantly according to subtreatment (interaction A1: **, AR1: *). The highest mean uptake rates were consistently observed in CO (***) while IA had lowest rates reaching flux means greater than -87 $\mu g\ m^{-2}\ h^{-1}$ starting from July (***, figure 10 and table 4). For more details of the descriptive statistics and pairwise treatment comparisons of CH_4 sink and weekly statistics, see Appendices E and G.

Within the exclusion subtreatments (CE and IE), soil CH_4 sink varied more according to soil layer and main treatment than months. The CH_4 uptake rates were significantly affected by the soil layer (A1: ***, AR1: *), organic layers consistently having lower uptake rates than

Table 4: Differences in CH_4 flux between paired treatment groups. The difference (diff.) and percentage change (% change) between the groups was calculated with same logic as with the previous variables (diff = $flux_{Imean}$ - $flux_{Cmean}$; % change = ($flux_{Imean}$ - $flux_{Cmean}$)/|$flux_{Cmean}$| *100). The significance of differences were determined with TukeyHSD multiple pairwise comparisons (see further details in Appendices E and G).

Time	**Whole period**		**June**		**July**		**August**		**September**	
Treatment	I	C	I	C	I	C	I	C	I	C
Mean	-146.50	-256.63	-180.12	-223.01	-143.50	-285.91	-130.72	-248.41	-143.63	-239.17
Median	-145.08	-221.16	-190.06	-221.16	-145.68	-274.25	-126.58	-221.50	-145.08	-222.36
Diff.	110.13		42.90		142.41		117.69		95.55	
% change	42.91		19.24		49.81		47.38		39.95	
Signif.	***		ns		***		***		***	
Treatment	IA	CA	IA	CA	IA	CA	IA	CA	IA	CA
Mean	-84.92	-256.42	-112.35	-202.35	-86.85	-296.84	-71.08	-247.91	-72.62	-237.51
Median	-81.96	-223.23	-90.44	-205.05	-89.57	-259.01	-75.11	-221.60	-64.14	-235.36
Diff.	171.49		90.00		209.99		176.83		164.89	
% change	66.88		44.48		70.74		71.33		69.43	
Signif.	***		ns		***		***		***	
Treatment	IE	CE	IE	CE	IE	CE	IE	CE	IE	CE
Mean	-172.10	-206.42	-207.80	-195.50	-168.43	-217.05	-153.02	-196.20	-175.52	-217.36
Median	-167.06	-191.16	-192.96	-183.14	-167.06	-200.35	-135.99	-176.18	-179.43	-192.78
Diff.	34.32		-12.30		48.62		43.18		41.85	
% change	19.07		-6.29		22.40		22.01		19.25	
Signif.	*		***		***		***		***	
Treatment	IO	CO	IO	CO	IO	CO	IO	CO	IO	CO
Mean	-169.24	-327.01	-196.89	-297.44	-168.73	-363.23	-152.82	-318.52	-170.20	-283.91
Median	-172.27	-304.24	-216.02	-283.89	-164.57	-338.92	-150.78	-301.43	-184.01	-268.22
Diff.	157.77		100.55		194.50		165.70		113.71	
% change	48.25		33.80		53.55		52.02		40.05	
Signif.	***		***		***		***		***	
Treatment	IT	CT	IT	CT	IT	CT	IT	CT	IT	CT
Mean	-132.53	-262.36	-173.22	-199.48	-126.84	-309.61	-119.29	-259.87	-120.76	-221.18
Median	-145.08	-263.91	-195.95	-193.50	-145.68	-291.40	-140.25	-262.15	-142.68	-207.94
Diff.	129.83		26.26		182.77		140.57		100.42	
% change	49.48		13.16		59.03		54.10		45.40	
Signif.	***		***		***		***		***	

mineral layers (***, table 5) and layers in irrigation site having lower uptake rates than those in control site after June with insignificant changes in effect along months. Lowest mean uptake rates were observed in the organic layers in the irrigation site in August (-136.63 $\mu g\ m^{-2}\ h^{-1} \pm 39.3$), and highest in mineral layers in the control site in September (-238.08 $\mu g\ m^{-2}\ h^{-1} \pm 63.54$, see table 5). However, the difference between irrigation and control was not significant in the mineral layers. The differences between the layers both within and between the main plots were insignificant during all months and remained relatively constant, with the exception of June when the difference was lowest in the control site and September with highest difference of 60.34 $\mu g\ m^{-2}\ h^{-1}$ in the irrigation site (table 5). The largest significant

Table 5: Differences in CH_4 flux between organic (O) and mineral (M) layers of the IE and CE groups. Difference (diff.) between the layers within main plots was calculated by subtracting the mean mineral layer flux value from that of organic (diff = $flux_{Omean}$ - $flux_{Mmean}$), resulting in positive values when the flux was greater than in the organic layer and vice versa. If the values of percentage change (% change = ($flux_{Omean}$ - $flux_{Mmean}$)/|$flux_{Mmean}$| * 100) between the layers within main plots are positive, it indicates a relative decrease in CH_4 sink in the organic layer as compared with mineral layer. In comparisons between main plots, differences and percentage change were calculated with similar logic as with other variables (diff = $flux_{I,O,mean}$ - $flux_{C,O,mean}$; % change = ($flux_{I,Omean}$ - $flux_{C,Omean}$)/|$flux_{C,Omean}$| * 100). The significance of differences were determined with TukeyHSD multiple pairwise comparisons (see further details in Appendices E and G).

Whole site

Time	**Whole period**		**June**		**July**		**August**		**September**	
Layer	**O**	**M**	**O**	**M**	**O**	**M**	**O**	**M**	**O**	**M**
Mean	-172.37	-209.71	-190.93	-212.63	-175.39	-217.04	-157.02	-194.99	-174.09	-223.25
Median	-164.41	-205.36	-183.51	-192.96	-172.18	-220.73	-152.89	-185.35	-166.88	-209.77
Diff.	37.34		21.70		41.65		37.97		49.16	
% change	17.81		10.20		19.19		19.47		22.02	
Signif.	***		ns		ns		ns		ns	

Irrigation

Time	**Whole period**		**June**		**July**		**August**		**September**	
Layer	**O**	**M**	**O**	**M**	**O**	**M**	**O**	**M**	**O**	**M**
Mean	-154.53	-193.28	-193.61	-223.76	-151.91	-190.04	-136.63	-171.93	-148.09	-208.43
Median	-157.42	-197.19	-181.07	-197.65	-162.64	-211-33	-119.67	-159.26	-147.04	-197.19
Diff.	38.75		30.16		38.13		35.30		60.34	
% change	20.05		13.48		20.06		20.53		28.95	
Signif.	*		ns		ns		ns		ns	

Control

Time	**Whole period**		**June**		**July**		**August**		**September**	
Layer	**O**	**M**	**O**	**M**	**O**	**M**	**O**	**M**	**O**	**M**
Mean	-189.84	-223.35	-188.26	-202.73	-197.56	-236.55	-177.42	-214.98	-200.10	-238.08
Median	-180.21	-209.26	-185.33	-180.33	-187.55	-222.14	-161.85	-193.84	-172.86	-222.36
Diff.	33.51		14.47		38.98		37.56		37.97	
% change	15.0		7.14		16.48		17.47		15.95	
Signif.	ns		ns		ns		ns		ns	

Organic

Time	**Whole period**		**June**		**July**		**August**		**September**	
Treatment	**I**	**C**	**I**	**C**	**I**	**C**	**I**	**C**	**I**	**C**
Diff.	35.31		-5.35		45.65		40.79		52.01	
% change	181.40		-2.84		23.11		22.99		25.99	
Signif.	*		ns		ns		ns		ns	

Mineral

Time	**Whole period**		**June**		**July**		**August**		**September**	
Treatment	**I**	**C**	**I**	**C**	**I**	**C**	**I**	**C**	**I**	**C**
Diff.	30.07		-21.03		46.51		43.05		29.65	
% change	13.46		-10.37		19.66		20.03		12.45	
Signif.	ns		ns		ns		ns		ns	

differences were found between organic layer in the irrigation site and mineral layer in the control site (***). Within the main plots, only difference between organic and mineral layer in the irrigation site was significant (*).

6.3 Variable correlations

According to the correlation analyses, soil CH_4 flux had significantly high positive correlation with soil moisture over the whole study period (r=0.65 ***, figure 11). In other words, increases in soil moisture levels subsequently led to significant decreases in soil CH_4 sink over the study period. Correlation between CH_4 flux and soil temperature, however, was small and statistically insignificant (r=0.016 ns), indicating that changes in soil temperature did not lead to a significant change in CH_4 sink. Because the correlation between soil moisture and soil temperature was r<|0.70| (r=0.29 ***), they were not considered multicollinear. In the treatment scales over the whole study period, correlations between CH_4 flux and soil moisture were highly significant (***) in both main plots (C: r=0.37 , I: r=0.41) and in all subtreatment groups with the exception of IE (**), CA, CO and CT (ns, figure 12). In contrast to all other subtreatment groups, CT and IE had negative correlations (CT r=-0.12 and IE r=-0.46 **), indicating that increases in soil moisture led to increases in CH_4 sink in those groups. The highest correlations in the irrigation site were in IT (r=0.6 ***) and CE in the control site (r=0.81 ***). In terms of soil temperature, both main plots had negative correlations (C: r=-0.45 ***, I: r=-0.18 **) which indicated a higher positive dependence of CH_4 sink on soil temperature in the control site (figure 12). In the subtreatment level, soil

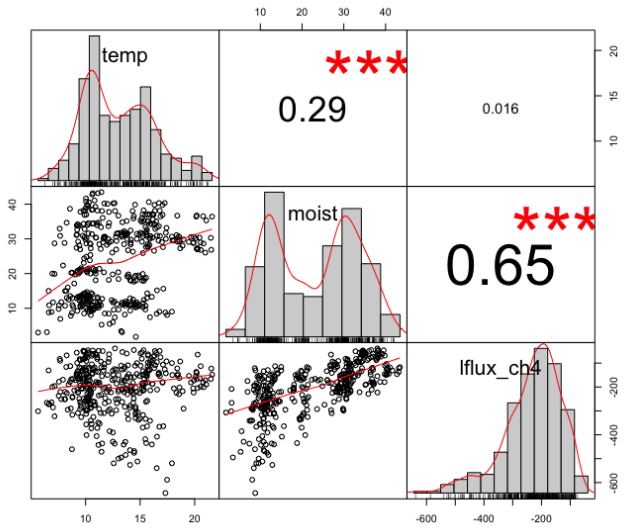

Figure 11: Correlation matrix of the measured variables. Correlation analyses were carried out using Pearson's correlation coefficient. Methane flux (lflux_ch4, $\mu g\ m^{-2}\ h^{-1}$) was significantly positively correlated with soil moisture (moist, VWC %), or in other words, soil CH_4 uptake rate correlated negatively with soil moisture. Correlation between soil temperature (temp, °C) and CH_4 uptake was not significant. Soil temperature and soil moisture were also significantly positively correlated.

temperature correlated significantly with CH_4 flux only in CA, CO and CT, meaning that measured CH_4 uptake rate in CE and all subtreatment groups in the irrigation site did not significantly follow changes in soil temperature and vice versa.

Correlation between CH_4 flux and soil moisture in the exclusion data set was highly significant but somewhat lower than in the pooled data with all subtreatments included (r=0.4 ***). Soil moisture in both layers had significant positive correlations with CH_4 flux, and negative ones with CH_4 sink, in the scale of the whole study site, but when divided into main plots moisture in both layers had significant negative correlations with flux (mineral r=-0.46 **, organic r=-0.33 *) in the irrigation site, the latter indicating an increase in CH_4 sink with an increase in soil moisture (figures 12 and 13). The opposite was true for the control site, in which soil moisture had high positive correlations (mineral: r=0.82 ***, organic: r=0.68 ***), indicating decreases in sink with increases in soil moisture. In contrast to soil

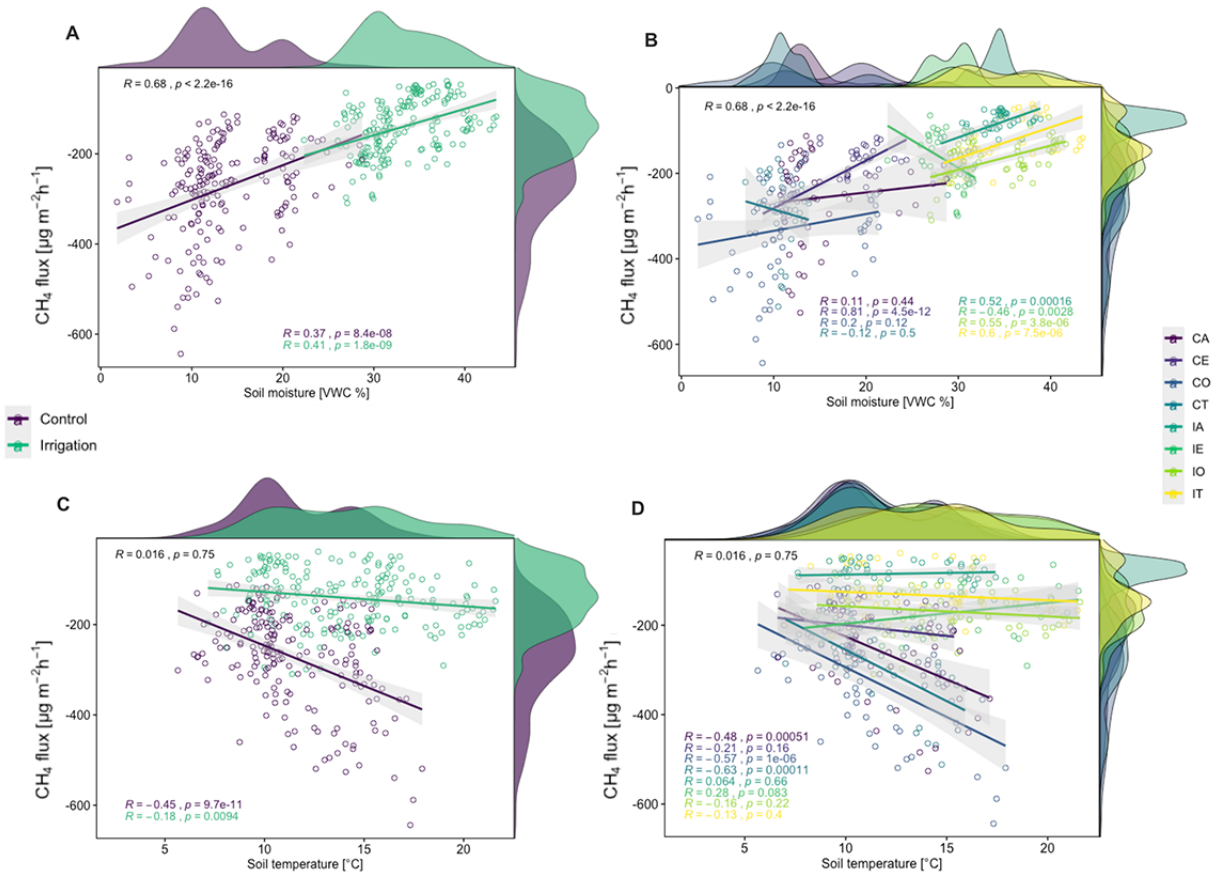

Figure 12: Correlations and frequency densities of the measured variables with linear regression trends in main plots (A and C) and subtreatment groups (B and D) over the whole study period. The plots include lines fit to linear regression at 95% confidence level. Soil moisture had high correlations with CH_4 uptake rate in both main plots and nearly all subtreatment groups. Soil temperature in general was not significantly correlated with CH_4 uptake rate but had higher correlations in the control site than in the irrigation site in both main plot and subtreatment level, with the exception of CE. Correlations between soil temperature and flux were negative in all except IA and IE, indicating decreases in sink by increases in soil temperature in the latter groups.

moisture, soil temperature had higher overall correlations with CH_4 flux than in the pooled data (r=0.19 *). However, temperature only had a significant correlation in organic layers (r=0.24 *). In the main plot level, soil temperature had relatively low negative correlations with CH_4 flux, or in other words low positive correlations with CH_4 sink, in both layers in the control site (ns), while the corresponding values in the irrigation site were both positive and higher (mineral r=0.31 and organic r=0.29), indicating negative correlations with CH_4 sink. In the soil layer data, correlation between soil temperature and soil moisture was higher than in the pooled data (r=0.42 ***). See the full correlation matrix of soil layer data in Appendix H.

In the temporal scale, soil moisture had positive and relatively high correlations with flux

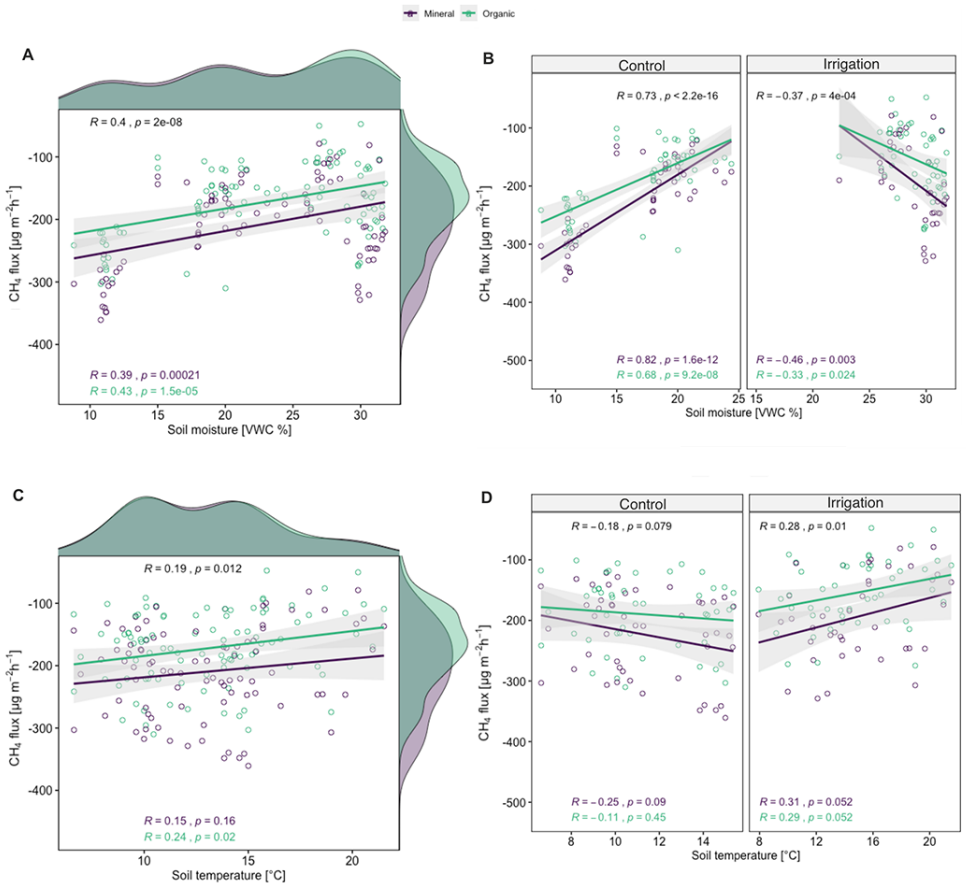

Figure 13: Correlations and frequency densities of the measured variables in the whole study site (A and C) and main plots (B and D) over the whole study period, divided into organic and mineral layers from CE and IE subtreatments. The plots include lines fit to linear regression at 95% confidence level. Soil moisture had significantly high positive correlation with CH_4 flux in general, but also in both layers with higher correlation in the organic layer. In other words, soil moisture correlated negatively with CH_4 sink. Correlation in the control site was higher and positive while irrigation site had a lower negative correlation, indicating strong decreases in sink with increases in soil moisture in control site and weak increases in sink with increases in soil moisture in irrigation site. In both sites, soil moisture in mineral layers had higher correlations with higher significance than in organic layer. Soil temperature had a significant and relatively low correlation with CH_4 flux in the whole study site, temperature in organic layers having higher correlation and significance. Correlations were also higher in the irrigation site in both layers.

in general, highest correlations occurring in July in both main plots (whole site r=0.75 ***, C: r=0.43 ***, I: r=0.49 ***). In other words, soil moisture correlated negatively with CH_4 uptake rate every month. Between the main plots, irrigation site had higher correlations in all months except in August. In the subtreatment level, there was more variation in the correlations between soil moisture and CH_4 sink along months (figure 14). In contrast to other treatments, IE had high negative correlations between soil moisture and flux in all months, ranging from -0.59 to -0.73, also indicating high positive correlations with CH_4 sink. The strong negative correlations of IE held true also in both its organic and mineral layers every month, ranging from -0.86 to -0.37 (organic) and -0.59 to -0.71 (mineral) but were mostly insignificant or of low significance. Highest correlations of organic layers in IE occurred in September (r=-0.86 *) and August in mineral layers (r=-0.71 **). Also, correlations with flux were negative in CT in June, August and September, the latter having almost perfect correlation of -0.99 (*) and all of them showing very strong positive correlations with CH_4 sink. The positive correlation trends between soil moisture and flux in CE were consistent also in both its organic and mineral layers, the coefficients of which ranged from 0.37 to 0.93 (organic) and 0.66 to 0.96 (mineral), the mineral layer having significantly stronger correlations than the organic layer. The strongest correlations of organic layers in CE were found in September (0.93 **) and those of mineral layers in July (0.96 ***), both indicating strong negative correlations between soil moisture and CH_4 sink.

Soil temperature had low, mostly statistically insignificant and negative correlations with CH_4 flux during the study period, indicating low positive correlations with CH_4 sink. The highest correlations between soil temperature and flux in the whole study site occurred in July (r=0.19 *) while in the control site highest correlations were in August (r=-0.6 ***) and in the irrigation site in September (r=-0.56 **). However, as with soil moisture, there was more temporal variation in the subtreatment level (figure 14). In general, there were more positive correlations between temperature and flux in June in nearly all subtreatment groups, after which they turned mostly negative until August. In other words, soil temperature correlated mostly negatively with CH_4 sink in June and positively in July and August. IE had low positive correlations between temperature and flux every month while those in CO remained negative, meaning that soil temperature in IE correlated negatively with CH_4 sink and in CO positively. Both layers in IE had very weak insignificant correlations every month, mineral layer showing stronger correlations ranging from 0.06 to 0.47 while those of organic layer ranged from 0.12 to 0.36, both indicating negative correlations with uptake rates. The highest correlations were observed in the control site and especially in CT and CO which had minimum correlations of $|0.32|$. Similar trend was observed also in both layers of CE, except in organic layers in September (0.91 *). The correlations of CE layers ranged from 0.15 to -0.91 in organic and 0.26 to -0.77 in mineral layer, highest correlations of both layers found in September. See temporal correlations of soil layers in Appendix H.

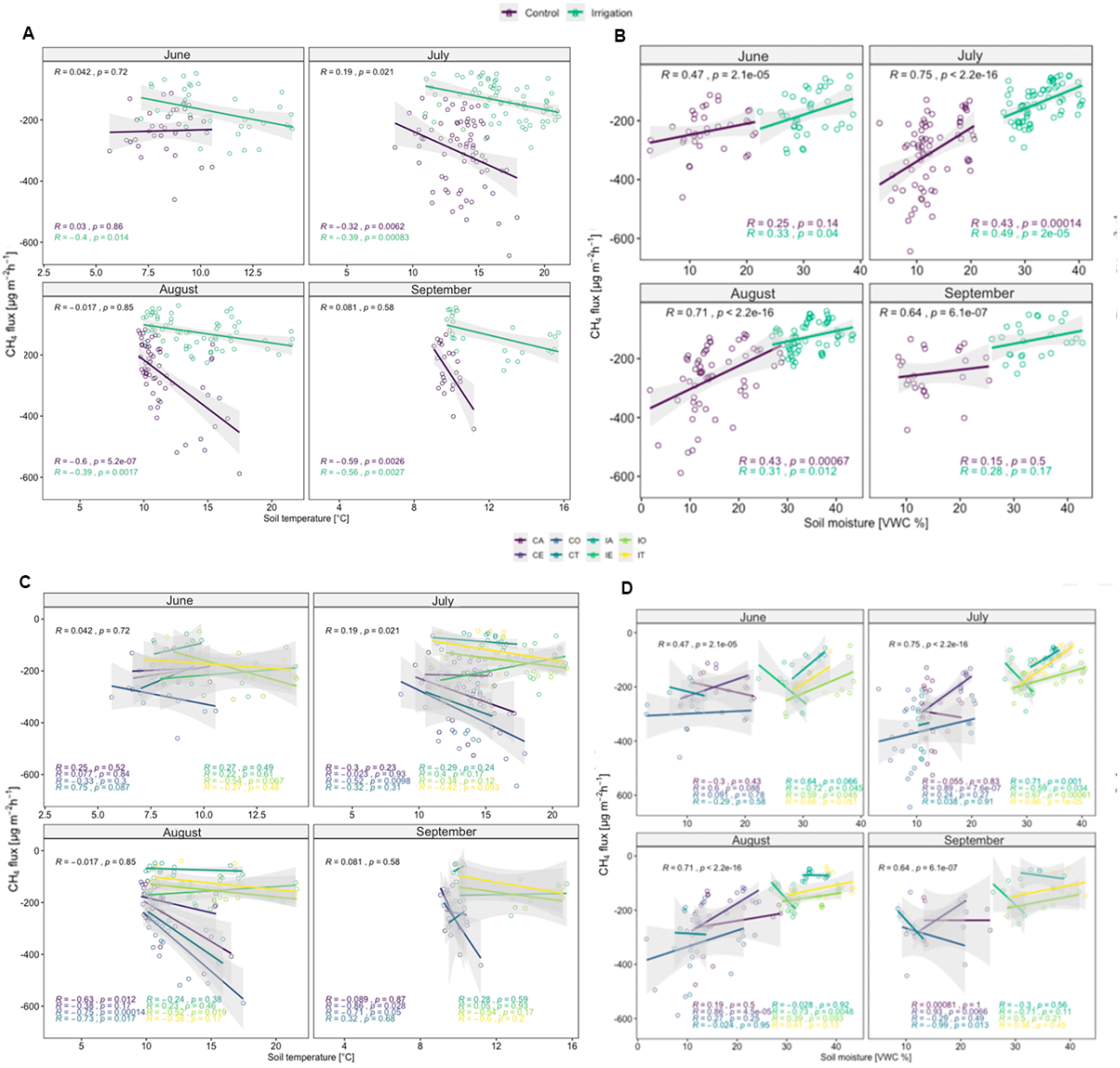

Figure 14: Correlations between the variables, divided into months by main plots (A and B) and subtreatment groups (C and D). The plots include lines fit to linear regression at 95% confidence level. Soil moisture correlated strongly with flux in all months, especially in the irrigation site. In both main plots, an increase in soil moisture led to decrease in uptake rate every month. Correlations were lowest in September and highest in July in both sites. In the subtreatment level, there was more variation in the temporal correlation trends. Soil temperature had generally low negative correlations with flux with low or no significance in all months, irrigation site having higher correlations in June and July, after which soil temperature in control site had stronger correlations until September. Correlation in the whole study site was highest in July and lowest in August. Control site in general had more variation in the correlation trends between soil temperature and flux and thus soil temperature and uptake rate.

6.4 Modelled relationship between methane flux and treatments

The significance of soil moisture as a predictor in the GLMs with CH_4 flux as the response variable varied in both temporal and experimental scales. The fit of the models was generally relatively low with highest D-squared values reached in the whole study site (max D^2=60 in August) and CE (D^2=0.78) and lowest in the control site (min D^2=0.06 in June) and irrigation site (min D^2=0.15 in July, table 6). All the models were also relatively poor in their predictive performance, with LOOCV-predictions not meeting the actual observations well (see Appendix I). In addition, the confidence intervals were shown to be relatively small but did not seem to include most of the actual observations (figure 15). The best predictive performance, however, was found in the IA (MAE=20.66 and RMSE=31.75) and CE (MAE=23.71 and RMSE=30.76) models. Models of the whole study site in whole study period (MAE=82.83 and RMSE=140.39) and control site in July (MAE=81.10 and RMSE=95.30) were most unable to predict fluxes reliably, possibly due to large amount of outliers which also may have raised the RMSE values. Soil moisture was highly significant in all models based on the whole study site (***) with some exceptions shown in the type III ANOVA (ns in August and whole study period). This was in agreement with the three-way ANOVA (AR1) which showed high significance for soil moisture in the level of the whole study site (***), but with significant interaction between soil moisture and month (*) which was not so apparent in the GLMs. The trends shown by the models were positive, indicating relatively clear decreases in uptake rates by increases in soil moisture (figure 15). Soil temperature was also included in all those models with varying significance and showed mainly negative flux response trends.

Models differed between the main plots as well. Irrigation models had soil moisture as a significant term only in June, July and whole study period while soil temperature was included in all models with high variation in significance. The June model showed a positive relationship between soil moisture and CH_4 flux and thus a negative relationship with CH_4 sink, while that of July and the whole period showed a curvilinear relationship with an increasing trend until approximately 30–32% of soil moisture, after which the flux had a more decreasing trend with increases in soil moisture (figure 15). In other words, CH_4 sink response had a decreasing trend in lower soil moisture levels and increasing in higher levels. In the control models, soil moisture was included in all models and had a high temporal variation in its significance from statistically insignificant (ns) in June and September to highly significant (***) in August and whole study period. Models for June, July, August and whole study period predicted a positive trend while that of September had a negative curvilinear response with decreasing flux by increases in soil moisture until approximately 15% of soil moisture, followed by positive increases in flux response. Therefore, the trend for CH_4 sink was negative until September in control site and the curvilinear response of September model was positive. A negative curvilinear response was also found with soil

temperature as the only predictor in the September irrigation model where the fluxes decrease and sink increases by increases in soil temperature until circa 13°C, followed by an increasing trend in flux and a decreasing trend in sink by increases in soil temperature. The response

Table 6: Goodness of fit and predictive performance of the models. Statistics of the whole study site and main plots were divided into months and the whole study period (all) while the subtreatment models were solely based on data from the whole study period. Depending on the model, included terms were soil moisture (moist), soil temperature (temp) and their interaction. If the term was not included in the model, it is marked with '-'. In some models, the two ANOVAs (type I and type III tests) showed differing significance levels of the terms, thus marked as type I/type III. D^2 is deviance squared, MAE is the mean absolute error and RMSE root mean squared error and r is the Pearson's correlation coefficient.

Whole site

Time	**June**	**July**	**August**	**September**	**All**
Moist signif.	***	***	***/ns	***	***/ns
Temp signif.	*	*	***	*	***
Interaction	-	-	**	-	***
D^2	0.29	0.58	0.60	0.50	0.51
MAE	55.68	60.38	59.01	55.40	82.83
RMSE	68.91	77.10	71.99	67.40	140.39
r	0.48	0.74	0.75	0.65	0.09

Irrigation

Time	**June**	**July**	**August**	**September**	**All**
Moist signif.	*	***/**	-	-	***
Temp signif.	*	ns/**	**	***	ns/*
Interaction	-	**	-	-	*
D^2	0.25	0.39	0.15	0.55	0.21
MAE	57.19	40.30	37.66	36.85	46.78
RMSE	67.08	53.66	45.56	43.70	56.37
r	0.37	0.45	0.33	0.66	0.39

Control

Time	**June**	**July**	**August**	**September**	**All**
Moist signif.	ns	**	***/**	ns	***
Temp signif.	-	*	***	***	***
Interaction	-	-	-	-	-
D^2	0.06	0.26	0.43	0.48	0.28
MAE	55.19	81.10	70.42	57.40	69.07
RMSE	73.80	95.30	86.98	65.66	84.72
r	0.06	0.41	0.60	0.56	0.51

Subtreatments

Treatment	IA	CA	IE	CE	IO	CO	IT	CT
Moist signif.	***	-	**	***/**	***	-	***	-
Temp signif.	-	**	*	**	-	***	ns	***
Interaction	-	-	-	*	-	-	-	-
D^2	0.46	0.20	0.31	0.78	0.30	0.27	0.59	0.36
MAE	20.66	73.35	44.04	23.71	34.52	76.18	27.88	58.54
RMSE	31.75	86.54	53.88	30.76	43.65	91.50	35.96	72.20
r	0.48	0.36	0.45	0.86	0.50	0.47	0.72	0.50

of flux was negative linear in August, indicating increases in uptake rate by increases in soil temperature. The effect of soil temperature and the high variation of its significance was apparent in models based on both sites but also in three-way ANOVA (AR1) that included main plots, soil temperature and months as independent variables, the latter of which showed

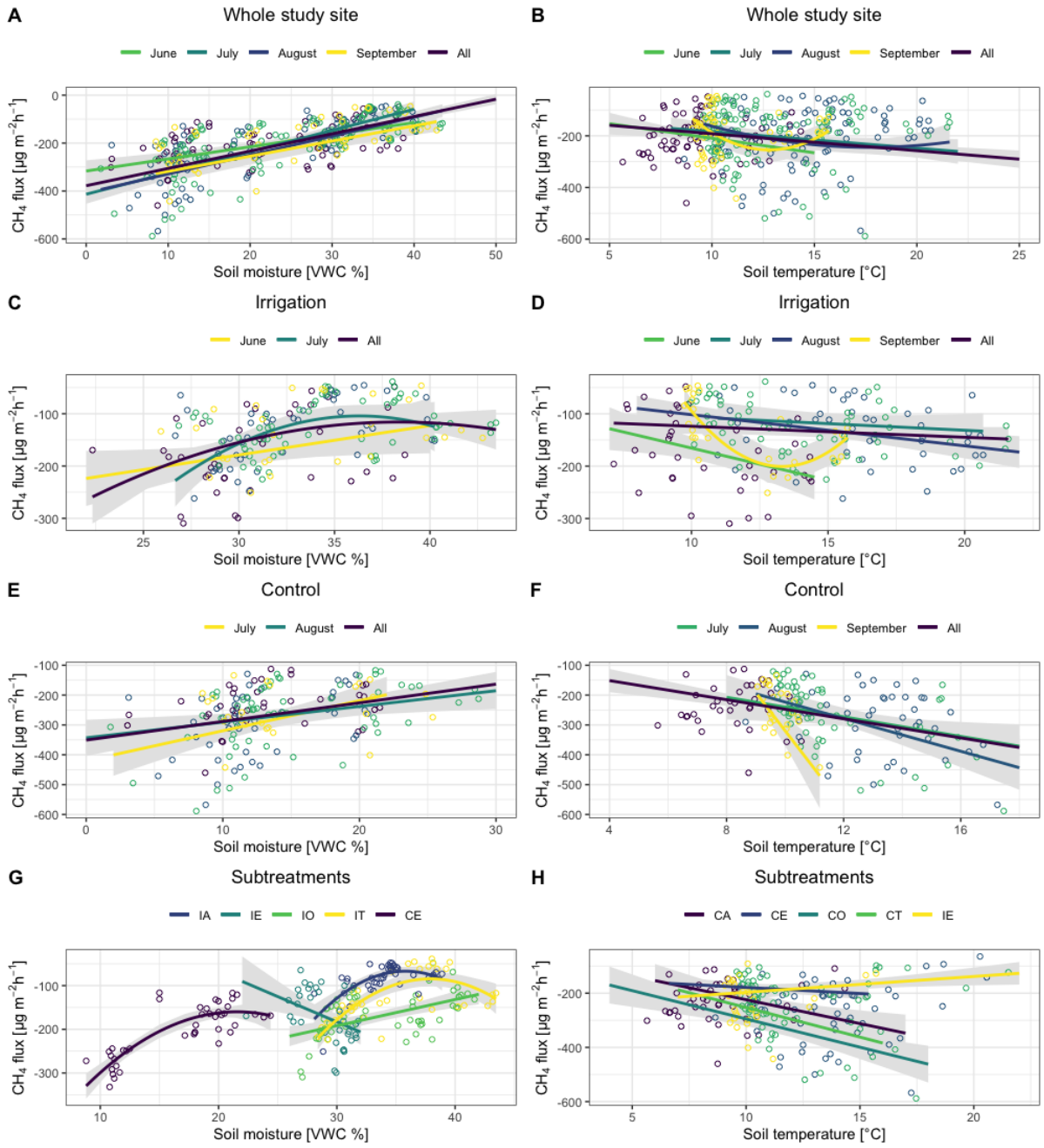

Figure 15: Response curves of CH_4 flux with soil moisture and soil temperature as significant predictors in GLMs. The confidence level is at 95%, meaning that 95% of the predicted values should be located within that area. The points and their colours represent either the corresponding monthly or subtreatment group observations of each data set used in the full models. Plots C, E and F include also data points of those months that did not include the predictor term in question in the models. In plots A, C, E and G, only models that had soil moisture as a significant predictor were included with soil temperature set at its mean. Plots B, D, F and H include models that had soil temperature as a significant predictor term and show its effect on CH_4 flux with soil moisture set at its mean. Subtreatment groups were modelled using the full monthly data and are thus in the same plot.

significant interaction effects with main plots (***) and months (**) separately and with main plots and months together (*). This indicates a varying and relatively complex effect pattern of soil temperature on CH_4 uptake rate along different spatiotemporal scales.

In the subtreatment level, soil moisture was generally highly significant over the whole study period, with the exception of CA, CO and CT, the models of which did not include the term. The latter models had significant soil temperature terms which affected the uptake rates primarily by increasing them by increases in temperature (i.e. decreases in fluxes, figure 15). The high significance was further affirmed in three-way ANOVA (AR1) containing subtreatment groups, soil temperature and months, where the interaction between subtreatment groups and soil temperature was highly significant, indicating significant changes in the subtreatment group-specific effects by changes in soil temperature (***). The temporal variation in the significance of soil temperature was also shown in ANOVA with a significant interaction with months (**). Soil moisture had a varying response in CH_4 flux with CE, IA and IT models showing positive curvilinear relationships while IO had a positive linear and IE a negative linear trend. Thus, IE was the only treatment to show a linear negative response to increases in soil moisture and to include a significant soil temperature term showing a positive response. The model term results somewhat differed from ANOVA (AR1) that included subtreatments, soil moisture and month, where the interaction of subtreatments and soil moisture was not significant which would indicate that there were no significant changes in the effect of soil moisture on CH_4 uptake rate as influenced by the different subtreatments. In other words, the soil moisture effect would not change in significance between subtreatments.

The interaction terms between soil moisture and soil temperature were included in only some of the models. However, according to three-way ANOVAs (AR1) with soil moisture, soil temperature and treatment level as independent variables, only the whole study site had a significant interaction effect (***). In all models, the interactions were clearly visible with non-parallel and intersecting response lines but seemed to vary according to the experimental level by which the model was built (figure 16). In the whole study site, higher soil moisture levels seemed to have a stronger positive effect on CH_4 flux at higher soil temperatures while lower moisture levels had stronger increasing effect at lower temperatures. In other words, uptake rate strongly decreased in both higher and lower soil moisture and temperature levels. Higher soil temperatures seemed to increase the effect of soil moisture on flux especially at soil moisture levels above approximately 25–30% in both whole site models. Similar trend was visible in the CE model but with a curvilinear relationship and the intersect with increasing effect of higher temperature on soil moisture effect occurring at circa 20%. The opposite was true for both irrigation models based on July and whole study period: until approximately 30–31% of soil moisture, high soil temperature together with increasing soil moisture had the highest flux responses, after which lower temperatures had strongest increasing impact

on the effect of soil moisture on CH_4 flux while higher temperatures had the opposite effect. Thus, the interaction relationships showed that the main effect of soil moisture on CH_4 uptake rate cannot be estimated without taking into account the interacting effect of soil temperature on soil moisture in the case of those five models.

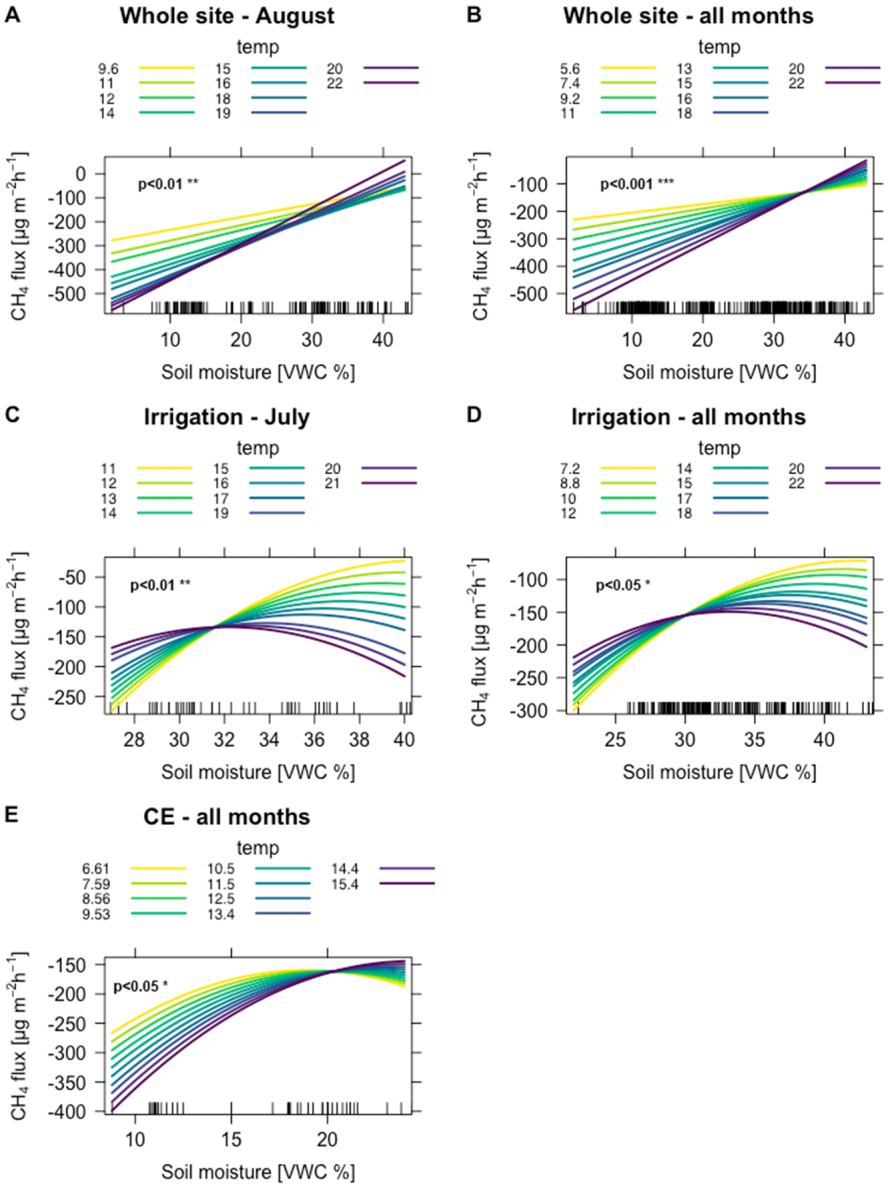

Figure 16: Effect plots of the interaction terms between soil moisture and soil temperature and their effect on CH_4 flux. All interaction terms shown were significant in the models in question (see table 6). "temp" in the plots refers to soil temperature in °C. The significance levels of the interaction terms in each model are included in the plots. The interaction trends were relatively similar in the models based on whole study site and CE group where soil moisture had strongest effect on CH_4 flux in lower soil temperatures until approximately 20–30% of soil moisture, after which higher soil temperature increased the effect of soil moisture on CH_4 flux. In other words, lower temperatures led to decreases in sink in lower soil moisture levels while higher temperatures in higher soil moisture levels resulted in more effective decreases in sink. Models of the irrigation site, on the other hand, had the opposite trend with lower temperatures increasing the soil moisture effect on flux after the intersect.

7 Discussion

The soil in this study was a methane sink with consistent negative values through the whole study period from 15.6 to 11.9.2018. Thus, the study failed to reproduce a similar CH_4 emission event as found in a significantly wet study period observed by Lohila et al. (2016). However, the timing of lowest uptake was similar to their study where positive fluxes were observed for multiple months starting from mid-August (max 92 $mg\ m^{-2}\ d^{-1}$). In this study, uptake rates reached by far higher values and a larger range than most studies located in boreal upland forests (table 7). However, there were some possible outliers in the control flux data, especially the all time minimum of -643.89 $\mu g\ m^{-2}\ h^{-1}$ (ca. -15.4 $mg\ m^{-2}\ d^{-1}$), which may have contributed to the large difference to the other boreal forest methane flux studies. It is also noteworthy that most studies regarding soil methane fluxes in boreal upland forest environments have been carried out in regards of methane consumption instead of methane production which was the perspective of this study.

Table 7: Summary of selected methane flux studies conducted in a number of boreal upland forest environments. The table includes measurements of CH_4 flux expressed as $mg\ m^{-2}\ d^{-1}$, so some of the values reported by different studies, such as this, were converted to daily flux unit for easier comparison between studies. Values of fluxes are either as ranges from min to max or average. The shown values of this study include minimum (CO, July, n=24) and maximum (IA, August, n=15) monthly averages of the observed fluxes due to possible outliers in the data. All flux measurements were carried out using chamber method. The study periods vary between June and October.

Author(s)	**Flux** ($mg\ m^{-2}\ d^{-1}$)	**Location**	**Forest type**
This study	-8.7 to -1.7	Kittilä, Finland 67°59'N, 24°14'E	coniferous
Lohila et al. (2016)	-2.3 to 92.0	Kittilä, Finland 67°59'N, 24°14'E	coniferous
Savage et al. (1997)	-2.6 to 0	Thompson, Manitoba, Canada 55°40'N, 97°52'W	coniferous/ deciduous
Gulledge and Schimel (2000)	-0.50	Fairbanks, Alaska, USA 64°45'N, 148°18'W	coniferous/ deciduous
Saari et al. (1998)	-2.13	central Finland 62°39'N 27°0'E	coniferous
Flessa et al. (2008)	ca. -1.6	Krasnoyarsk Krai, Russia 67°29'N 86°25'E	coniferous/ deciduous
Billings et al. (2000)	-0.95 to -0.10	Fairbanks, Alaska, USA 64°45'N, 148°18'W	coniferous/ deciduous
Whalen et al. (1991)	-1.81 to 0	Fairbanks, Alaska, USA 64°45'N, 148°18'W	coniferous/ deciduous
Klemedtsson and Klemedtsson (1997)	ca. -0.9 to -0.1	Gårdsjön, Sweden 58°04'N, 12°01'E	mixed coniferous/ deciduous
Pihlatie et al. (2008)	ca. -1.9	Hyytiälä, Finland 61°50'N, 24°17'E	coniferous

7.1 Relationship between soil moisture and methane flux

The experiment successfully created significant differences in soil moisture between control and irrigation site. In comparison with the year 2011 during which the large methane emissions were observed in Kenttärova, soil moisture reached by far higher values in year 2018:

according to Lohila et al. (2016) (supporting information file), soil moisture at 10 cm depth in 2011 was 19–26% whereas this study observed values between 1.6–44.3%, the highest values consistently found in the irrigation site, as expected. In addition, the summer in 2018 was exceptionally dry which led to significantly lower natural precipitation amounts and, via evapotranspiration, lower soil moisture especially in the control site (e.g. Seneviratne et al. 2010). However, it should be noted that the soil moisture values in the irrigation site were measured by HydraProbe and Soil Scout sensors, both of which were found to produce systematically higher values than HOBO sensors (see Appendix G). Therefore, the significantly high difference in soil moisture may have actually resulted more from the systematic error caused by the HydraProbe and Soil Scout sensors and not necessarily from actual soil moisture differences. Soil temperature was also found to be consistently higher in the irrigation site, the difference remaining relatively constant through all months which was completely opposite to the findings of Gulledge and Schimel (2000). This may have resulted from the increased specific heat capacity of the soil due to the increased amount of soil water, thus resulting in higher soil temperature minima and maxima and lower sensitivity to diurnal changes in air temperature as the air temperatures stayed relatively high through all summer (e.g. Al-Kayssi et al. 1990). On the other hand, higher soil moisture is often estimated to lead to higher amount of evaporation and, thus, higher amount of heat loss and lower soil temperature especially in soils with coarse texture, which is opposite to the findings of this study (Gulledge and Schimel 2000). Furthermore, the location of the irrigation site itself may have also received more sun radiation than the control site, resulting in higher soil temperatures but this cannot be fully confirmed by the data in this study. Moreover, the systematically higher soil temperatures recorded by the HydraProbe sensors located solely in the irrigation site may have severely overestimated the soil temperature statistics and analyses for the irrigation site (see Appendix G). Thus, the differences in soil moisture and soil temperature between the main plots may be significantly biased and unreliable.

Despite the higher soil moisture levels in the irrigation site, the soil did not turn into a methane source. The amount of irrigated water combined with natural precipitation did not exceed the long-term precipitation averages, also leading to lower soil moisture content than was expected which may have partially caused the consistent negative flux values in the irrigation site (see table 1). However, while Savage et al. (1997) found maximum values of soil moisture of only 20% (gravimetric water content, GWC), the soil was still found to turn into a small methane source after a strong rainfall event with 38.5 mm precipitation. On the other hand, Saari et al. (1998) found that CH_4 consumption was decreased but not fully restricted in the maximum water content of 79% (GWC) in laboratory manipulations, which may suggest that even in the maximum soil moisture content of 44.3% recorded in this study methanotrophic activity may have been more prevalent than methanogenesis, resulting in negative flux. This is further supported by Christiansen et al. (2012) who also found that methane emissions from the soil started at soil moisture above 45% (VWC) which

was generally not found in the upland forest soils. Also, as Castro et al. (1995) and Le Mer and Roger (2001) point out, the alternating sequences of addition of irrigated water and the subsequent effective evapotranspiration of the water may have resulted in very short-lived increases in soil moisture and, subsequently, very short-term low methane emissions or significant decreases in methane sink, before returning back to the original soil moisture level with mostly methanotrophic activity. Thus, the possible decreases in methane sink and emissions immediately after irrigation may have been missed as the fluxes were always measured prior to water addition in this study.

The effect of soil moisture on CH_4 sink varied according to treatment levels in the scale of the whole study period. Strong negative CH_4 sink responses to soil moisture in both main plots were expected and found in many earlier studies (e.g. Castro et al. 1995; Smith et al. 2000; Christiansen et al. 2012). The main plot models and correlations may indicate that a similar curvilinear response of irrigation site could be possible also in control site if the soil moisture increased to similar levels as in the irrigation site for a longer time period. However, it should be noted that the models had relatively poor fit and predictive performance so they should not be considered as reliable generalisations of the variable relationships. Together with high soil moisture difference, the results of higher soil moisture dependence in IO and soil temperature in CO may suggest that when soil moisture level decreases under a certain level, soil temperature becomes a factor with higher effect on CH_4 sink and possibly affects methanotrophy more than methanogenesis in the absence of anoxic conditions (see figures 12 and 15). Many studies have found that methanotrophic activity is rarely reduced by drought in boreal upland forest soils while methanogens are more affected by the lack of sufficient soil moisture, further supporting this idea (e.g. Le Mer and Roger 2001; Pihlatie et al. 2008). Furthermore, as soil moisture decreases, diffusivity of methane from the atmosphere and inside the soil increases along with oxygen concentration, which leads to a higher effect of soil temperature on methane consumption (Crill 1991). However, methanotrophs are generally not as strongly affected by soil temperature as methanogens especially in upland mineral soils but rather primarily by soil moisture and secondarily by soil temperature (Le Mer and Roger 2001; Smith et al. 2003; Pihlatie et al. 2008). Therefore, higher soil temperatures may have caused stronger evapotranspiration and lower soil moisture levels which increased diffusivity and aerobiosis (i.e. oxic conditions), thus increasing methane consumption and methane sink in the CO group but also possibly in the control site as a whole.

Similar to Lohila et al. (2016), the lowest uptake rates in the irrigation site and the study site as a whole were recorded in August but with no emissions, low monthly differences and a subsequent increase in mean uptake rates in September (see table 4). Unfortunately, this study was not able to analyse the monthly differences in significance of soil moisture as a predictor for CH_4 flux and uptake rate further by creating monthly models of IO and CO groups which represented only soil moisture manipulation and thus the temporal changes

are discussed more based on the correlation, ANOVA and TukeyHSD analyses. The higher significance of soil temperature as a predictor in August and September in both irrigation and control may have resulted from the fact that soil temperature was close to the whole period average or lower (below 15°C) in both main plots together with high soil moisture levels during those months (see tables 2 and 3). Similar results with weakened methane consumption and lower sink via lower temperatures have been found by Billings et al. (2000) but in early summer. However, according to Castro et al. (1995), methane consumption is relatively constant between 10–20°C and is not affected by changes in soil temperature within that range. Higher soil moisture levels may have led to lower methane consumption rates and lower total sink primarily due to lower CH_4 diffusion from the atmosphere into the soil and not necessarily due to increases in methanogenic activity (Crill 1991; Castro et al. 1995). However, methane production can also be enhanced by soil wetting in upland soils, as could be the case in this study as well (Crill 1991; Megonigal and Guenther 2008). As methanogens are more sensitive to changes in soil temperature than methanotrophs, the high significance in soil temperature may also suggest that in adequately high soil moisture levels, methanogenic activity increased and, therefore, changes in soil temperature may have become the more limiting factor for methane production and, thus, its effect was more significant (Crill 1991; Le Mer and Roger 2001; Pihlatie et al. 2008; Xu et al. 2013). According to the models, the latter effect may have been more relevant in September when the sink started to decrease in above soil temperature of circa 13°C, while in August (n.b. D^2=0.15) the negative linear trend would suggest a more methanotrophy-dependent flux response. Nevertheless, the significant effect of soil temperature on CH_4 sink in the irrigation site in August and September remains largely unexplained.

As mentioned previously, the interaction between soil moisture and soil temperature as a predictor of CH_4 flux was found to be significant in some models and should not be neglected when assessing the main effects. The trend showing enhanced soil moisture effect in higher soil temperatures (figure 16) in the whole site models may suggest a more temperature-dependent response via soil moisture levels in a larger scale, possibly indicating the enhancement of methanogenic activity by increases in both soil temperature and soil moisture (Le Mer and Roger 2001; Xu et al. 2013). The opposing interaction trends in the irrigation models may be related to similar phenomena as described earlier about the relationship between high soil moisture and low soil temperature in the August and September models. However, the August and September models did not include interaction term and the soil temperatures were generally highest in July when the interaction term was found (see table 2). The high significance of the interaction term may also actually further emphasise the effect of lower temperatures in higher soil moisture: since the soil temperature was high in July, changes to lower temperatures during that month significantly showed decreases in CH_4 sink in higher soil moisture levels which were consistently observed in the irrigation site. In addition, the fact that none of the control site models included the interaction term and soil moisture was

very low further supports the idea. Since soil temperature was highest in July and uptake rates were relatively high, methanotrophy may have been the more active phenomenon behind the total fluxes during that month because even with increases in soil temperature in high soil moisture levels methane production did not increase noticeably. However, conclusions concerning the interaction between soil temperature and soil moisture cannot be made reliably due to the possible systematic measurement errors in the temperature and moisture data.

All in all, the results of soil moisture manipulation suggest the simultaneous presence of both methanotrophic and methanogenic activities, with possibly higher effect on CH_4 sink being on the former. In this study, the estimates of the magnitude of the ratio between them are solely based on literature from few earlier studies carried out in boreal and temperate forests and mostly from the perspective of methane uptake (e.g. Yavitt et al. 1990; Crill 1991; Saari et al. 1998; Smith et al. 2000). Therefore, further research is required for understanding the temporal changes in the consumption-production ratio of methane as a response from changes in soil moisture and soil temperature.

7.2 Relationship between subtreatments and methane flux

7.2.1 Soil warming

The soil warming manipulation failed to create significantly higher soil temperatures in IT and CT groups when compared with the other subtreatments (see Appendix G). Sjögersten and Wookey (2002) also found that, for a largely unknown reason, OTCs did not increase soil temperature significantly at 5 cm depth which was also the approximate depth of soil temperature sensors in this study. However, the hydrological conditions within the OTCs varied strongly, with IT having significantly high and CT low soil moisture which may have resulted from OTCs drying the subplots by sheltering the plots from precipitation in the control site where the OTCs were only removed during flux measurements while those in the IT subplots were always removed during irrigation, thus allowing a more enhanced water addition. Similar effects of OTCs to soil moisture have been reported also by Sjögersten and Wookey (2002).

Methane uptake was significantly lower in IT in comparison with CT, possibly as a result of higher soil moisture. According to the models and correlation analyses, soil moisture was a better predictor of CH_4 flux in IT whereas in CT it was soil temperature. Therefore, the analyses support the idea that since the OTC manipulation failed to create higher temperatures in IT, soil temperature was unlikely to cause the lower uptake rates which may be more linked to the effect of high soil moisture content. With the very low soil moisture content in CT taken into account, the large difference in uptake rate between CT and IT may be due to similar phenomenon as was suggested between CO and IO. That is, in significantly low soil

moisture content the diffusion of CH_4 into the soil was increased and in the prevalence of oxic conditions methanogenic activity was inhibited and methane consumption was effective, thus resulting in negative flux (e.g. Crill 1991; Whalen et al. 1991). However, despite soil moisture being by far lower in CT, CO had higher uptake through the whole period. This may have been due to lower methanotrophic activity in lower soil moisture content but, on the other hand, such an inhibition of methane consumption is unlikely in northern boreal forest soils (e.g. Castro et al. 1995; Pihlatie et al. 2008). Also, the generally slightly higher soil temperatures in CT were unlikely to affect the methanotrophic communities (Le Mer and Roger 2001; Pihlatie et al. 2008).

Temporal changes in CH_4 sink in the two groups followed relatively clearly changes in soil moisture and soil temperature. The lowest uptake rates in IT were observed in August and September which followed a similar temporal pattern as was found by Lohila et al. (2016). If the possible systematic error of the moisture data is not taken into account, the results may strongly suggest that the change to lower uptake rates during that time was primarily a result of an increase in soil moisture after approximately two months of irrigation. Lohila et al. (2016) found that the soil turned into a methane source in mid-August after approximately three months of high precipitation, which further emphasises the importance of soil moisture behind the decrease in uptake. However, while they suspected soil and air temperatures to be additional significant variables affecting the methane emissions in autumn, this study did not find any significant correlations between soil temperature and CH_4 sink or effects with or without interactions with soil moisture in IT. However, it remains unsolved whether a successful OTC soil warming would have led to higher soil temperatures and thus lower methane uptake rates or even emissions in the IT group. Together with the findings of Lohila et al. (2016), it would seem that increases in soil temperature together with soil moisture may possibly result in significantly lower uptake rates especially by further enhancing methanogenesis.

The lowest uptake rates in CT occurred in June which may be associated with both low soil moisture and soil temperature levels. Since soil moisture was not a significant predictor in lower levels, the lower temperatures may have become a more important control for methanotrophic activity as the June soil temperature mean of 7.9°C was well within the range of -5 to 10°C, in which methanotrophs are more affected by soil temperatures (Castro et al. 1995). Therefore, methane consumption may have remained lower than average during that month despite the low soil moisture levels. In addition, both methanotrophs and methanogens have been found to be more sensitive to temperatures below 10°C but, on the other hand, it is not extensively studied and their tolerance of low temperatures remains relatively uncertain especially in boreal upland forest soils with diverse methanotroph communities (Dunfield et al. 1993; Liebner 2007). All in all, the results from warming manipulation strongly indicate that soil moisture may be a significant factor controlling the methane uptake rates,

especially by affecting methanotrophic activity, but the combined effect with increased soil temperature especially in higher soil moisture levels remains unsolved, emphasising the need for multi-year replications.

7.2.2 Organic litter addition

The organic litter addition succeeded in creating significant differences in uptake rates between IA and CA groups but also in comparison with the other subtreatments. Based on the models and correlation analyses, it could be argued that the lower uptake rates in IA in relation to CA were in part a clear result from higher soil moisture levels whereas the higher uptake rates in CA may have resulted from significantly higher methane consumption with stronger soil temperature effect. However, as with other irrigation treatments, it should be noted that the soil moisture differences were possibly unreliable which also increases the uncertainty related to the interaction effect between soil moisture and litter addition. Since decomposition rates of organic litter are generally low in northern boreal region, the significantly lower uptake rates may be more linked to the added organic litter itself which contained more broad-leaved deciduous litter than the other subtreatments. It may also be that the amount of soil mineral nitrogen increased along with litter additions, resulting in higher nitrogen toxicity for methanotrophs (Kähkönen et al. 2002; Pihlatie et al. 2008). The higher amount of broad-leaved litter in those subplots resulted from the addition of old organic litter collected from all the other subplots, thus containing more deciduous leaves that had accumulated over multiple years in the otherwise spruce-dominated forest. By horizontally blocking the diffusion of atmospheric methane into the topmost layer of the mineral soil most active in methanotrophic activity the broad leaves may have effectively reduced methane consumption and, thus, decreased CH_4 sink (Saari et al. 1997, 1998; Brumme and Borken 1999; Pihlatie et al. 2008). However, CA did not have significantly lower uptake rates than the other control subtreatments and was overcome by especially CE. Thus, when combined with possibly higher soil moisture levels, deciduous organic litter addition was highly effective in decreasing methane sink, as has been suggested by Smith et al. (2003).

The differences in uptake rates between IA and other subtreatments did not change significantly over months. As with the general trends in other irrigation groups, the lowest uptake rates occurred in August and September, similar to Lohila et al. (2016), but as a difference to the other subtreatments, the means in both months were above -100 $\mu g\ m^{-2}\ h^{-1}$. As the temporal decreases to lower mean uptake rates followed increases in soil moisture in IA, the previous discussion of the high importance of soil moisture as a possible primary controlling factor holds true in the temporal scale as well. However, according to the correlation analyses, soil moisture was not a significant factor controlling the sink in August and September. This may possibly suggest a higher temperature-dependence of uptake rates in high soil moisture levels, since especially methanogens are more sensitive to changes in soil

temperature in anoxic conditions (e.g. Megonigal and Guenther 2008). Still, soil temperature did not correlate well with fluxes in all months in IA which may actually suggest that other factors not measured and included in the analyses were affecting the uptake rates more than soil moisture and soil temperature. In addition, since the soil temperature data in irrigation site were likely overestimated, the discussion of its effect on uptake rates of IA is highly uncertain. Uptake rates in CA followed changes in soil temperature well, with both highest uptake and highest soil temperatures occurring in July and lowest uptake with lowest temperatures in June, confirming the model findings of high temperature significance. However, correlations between soil temperature and flux in that group were weak and insignificant in all months except in August when the soil moisture was at its highest. It may be that since soil temperature remained relatively high in August, further increases in it affected the methanotrophic activity more than changes in soil moisture, as was suggested by, for example, Sjögersten and Wookey (2002).

Since the organic litter addition seemed to produce significant decreases in CH_4 sink together with heightened soil moisture levels, the experiment should be repeated in the future for a more thorough examination of their interaction. The results of this study clearly indicate that a soil with a relatively thick deciduous litter layer under prolonged precipitation period with sufficiently high water inputs could turn into a methane source during autumn. By repeating the experiment including the combination of organic litter addition and irrigation, the effect of natural precipitation and air temperature anomalies, such as those in year 2018, could be better taken into account.

7.2.3 Organic litter and root exclusion

The effect of soil moisture and soil temperature on uptake rates in the exclusion treatment clearly differed from other subtreatments in all temporal scales. Without taking the different layers into account, the generally lower uptake rates in the IE group (see table 4) were possibly a result of higher soil moisture levels as with other irrigation treatments. However, the flux responses to soil moisture and soil temperature were completely opposite to those found in the other irrigation treatments, with sink significantly increasing by increases in soil moisture and decreasing by increases in soil temperature. In addition, CE showed trends more similar to those found in the irrigation site and opposite to IE. The positive trend between soil moisture and flux in CE may have resulted from the fact that it had higher soil moisture levels than all the other control groups, also resulting in the lowest uptake within control site as a consequence of decrease in methanotrophic activity. However, since soil moisture in CE was mostly measured by possibly biased Soil Scout sensors, the soil moisture effect may be overestimated. In contrast, IE had the lowest soil moisture levels through the whole period (mean=28.8%) within the irrigation site, leading to higher oxygen availability and methane consumption and, thus, higher uptake rates than the other irrigation groups.

As with CE, the soil moisture effect may, however, be also overestimated. In terms of IE, the largest difference in uptake rate was to the IA treatment which could further confirm the findings of litter addition negatively affecting the sink especially in high soil moisture levels: even though soil moisture in IE was relatively high in comparison with the control groups, the exclusion of organic litter and root exudates effectively increased the sink. It may also be that in smaller amount of organic litter and thus soil nitrogen, methanotrophic activity and consumption was enhanced (Kähkönen et al. 2002; Pihlatie et al. 2008). However, it should be noted that the cut roots still possibly remained as a substrate pool for the decomposers in the soil and the effect of their exclusion was unlikely to be detected during one summer (Minkkinen et al. 2007).

The observed unusual response trends may have been a result of soil moisture being significantly changed due to the manipulation method. Similar exclusion-related disturbances were also found by Minkkinen et al. (2007) who suggested that with the removal of transpiring vegetation and roots in warm air temperatures, soil temperature was more subject to extreme temporal changes and soil moisture may have been more preserved within the lower soil layers, thus possibly raising the soil moisture levels of the mineral soil where also the moisture sensors were located in this study. Furthermore, the ground vegetation in CE was mostly dead due to the low precipitation and possibly the acute effects of root cutting, reducing the amount of plant transpiration. Similar disturbances in the hydrological and temperature regimes likely occurred in IE as well. It may be that the root exclusion fabric collected the irrigated water more efficiently into the excluded organic layer and then a significant part of it evaporated before infiltrating through the fabric into the mineral soil. In addition, the litter collection nets above the exclusion plots may have effectively decreased the amount of natural precipitation inputs into the soil, thus decreasing the amount of soil moisture especially in IE. It may also be that the nets protected the CE plots from direct sun radiation, thus possibly leading to lower rates of heating and water loss. As Minkkinen et al. (2007) point out, the results of the effect of soil moisture and soil temperature on carbon fluxes, and in this case methane sink, may be overestimated in the models due to these disturbances and the overall results from the IE and CE groups as a whole should be interpreted with caution. Since flux measurements were taken from both organic and mineral layers of the exclusion plots and the whole plot results are relatively unreliable, further discussion will be based more on the specific measurement layers.

In the scale of the whole study period, organic layers had lower uptake rates than mineral layers which was in agreement with the results from studies carried out by Saari et al. (1997, 1998) and Kähkönen et al. (2002) (figure 13). In addition, the positive correlations of both layers between soil temperature and flux were in agreement with similar findings by Saari et al. (1998). The exclusion of the organic layer may have increased the diffusivity of atmospheric methane into the soil and enhanced methane consumption which may have led

to higher methane sink in the mineral soil and higher water retention and lower sink in the organic layer (Saari et al. 1998). While methane consumption was decreased in the irrigated organic and mineral soil, the consumption still may have remained active which may also be the cause behind the negative flux values in the organic layers in the irrigation site despite high soil moisture levels (Saari et al. 1998).

The lower sinks in both layers in the irrigation site were most likely explained by the higher soil moisture levels, as with other irrigation treatments. In addition to the effect of possible lack of carbon substrates, the negative flux response in irrigation layers may have resulted from the fact that the soil moisture, which was lower than irrigation average, turned out to be within the optimum for methanotrophic bacteria, thus resulting in increases in uptake rates by increases in soil moisture (Whalen and Reeburgh 1996; Gulledge and Schimel 1998; Saari et al. 1998). This would then indicate an optimum of approximately 22–32% VWC (IE min-max) in the soil of this study. However, if the optimum really was within that range, the positive flux responses of the other irrigation groups within that range of soil moisture would then possibly prove that theory wrong. In addition, decreases in flux response in IA and IT models started above 35% soil moisture which is not within the range of the estimated optimum. In northern boreal upland forests the optimum soil moisture is estimated to be between 20 and 35% of water holding capacity, but without measuring the bulk density and water holding capacity of the soil, the comparisons of the results of this study to other measurements carried out in various boreal and temperate soils in other studies are difficult to make reliably (Gulledge and Schimel 1998; Pihlatie et al. 2008). Furthermore, it has been found that soils with lower amounts of carbon substrates and higher variability in soil moisture caused by alternating submersion and drying, such as the soils in IE group, have high methane consumption potential and are more readily influenced by changes in soil moisture (Le Mer and Roger 2001). These results may also indicate that there were some other factors at play not measured in the exclusion treatment that may have contributed to the strong negative responses of IE fluxes independently or as interactions with soil moisture or temperature. However, the fact that the moisture sensors were located in the mineral soil and not in the organic layer which most likely experienced largely different hydrological conditions, the low correlations and responses of flux to changes in the measured soil moisture may not, in fact, reflect the actual phenomena that occurred during the study period. As mentioned earlier, the soil moisture values measured in this study were also very likely biased, thus preventing a reliable assessment of the possible soil moisture optimum.

As with other treatments, the timing of lowest uptake rates followed changes in soil moisture and was somewhat similar to that found by Lohila et al. (2016) but with no significant temporal changes. The contrasting occurrence of lowest uptake rates of control mineral layers in June may be best explained by the lower soil temperature and moisture which may have lowered the methanotrophic activity in the mineral soil (Crill 1991; Whalen et al. 1991). This

idea was confirmed by the interaction term showing decreases in sink in soil moisture below circa 20% and lower soil temperatures starting from approximately 6°C (figure 16). Same cause may also be behind the lower uptake rates of both control layers in June because soil temperature was higher in IE, resulting in more efficient methane consumption rates despite higher soil moisture levels. After June, the higher soil moisture levels in the irrigation site turned to be the more influencing factor by primarily affecting gas diffusion, as has been found by multiple studies (Crill 1991; Whalen et al. 1991; Castro et al. 1995). However, the weak correlations between flux and soil temperature in contrast to higher correlations with soil moisture in June in the control layers may not support this idea. The lower uptake rates may also be due to relatively high CH_4 concentrations in the soil profile after winter and the reestablishment of the methanotroph populations when soil temperature begins to rise in June, as suggested by Crill (1991). Based on their study, when the soil moisture level started to increase after June in CE, diffusion became the more important factor providing CH_4 substrates for methanotrophs. The trend of organic layers having lower uptake rates than those of mineral layers held true for each month, further possibly emphasising the importance of organic horizon as a gas diffusion barrier. It is also very likely that since the sensors measured soil moisture and temperature only in the mineral soil, the measured values were not appropriate for analyses of the flux responses in organic layers, leading to weaker correlations and significance.

The results of the exclusion manipulation show complex and unexpected trends in flux responses which were difficult to analyse based on the data collected in this study. All things considered, the results indicate that the exclusion of both organic litter and root exudates did not significantly affect the temporal changes in CH_4 sink but may have confirmed the importance of organic litter addition and root exudates in the scale of the whole study period. However, the results are highly contrasting with the other treatments and the manipulation method together with the biased data provided by the soil moisture and temperature sensors may have caused large uncertainties on the results. Therefore, in future research it is highly recommended that the manipulation is repeated multiple times for especially assessing the strongly negative responses of flux in IE to increases in soil moisture and whether those findings may actually result from optimum soil moisture content for methanotrophs in lack of carbon substrates or something else not measured here.

7.3 Uncertainties

7.3.1 Experimental design and methods

The design of the experiment may have led to multiple uncertainties mostly related to statistical analyses. Split-plot design is estimated to often lead to lower precision in the results of the main treatment in comparison with the subtreatments. The higher precision of subtreatments is caused by the higher number of replications in the subtreatments than the main

plots (Cochran and Cox 1957; Jeffers 1960; Altman and Krzywinski 2015). In this study, the irrigation and control treatments were not replicated at all, leading to only one block (irrigation + control), whereas subplots were replicated 1 x 3 = 3 times for A, E and T treatments and 1 x 4 = 4 times for O treatment in each main plot. Therefore, it is clear that the precision of the irrigation treatment was lower than that of the subtreatments and the lack of block replications in a very heterogeneous environment led to high amount of uncertainties in the differences between irrigation and control treatments. However, the precision of the evaluation of the effects of the irrigation manipulation was increased by including the O subplots which showed only the effect of increased soil moisture on CH_4 sink. The amount of replications of the other subtreatments may have also been good to increase to four in order to obtain as precise results as with the O groups, as suggested by Jeffers (1960). However, the number of subtreatment replications was kept at three in this study due to practical lack of space in the study site. In future research it is highly recommended that the main plots (block) are replicated at least twice for obtaining higher precision and power for the statistical analysis of irrigation effects but also of the subtreatments in temporal analyses (Dean 1999). However, the spatial replication of the experiment is much less convenient and expensive and may cause a considerable amount of disturbance in the relatively fragile northern boreal forest environment.

The experimental error was also very likely high due to the large heterogeneity of the study site. Despite having a concurrent control in the experiment, both the main plots and subtreatments were likely subject to differing amounts of confounding factors, such as weather and soil conditions. Especially the total sun radiation and its timing together with precipitation inputs and variation in the local soil structure were likely different to most of the experimental units, leading to higher experimental error and uncertainty especially regarding soil moisture and flux measurements. As Jeffers (1960) points out, controlling all possible confounding factors in forest experiments is impossible and the only means of reducing the error would be the adequate replication of the treatments. This further emphasises the need to have more replications of the main treatment level of this experiment in the future if the effect of increase in soil moisture is to be studied more precisely.

In this study, randomisation of the subplots may have been carried out more haphazardly than a normally completely randomised design would have required. In a randomised experiment, the subplots are assigned to different treatments or experimental units randomly without a subjective influence of selection and are similar on average (Kirk 2012). After establishing the main irrigation and control sites the subplots were assigned by the field workers without carrying out a more objective random allocation beforehand. This may have led to bias in the comparisons of the results and the drawn conclusions of the causality between the manipulated factors due to field workers' subjective thinking processes (Jeffers 1960; Kirk 2012). According to Logan (2010), such a reliable method could be carried

out, for example, by using sampling functions (e.g. *sample()* or *spsample()* in R) which would randomly allocate experimental units within a grid representing the main plots and then treatments to them based on coordinates or locations within a matrix. However, the randomised coordinates may not often be possible to assign in practice due to the large heterogeneity of the study site. For example, the location of large tree roots and coarse soil fragments such as stones and boulders which are common in glacial till, are often invisible before actually setting up the chamber collars and other research equipment into the soil, which may lead to the practical need of choosing a spot with better fit.

Since the experiment was run through one summer, the year- and month-specific confounding factors may have produced large uncertainties in the results and decreased their applicability in further studies. The anomalous weather conditions during the study period may have led to significant experimental errors especially in the soil moisture manipulation which is more subject to changes via evapotranspiration (e.g. Gulledge and Schimel 2000; Seneviratne et al. 2010). In addition, the OTC warming and organic litter addition and exclusion manipulations should be repeated in order to understand the specific causes behind the flux responses in those subtreatment groups. Thus, the results of this study represent only the responses found in specific weather conditions and a specific study site within the wide boreal region. In order to minimise the uncertainty in the accuracy in the overall estimates of the flux responses to the treatments and increase the applicability of the results to other boreal forest areas, it is highly recommendable to repeat the experiment in multiple years and possibly in different upland forest areas, as suggested by Cochran and Cox (1957) and Jeffers (1960). By repeating the experiment in multiple subsequent summers, the estimations of the actual flux response to the different treatments could be more reliable and more free from the effects of the time-related confounding factors. However, with the time limitations of this study, such a broad and long experiment was not possible to establish.

7.3.2 Field methods and conditions

The methods of treatment manipulations may have caused multiple uncertainties in the results. In soil moisture manipulation, the irrigated water amount was not enough for exceeding the long-term average, the effect of which may have been further enhanced by the low amount of natural precipitation. According to Jeffers (1960), since the area of irrigation was spread over the borders of the site the edge effects of the treatment were likely located well outside of the subplots, guaranteeing a more homogeneous distribution of the irrigation. However, the wind conditions undoubtedly made the distribution of the irrigated water uneven within the irrigation site, resulting in uneven amounts of water per subplot. If the amount of irrigated water and irrigation frequency was kept higher and more constant through the whole summer, the precipitation amount could have possibly exceeded the amount of evapotranspiration which could have led to significantly higher soil

moisture and anoxic conditions (Seneviratne et al. 2010). By calculating the required water amount based on the long-term precipitation average and repeating the experiment during multiple years, the unexpected heat waves and other weather anomalies would not affect the results as much as in this study. However, such improvements would require much more efficient water carrying logistics and capacity than what was possible in this study. For ensuring a more efficient irrigation system, one option would be to establish the experiment in closer vicinity of a water source which was not, however, possible in this study due to flux measurement devices being set specifically in the Kenttärova forest. In addition, better adjustments may be required for the water sprinklers and within the financial capabilities improve the irrigation system so that it would be operating longer periods of time per day, for example with automatic sprinklers providing irrigation through the evening and possibly night when evapotranspiration is at lowest.

The results concerning soil moisture differences between the main plots and all the correlation analyses and models based on them were likely biased as a result from possible systematic error in the soil moisture data. As mentioned previously, since the HydraProbe and Soil Scout sensors consistently produced significantly higher soil moisture values than HOBO sensors and were the only sensors included in the irrigation site, the high difference between the main plots may have been significantly overestimated and thus not correspond to the actual soil moisture. In addition, due to the coarseness, low water storage ability and large heterogeneity of the forest soil, the irrigated water may not have actually increased the soil moisture levels very efficiently and created as large soil moisture differences as the biased soil moisture values indicated (e.g. Kljun et al. 2007). Therefore, more reliable results could have been obtained by normalising the erroneous soil moisture data by subtracting the monthly and whole period differences from the HydraProbe and Soil Scout data as compared to HOBO sensors, for instance (see Appendix G). Based on literature, despite the possible systematic error and large uncertainty related to the measured soil moisture, it can still be assumed that the differences in uptake rates were likely caused by differences in soil moisture (e.g. Crill 1991; Castro et al. 1995; Smith et al. 2003; Christiansen et al. 2012). Furthermore, soil moisture was measured as volumetric water content (%VWC) which may not be a good measure for comparison with other soil types with various soil textures. Another alternative or addition would have been to include measurements of soil bulk density for calculating the water holding capacity (WHC) and the percentage of water-filled pore space (%WFPS) of the soil in question. Percentage of water holding capacity (%WHC) is often considered a more comparable measure of soil moisture than VWC (Gulledge and Schimel 1998; Seneviratne et al. 2010). However, in order to calculate the %WHC, the experiment needs to apply destructive soil sampling and laboratory analyses which increase the costs of the experiment (Seneviratne et al. 2010). Comparisons with other studies are most crucial in terms of the organic litter and root exclusion manipulation of this study where the measured soil moisture level in %VWC is not as well comparable with other earlier studies that have found specific

optima for methanotrophic activity (e.g. Whalen and Reeburgh 1996; Saari et al. 1998; Billings et al. 2000).

As has been discussed earlier, the three different sensors measuring soil temperature produced highly varying estimations of the values which undoubtedly resulted in biased statistical analyses of the soil temperature differences and effects. By averaging the temperatures measured by HydraProbe and HOBO sensors in the IO2, IO3 and IE2 subplots, the resulting soil temperature values may have been overestimated, resulting in too high subtreatment temperature averages. In addition, the higher soil temperatures observed in the irrigation site may have resulted from the systematically higher values measured by HydraProbe sensors which were only located in the irrigation site. However, the effect of the possibly biased soil temperature observations was probably smaller due to the replications in the subtreatment groups which may have improved the accuracy of the calculated average while clearly still affected by the biased observations. In addition, if the HydraProbe sensor observations would have been completely removed, the overestimated temperatures would still have been present in those plots which did not have any other sensor measuring the variable (IO1 and IT1), still resulting in systematic error. As with the biased soil moisture data, the soil temperatures measured by HydraProbe sensors could have been normalised for example by subtracting the average monthly and whole period difference in relation to the other two sensors, which could have produced more reliable results (see Appendix G). Furthermore, the malfunctioning of the HOBO sensor in the CT2 subplot led to no temperature data and, thus, a significant decrease in CT replications and precision. Two replications were most likely not enough for providing reliable estimates of the soil temperature average in the CT group especially since the environment was very heterogeneous (e.g. Cochran and Cox 1957; Jeffers 1960).

Since the OTC warming treatment was inefficient in producing significant differences in soil temperature among the subplots, the manipulation needs to be repeated in the future. In addition, the pentagon-shaped OTCs instead of hexagons may have influenced the insignificant soil temperature changes by having a different inclination degree (60°in hexagonal OTCs) but this is rather unlikely (Marion 1996). As discussed earlier, the OTCs themselves may have also blocked natural precipitation inputs in the IT and CT subplots, resulting in lower soil moisture levels, as was found by Sjögersten and Wookey (2002).

As described earlier, the organic litter and root exclusion may have caused significant alterations in the hydrological conditions of the soil. The soil disturbances caused by the excavations may have lasted for a significantly long time during the study period and affected the measured fluxes as well as hydrological conditions in many unknown ways. The uncertainties in analysing the results of the exclusion manipulation were further added to by the location of the soil moisture and soil temperature sensors in the mineral soil layers. Therefore, the results concerning the whole IE and CE subplots and organic layers but also

the differences between the organic and mineral layers are highly uncertain and require further assessment with careful consideration of the exclusion methods and their effects to the hydrological and thermal conditions of the soil. If the separation of the organic and mineral layers are considered in the future studies, the inclusion of the sensors in the organic layers is recommended. However, their practical installment in the occasionally thin organic layer may be highly impractical and laboratory measurements may provide more accurate results of the temperature and moisture-related responses of CH_4 flux, as was done for example by Saari et al. (1998). In the light of the results of organic litter addition and the earlier studies made by excluding roots, the exclusion of the organic layer could be omitted in future studies especially if the study will not be repeated multiple times since the exclusion of root exudates most likely will be more visible in multi-year analyses and not in one summer (Minkkinen et al. 2007). Also, the root exclusion itself could be left out entirely and the exclusion of organic litter may be sufficient which would also reduce the amount of unnecessary disturbance in the hydrological and thermal conditions of the soil and thus increase the reliability of the results. However, since this study did not reliably confirm any significant effects of roots in CH_4 sink, the root exclusion manipulation should be repeated in longer-term experiments, as was done for example in a similar exclusion manipulation by Vincent et al. (2010).

The methane fluxes in this study were measured using cavity ring-down spectroscopy which is considered one of the most precise and accurate methods of gas concentration measurements (Rella et al. 2013). The addition of measurements of multiple gas species further added to the high precision of the CH_4 and H_2O mole fraction measurements and calculations (Rella et al. 2013; Korkiakoski 2014). Therefore, most of the uncertainties of flux observations may have been more related to the chamber measurements carried out in the field. Most of the uncertainties in static chamber technique are often caused by the flow of air from outside the chamber during closure and soil disturbances (Pihlatie et al. 2013). However, the leakage was minimised by using permanent steel collars set in the ground and the foam edges of the chamber which provided enhanced sealing. Since the soil surface in the study site was relatively uneven at some subplots, also the collars may have been more unbalanced, resulting in potential small openings between the chamber and the collar and, thus, possible leakages. However, this problem was acknowledged already during the beginning of the study period and the possible leakage was minimised by gently pressing the chamber towards the unbalanced collar with minimal disturbance to the soil and the measured fluxes. Nevertheless, the added pressure may have also been a source of bias in the observed results. In addition, the chambers were ventilated with open air before and after each measurement and the circulation of air within the chamber during closure was ensured using a fan, both of which provided more reliable estimations of the CH_4 and water vapour concentration changes (e.g. Pihlatie et al. 2013; Korkiakoski et al. 2017).

7.3.3 Statistical analysis and modelling

Since the CH_4 flux observations used in this study were calculated using linear fit, the resulting flux estimations may be underestimated. According to Pihlatie et al. (2013), when linear regression is used for the flux calculations, the results are often significantly underestimated while non-linear exponential fitting may sometimes provide more accurate results. However, the exponential fit is often estimated to result in large uncertainties and sometimes overestimations especially due to its sensitivity to the conditions within the chamber during the first minutes (Pihlatie et al. 2013). Therefore, the linear fit may have been a better choice in this case since there may have been some disturbances affecting the flux especially during the beginning of closure, caused by the pressing of chamber and unevenness of the collars. Still, it may be recommendable that the fluxes in similar experiments are calculated using both methods for being better able to estimate the causal effects of the manipulations on uptake rates. Otherwise the accuracy of the flux calculations was improved by executing the water vapour corrections before the linear fitting (Rella et al. 2013; Korkiakoski 2014). However, an additional uncertainty in the calculated flux values may have also resulted from using atmospheric air temperature measured at the Kenttärova station instead of the temperature within the chamber. Atmospheric air temperature has sometimes been used in flux calculations when temperature measurements inside the chamber are not accessible (e.g. Pihlatie et al. 2013).

The analyses of variance may have contained multiple uncertainties related to the error terms of split-plot design. Split-plot design includes two error terms: main-plot error and subplot error, both of which have different variations within the design and should be taken into account in the ANOVA procedure (Logan 2010; Altman and Krzywinski 2015). In this study, the error terms were not specified in the ANOVAs which may be a significant source of uncertainty in the assessment of causal relationships. However, the uncertainty would have been greater if there was more than one block consisting of irrigation and control plots, so this study did not include any between-block effects and errors (Logan 2010; Altman and Krzywinski 2015). A better alternative for the two- and three-way ANOVAs used in this study may have been linear mixed effects models (LMM, *lme()* from package *nlme* or *lmer()* from package *lme4* in R) which are more efficient in analysing the main treatment effects while considering the different nested error terms within an unbalanced design (Logan 2010). In addition, the computed ANOVAs used the standard type I sums of squares method in which the order of the model terms is of high significance, and changing it may lead to significantly different results (Langsrud 2003; Logan 2010). Therefore, the use of type III may have resulted in more accurate estimations of the effects of different treatment levels especially due to its ability to estimate effects without being affected by the unbalanced sample sizes (Logan 2010). However, some studies have argued that type II would be more powerful in the analysis of unbalanced designs (Langsrud 2003).

The temporal correlation analyses of the variables were carried out using simple linear regression models and Pearson's correlation coefficient which may have produced uncertainties in changes within the subplots. The simple regression model with correlation analysis treats each observation as independent and produces correlation values that are often best fit for estimating changes over time in between-individual observations (here, between subtreatment groups and between main plots) (Bakdash and Marusich 2017). Therefore, the correlation analyses in this study left out the analysis of within-individual (here, within subtreatment groups and main plots) correlation changes and likely violated the independence of observations in that scale, as is often the case in studies with repeated measures (Barnett et al. 2010; Tabachnick 2014). As Bakdash and Marusich (2017) suggest, the addition of within-individual analysis (e.g. *rmcorr* package in R) which takes into account the dependency of the observations with each other, would possibly improve the accuracy of the relationship assessments. However, no examples of studies using this method in the field of environmental science were found for this study.

Since GLM is a fixed-effect model, it does not include random effect terms from the different treatment levels. A fixed effect in a model is the effect of an experiment that is known and of primary interest for the researcher while random effects are those describing the variation among the treatments, or in this study, variation between the different treatment levels which is often not the goal of the study (Bolker et al. 2009). This is why the modelled flux responses in this study may not be as accurate as they would be if the used model would have included multiple random effect terms representing the variation in main plot and subtreatment levels. An alternative to GLM in this study could have been either linear mixed model due to the normality of the response and predictor variables or generalized linear mixed model (GLMM) which combines methods of generalized linear and linear mixed effect models and is able to specify the treatment-specific and nested random effects in the model (Bolker et al. 2009; Barnett et al. 2010; Fang and Loughin 2013). GLMM and LMM often also have greater statistical power than GLM and linear models which do not include random effects (Fang and Loughin 2013). In addition, since the distribution of the CH_4 flux data was skewed to left, GLMs with only first and second-order polynomials may not have captured the true flux response trend well (Guisan and Zimmermann 2000). Moreover, the analyses of model term significance may have been more accurate if instead of types I and III ANOVA methods the study used types II and III which are considered more suitable for unbalanced designs (Langsrud 2003; Logan 2010). Due to the repeated measures both in the monthly and whole period models, the assumption of independence between observations was also likely violated because no variance-covariance structure was specified in the models, leading to temporal autocorrelation (Littell et al. 2000; Barnett et al. 2010; Tabachnick 2014). Therefore, the modelled predictions of flux responses may be less reliable and should be interpreted with caution.

Most of the statistical analyses regarding causality between the variables in this study were based on the significance levels (p-values) which is always a source of uncertainty in statistics (Halsey et al. 2015). The sole application of p-values in hypothesis testing, such as ANOVA and TukeyHSD, without them being based on predictive models may have led to uncertainties in the determination of the actual magnitudes of the detected effects (Harrell 2015). Furthermore, since the sample sizes and number of replications was relatively small in this study, the statistical power was lower which may have led to higher uncertainties and exaggerations related to the significance levels shown by the p-values (Halsey et al. 2015). However, the repeated measures ANOVAs were based on GLS models containing correlation structure specifications which may have improved the accuracy of the effect estimates in this context. Moreover, all the GLMs were built following the principle of parsimony and backward variable selection where the simplest model was determined by the significance level of the model terms. According to Harrell (2015), step-wise variable selection leads so severe biases in the model term significance, D^2 values and confidence intervals, the latter of which may also explain the very narrow confidence intervals of the GLMs in this study (see figure 15). However, backward step-wise selection is considered a better alternative to the forward method due to the better assessment of the full model fit and multicollinearity between predictors (Harrell 2015).

Since the subtreatment models from the whole study period contained significantly less observations (min n=28) than those based on the main plots (min n=168), the reliability of their predictions is also lower. In addition, the number of observations in the monthly models of main plots were also low (min n=24). This may have led to over-fitting of the model predictions with the few observations having too much influence on the overall response (Harrell 2015). Therefore, if the amount of block replications were increased from one to two or more, it would have been possible to build all the models with higher reliability, including monthly models of the subtreatments, with an adequate amount of observations for each month and whole study period. Hence, it is highly recommended that future studies establish multiple block replications in order to being able to assess the temporal variation of CH_4 flux response to changes in soil moisture and soil temperature as affected by subtreatments, with much higher precision.

The models in this study included only two predictors, soil temperature being the only confounding factor considered. In reality, however, there may have been numerous other extraneous factors affecting the flux response, either directly or by influencing the manipulations in one way or another. Therefore, several other confounding factors could have been included in the models as predictors. It may have been more insightful to include monthly precipitation sums calculated separately for irrigation and control sites for assessing the combined and separate influence of both precipitation and soil moisture on the sink, as was done in studies by Savage et al. (1997) and Lohila et al. (2016). In addition, soil

redox potential may provide more depth for the analysis of soil moisture effects on methane consumption and production (Wang and Bettany 1997). Also, the impact of soil texture and bulk density has been found to be an important possible confounding factor in studies which have not specifically measured consumption-production ratio (e.g. Billings et al. 2000; Smith et al. 2000). As discussed earlier, CH_4 concentrations along the soil profile may also prove to be an appropriate predictor especially if the exclusion manipulation is to be repeated using the same method as in this study (Crill 1991; Kähkönen et al. 2002). Furthermore, the investigation of moss growth and its moisture content within the irrigation site could be a possible addition to the models since it is found to affect methane oxidation in boreal forests in complex ways related to water retention and evapotranspiration, and moss growth is increased in higher soil moisture (Whalen et al. 1991; Heijmans et al. 2004). In the light of the findings from organic litter addition, other suitable predictors may include the specific measures of broad-leaf and needle ratio and weights, pH and carbon and nitrogen content of the added organic litter especially in long-term experiments when decomposition becomes a factor of higher significance (Brumme and Borken 1999; Smith et al. 2000). If the experiment is executed in multiple locations at the same time and the results are analysed in a larger spatial scale, the nearby lake water level could be added to the models and other analyses as well, as suggested by Lohila et al. (2016).

8 Conclusions

This study aimed to find causal relationships between soil moisture and methane flux both independently and together with organic litter and roots and soil temperature. Since multi-factorial experiments in methane flux research especially in the boreal zone are very few, this study was able to produce new interesting findings to the field. Despite high precipitation amount and frequency with a significant increase in soil moisture, the soil did not turn into a methane source during the study period. However, the timing of highest fluxes, and thus lowest uptake rates, was observed in August and September in all irrigation treatment levels which confirmed the hypothesis related to the timing of sink-source switch and the findings of Lohila et al. (2016) in the same study area.

All treatments showed significant relationships between soil moisture and soil methane flux. Increases in soil moisture had a significant positive effect on methane flux, and thus a negative one on methane sink, in all treatment levels but the effect size varied according to subtreatments and months (figure 17). The effect of soil temperature increase on methane sink remained uncertain and hypothesis was left unconfirmed but its interactions with soil moisture were found significant especially in the levels of the whole study site and irrigation site. Compared to all other treatment levels of the study, organic litter addition produced significantly higher fluxes, and therefore lower uptake rates, when combined with higher soil

moisture levels which may indicate the possibility of significant methane emissions in higher and more constant soil moisture levels in autumn. Organic litter and root exclusion showed complex and contrasting flux responses without significant temporal changes, with decreases in fluxes, or in other words, increases in uptake, by increases in soil moisture within generally high soil moisture levels, in part confirming the hypothesis. As expected, lower uptake rates were observed in the organic layer. The results of exclusion treatment effects in both layer and whole subplot level were highly uncertain due to the significant disturbances and bias caused by the manipulation technique and sensor locations, thus leaving the causes largely unexplained. Also, some sensors measuring soil moisture and soil temperature were found to possibly have produced systematic errors to the data which further added to the high uncertainty of the effects of those variables on uptake rates. In general, the results of this study may strongly indicate that the treatments had a higher influence on methane consumption rather than production.

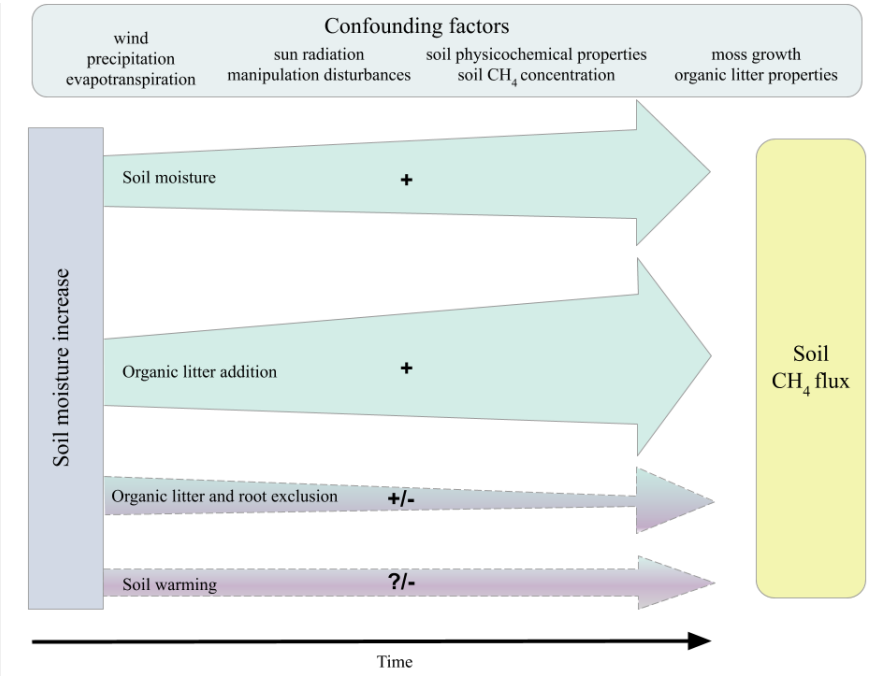

Figure 17: The effects of soil moisture increase and its interaction with the treatments of this study on soil CH_4 flux in temporal scale. The size of the arrows representing different treatments and factors refers to the relative importance and size of the effect on soil CH_4 flux over the study period. Increasing trends are marked with green colours and plus signs, decreasing trends with purple and minus, and unclear or uncertain trends with a combination of the former or a question mark with dashed arrow borders. The arrow of organic litter and root exclusion shows a decreasing trend toward the end of the period because such a trend was observed in higher soil moisture levels while it simultaneously had higher fluxes and thus lower uptake in the irrigation site in comparison to control site. Since the term "soil CH_4 flux" has no direction specification, the increases refer to changes from a lower negative flux value to a higher one and vice versa. From the perspective of the soil CH_4 sink, the arrow sizes and signs would be the opposite from the ones shown in the figure. The listed confounding factors do not include all possible variables that may have affected the results of the experiment, and are only mentioned as possible sources of uncertainty and as a guideline for choice of predictor variables in future studies.

The results of this study emphasise the importance of understanding the complex network behind soil methane flux dynamics in boreal upland forests. Since precipitation amounts, extreme precipitation events and soil moisture contents of especially Finnish and northern boreal forests have been increasing and are estimated to increase in the future as a result of climate warming, both temporal and spatial replications of similar soil moisture manipulation experiments are needed. By re-running the experiment for multiple subsequent years and possibly in various locations, the experiment could give a more consistent image of the soil moisture-dependent methane flux dynamics in the forest soil in the Pallas region but also in boreal regions in general, with a better understanding of the influence of weather anomalies such as the ones during summers of 2011 and 2018. In the light of the findings of this study, more emphasis should especially be put on the experimental combinations of organic litter addition, soil warming and soil moisture increase. Therefore, with some improvements in experimental design, manipulation techniques, sensor measurements and temporal replications this experiment could become a significant tool in examining several causal chains and their interactions in the soil methane flux dynamics in boreal upland forests under changing climate.

Acknowledgements

First and foremost I would like to thank associate professor Annalea Lohila from the Finnish Meteorological Institute and professor Miska Luoto for excellent guidance and support throughout the whole research process. I am also very thankful for Mika Korkiakoski for calculating the methane fluxes from a large pool of data and guiding me with the flux calculations and field measurements, and Timo Penttilä for helping with designing and building the experiment. Also, I want to thank Timo Hurme from the Natural Resources Institute for giving me valuable advice in the statistical analyses of the data. A big thank you goes to Valtteri Hyöky and Matti Peltonen for carrying thousands of litres of water up to the Kenttärova forest five days a week in all kinds of weather and helping me with various field measurements over the summer. I would especially like to thank Valtteri for being great company and helping me feel at home in Pallas.

I want to thank my study mates, especially Aino-Maija Määttänen and Sara Todorović for support and laughs during the whole thesis process. Also thank you Vilna Tyystjärvi for introducing me to LaTeX language and providing help with coding with great patience, and Lucrezia Slinn and Tiia Seeve for proof-reading. Finally, a warm thank you for my family and friends, especially Oona Mehtälä and Elina Pallaspuro without whom I would not be writing these words.

References

Allison, S. D. and K. K. Treseder (2008). Warming and drying suppress microbial activity and carbon cycling in boreal forest soils. *Global change biology* 14 (12), 2898–2909.

Altman, N. and M. Krzywinski (2015). Points of significance: split plot design. *Nature Methods* 12 (3), 165–166.

Anderson, J. P. E. and K. H. Domsch (1980). Quantities of plant nutrients in the microbial biomass of selected soils. *Soil Science* 130 (4), 211–216.

Arnold, K. von, M. Nilsson, B. Hånell, P. Weslien, and L. Klemedtsson (2005). Fluxes of CO2, CH4 and N2O from drained organic soils in deciduous forests. *Soil Biology and Biochemistry* 37 (6), 1059–1071.

Aurela, M., T. Laurila, and J.-P. Tuovinen (2004). The timing of snow melt controls the annual CO2 balance in a subarctic fen. *Geophysical Research Letters* 31 (L16119), 1–4.

Aurela, M., A. Lohila, J.-P. Tuovinen, J. Hatakka, T. Penttilä, and T. Laurila (2015). Carbon dioxide and energy flux measurements in four northern-boreal ecosystems at Pallas. *Boreal Environment Research* 20 (4), 455–473.

Bache, S. M. and H. Wickham (2014). *magrittr: A Forward-Pipe Operator for R*. R package version 1.5. URL: https://CRAN.R-project.org/package=magrittr.

Bakdash, J. Z. and L. R. Marusich (2017). Repeated measures correlation. *Frontiers in Psychology* 8, 456.

Ball, B. C., K. E. Dobbie, J. P. Parker, and K. A. Smith (1997). The influence of gas transport and porosity on methane oxidation in soils. *Journal of Geophysical Research: Atmospheres* 102 (D19), 23301–23308.

Barnett, A. G., N. Koper, A. J. Dobson, F. Schmiegelow, and M. Manseau (2010). Using information criteria to select the correct variance–covariance structure for longitudinal data in ecology. *Methods in Ecology and Evolution* 1 (1), 15–24.

Bartlett, K. B. and R. C. Harriss (1993). Review and assessment of methane emissions from wetlands. *Chemosphere* 26 (1–4), 261–320.

Beier, C., C. Beierkuhnlein, T. Wohlgemuth, J. Penuelas, B. Emmett, C. Körner, H. de Boeck, J. H. Christensen, S. Leuzinger, I. A. Janssens, and K. Hansen (2012). Precipitation manipulation experiments–challenges and recommendations for the future. *Ecology Letters* 15 (8), 899–911.

Bender, M. and R. Conrad (1992). Kinetics of CH4 oxidation in oxic soils exposed to ambient air or high CH4 mixing ratios. *FEMS Microbiology Ecology* 101, 261–270.

Bengtsson, H. (2020). *matrixStats: Functions that Apply to Rows and Columns of Matrices (and to Vectors)*. R package version 0.56.0. URL: https://CRAN.R-project.org/package=matrixStats.

Billings, S. A., D. D. Richter, and J. Yarie (2000). Sensitivity of soil methane fluxes to reduced precipitation in boreal forest soils. *Soil Biology and Biochemistry* 32 (10), 1431–1441.

Blankinship, J. C., J. R. Brown, P. Dijkstra, and B. A. Hungate (2010). Effects of interactive global changes on methane uptake in an annual grassland. *Journal of Geophysical Research: Biogeosciences* 115 (G2).

Boeckx, P., O. Van Cleemput, and I. Villaralvo (1997). Methane oxidation in soils with different textures and land use. *Nutrient cycling in Agroecosystems* 49 (1-3), 91–95.

Bolker, B. M., M. E. Brooks, C. J. Clark, S. W. Geange, J. R. Poulsen, M. H. H. Stevens, and J.-S. S. White (2009). Generalized linear mixed models: a practical guide for ecology and evolution. *Trends in ecology & evolution* 24 (3), 127–135.

Bousquet, P., P. Ciais, J. Miller, E. J. Dlugokencky, D. Hauglustaine, C. Prigent, G. R. Van der Werf, P. Peylin, E.-G. Brunke, C. Carouge, R. L. Langenfelds, J. Lathiere, F. Papa, M. Ramonet, M. Schmidt, L. P. Steele, S. C. Tyler, and J. White (2006). Contribution of anthropogenic and natural sources to atmospheric methane variability. *Nature* 443 (7110), 439.

Brumme, R. and W. Borken (1999). Site variation in methane oxidation as affected by atmospheric deposition and type of temperate forest ecosystem. *Global Biogeochemical Cycles* 13 (2), 493–501.

Cajander, A. K. (1926). The theory of forest types. *Acta Forestalia Fennica* 29 (3), 1–108.

Campitelli, E. (2020). *ggnewscale: Multiple Fill and Colour Scales in 'ggplot2'*. R package version 0.4.1. URL: https://CRAN.R-project.org/package=ggnewscale.

Castro, M. S., P. A. Steudler, J. M. Melillo, J. D. Aber, and R. D. Bowden (1995). Factors controlling atmospheric methane consumption by temperate forest soils. *Global Biogeochemical Cycles* 9 (1), 1–10.

Chai, X., D. J. Tonjes, and D. Mahajan (2016). Methane emissions as energy reservoir: Context, scope, causes and mitigation strategies. *Progress in Energy and Combustion Science* 56, 33–70.

Chan, A. S. K. and T. B. Parkin (2001). Methane oxidation and production activity in soils from natural and agricultural ecosystems. *Journal of Environmental Quality* 30 (6), 1896–1903.

Christensen, T. R., S. Jonasson, T. V. Callaghan, and M. Havström (1995). Spatial variation in high-latitude methane flux along a transect across Siberian and European tundra environments. *Journal of Geophysical Research: Atmospheres* 100 (D10), 21035–21045.

Christiansen, J. R., L. Vesterdal, and P. Gundersen (2012). Nitrous oxide and methane exchange in two small temperate forest catchments—effects of hydrological gradients and implications for global warming potentials of forest soils. *Biogeochemistry* 107 (1-3), 437–454.

Cochran, W. G. and G. M. Cox (1957). *Experimental designs*. 2nd ed. Wiley series in probability and mathematical statistics. New York: Wiley and Sons.

Conrad, R. (2009). The global methane cycle: recent advances in understanding the microbial processes involved. *Environmental microbiology reports* 1 (5), 285–292.

Crill, P. M. (1991). Seasonal patterns of methane uptake and carbon dioxide release by a temperate woodland soil. *Global biogeochemical cycles* 5 (4), 319–334.

Crill, P. M. and B. F. Thornton (2017). Whither methane in the IPCC process? *Nature Climate Change* 7 (10), 678–680.

Dean, A. (1999). *Design and analysis of experiments*. Springer texts in statistics. New York: Springer, p. 740.

Dlugokencky, E. J., E. G. Nisbet, R. Fisher, and D. Lowry (2011). Global atmospheric methane: budget, changes and dangers. *Philosophical Transactions of the Royal Society A* 369, 2058–2072.

Dunfield, P., R. Knowles, R. Dumont, and T. R. Moore (1993). Methane production and consumption in temperate and subarctic peat soils: response to temperature and pH. *Soil Biology and Biochemistry* 25 (3), 321–326.

Dutaur, L. and L. V. Verchot (2007). A global inventory of the soil CH4 sink. *Global Biogeochemical Cycles* 21 (4).

Fang, L. and T. M. Loughin (2013). Analyzing binomial data in a split-plot design: classical approach or modern techniques? *Communications in Statistics-Simulation and Computation* 42 (4), 727–740.

Ferretti, D. F., J. B. Miller, J. W. C. White, K. R. Lassey, D. C. Lowe, and D. M. Etheridge (2007). Stable isotopes provide revised global limits of aerobic methane emissions from plants. *Atmospheric Chemistry and Physics* 7 (1), 237–241.

Fetzer, S., F. Bak, and R. Conrad (1993). Sensitivity of methanogenic bacteria from paddy soil to oxygen and desiccation. *FEMS Microbiology Ecology* 12 (2), 107–115.

Finnish Meteorological Institute (2018a). GHG measurement sites - Pallas (GAW). https://en.ilmatieteenlaitos.fi/GHG-measurement-sites#Pallas.

Finnish Meteorological Institute (2018b). Kittilä Kenttärova June 7, 2018 12:00 AM — September 12, 2018 11:59 PM. URL: https://en.ilmatieteenlaitos.fi/download-observations#!/.

Fischer, H., M. Behrens, M. Bock, U. Richter, J. Schmitt, L. Loulergue, J. Chappellaz, R. Spahni, T. Blunier, M. Leuenberger, and T. F. Stocker (2008). Changing boreal methane sources and constant biomass burning during the last termination. *Nature* 452 (7189), 864–867.

Flessa, H., A. Rodionov, G. Guggenberger, H. Fuchs, P. Magdon, O. Shibistova, G. Zrazhevskaya, N. Mikheyeva, O. A. Kasansky, and C. Blodau (2008). Landscape controls of CH4 fluxes in a catchment of the forest tundra ecotone in northern Siberia. *Global Change Biology* 14 (9), 2040–2056.

Fox, J. and J. Hong (2009). Effect Displays in R for Multinomial and Proportional-Odds Logit Models: Extensions to the effects Package. *Journal of Statistical Software* 32 (1), 1–24. URL: http://www.jstatsoft.org/v32/i01/.

Garcia, J.-L., B. K. C. Patel, and B. Ollivier (2000). Taxonomic, phylogenetic, and ecological diversity of methanogenic Archaea. *Anaerobe* 6, 205–226.

Garnier, S. (2018). *viridis: Default Color Maps from 'matplotlib'*. R package version 0.5.1. URL: https://CRAN.R-project.org/package=viridis.

Gorham, E. (1991). Northern peatlands: role in the carbon cycle and probable responses to climatic warming. *Ecological applications* 1 (2), 182–195.

Grolemund, G. and H. Wickham (2011). Dates and Times Made Easy with lubridate. *Journal of Statistical Software* 40 (3), 1–25. URL: http://www.jstatsoft.org/v40/i03/.

Guisan, A. and N. E. Zimmermann (2000). Predictive habitat distribution models in ecology. *Ecological modelling* 135 (2-3), 147–186.

Gulledge, J. and J. P. Schimel (1998). Moisture control over atmospheric CH4 consumption and CO2 production in diverse Alaskan soils. *Soil Biology and Biochemistry* 30 (8-9), 1127–1132.

Gulledge, J. and J. P. Schimel (2000). Controls on soil carbon dioxide and methane fluxes in a variety of taiga forest stands in interior Alaska. *Ecosystems* 3 (3), 269–282.

Gulledge, J., P. A. Steudler, and J. P. Schimel (1998). Effect of CH4-starvation on atmospheric CH4 oxidizers in taiga and temperate forest soils. *Soil Biology and Biochemistry* 30 (10-11), 1463–1467.

Halsey, L. G., D. Curran-Everett, S. L. Vowler, and G. B. Drummond (2015). The fickle P value generates irreproducible results. *Nature methods* 12 (3), 179.

Hanson, R. S. and T. E. Hanson (1996). Methanotrophic bacteria. *Microbiological Reviews* 60 (2), 439–471.

Hari, P., P. Kolari, E. Nikinmaa, M. Pihlatie, J. Pumpanen, L. Kulmala, A. Simojoki, T. Vesala, and M. Kulmala (2008). Chapter 7.9: Annual energy, carbon, nitrogen and water fluxes and amounts at SMEAR II. *Boreal forest and climate change*. Ed. by P. Hari and L. Kulmala. Advances in global change research. Dordrecht: Springer, pp. 416–423.

Harrell, F. E. (2015). *Regression modeling strategies : with applications to linear models, logistic and ordinal regression, and survival analysis*. Second edition. Springer series in statistics. Cham: Springer, p. 582.

Heijmans, M. M., W. J. Arp, and F. S. Chapin III (2004). Controls on moss evaporation in a boreal black spruce forest. *Global Biogeochemical Cycles* 18 (2).

Hunter, J. D. (2007). Matplotlib: A 2D graphics environment. *Computing in Science & Engineering* 9 (3), 90–95.

Imdadullah, M., M. Aslam, and S. Altaf (2016). mctest: An R Package for Detection of Collinearity among Regressors. *The R Journal* 8(2), 499–509. URL: https://journal.r-project.org/archive/2016/RJ-2016-062/index.html.

Jeffers, J. (1960). *Experimental design and analysis in forest research*. Stockholm, Sweden: Almqvist and Wiksell, 172 pp.

Jones, A., V. Stolbovoy, C. Tarnocai, G. Broll, O. Spaargaren, L. Montanarella, and C.-L. Ping (2010). *Soil atlas of the northern circumpolar region*. European Commission, 144 pp.

Jögiste, K., L. Kulmala, J. Bäck, and P. Hari (2008). Chapter 5.2.7: Boreal zone. *Boreal forest and climate change*. Ed. by P. Hari and L. Kulmala. Advances in global change research. Dordrecht: Springer, pp. 124–126.

Kassambara, A. (2020). *rstatix: Pipe-Friendly Framework for Basic Statistical Tests*. R package version 0.4.0. URL: https://CRAN.R-project.org/package=rstatix.

Al-Kayssi, A., A. Al-Karaghouli, A. Hasson, and S. Beker (1990). Influence of soil moisture content on soil temperature and heat storage under greenhouse conditions. *Journal of Agricultural Engineering Research* 45, 241–252.

Keppler, F., J. T. Hamilton, M. Brass, and T. Rockmann (2006). Methane emissions from terrestrial plants under aerobic conditions. *Nature* 439, 187–191.

Kettunen, A., V. Kaitala, J. Alm, J. Silvola, H. Nykänen, and P. J. Martikainen (1996). Cross-correlation analysis of the dynamics of methane emissions from a boreal peatland. *Global Biogeochemical Cycles* 10 (3), 457–471.

Kirk, R. E. (2012). Experimental design. *Handbook of Psychology, Second Edition* 2, 23–45.

Kirk, R. E. (2013). *Experimental Design: Procedures for the Behavioral Sciences*. Thousand Oaks, California: SAGE Publications, Inc., p. 1056.

Kirschbaum, M. U. F., D. Bruhn, D. M. Etheridge, J. R. Evans, G. D. Farquhar, R. M. Gifford, K. I. Paul, and A. J. Winters (2006). A comment on the quantitative significance of aerobic methane release by plants. *Functional Plant Biology* 33 (6), 521–530.

Kirschke, S., P. Bousquet, P. Ciais, M. Saunois, J. G. Canadell, E. J. Dlugokencky, P. Bergamaschi, D. Bergmann, D. R. Blake, L. Bruhweiler, P. Cameron-Smith, S. Castaldi, F. Chevallier, L. Feng, A. Fraser, M. Heimann, E. L. Hodson, S. Houweling, B. Josse, P. J. Fraser, P. B. Krummel, J.-F. Lamarque, R. L. Langenfelds, C. Le Quéré, V. Naik, S. O'Doherty, P. I. Palmer, I. Pison, D. Plummer, B. Poulter, R. G. Prinn, M. Rigby, B. Ringeval, M. Santini, M. Schmidt, D. T. Shindel, I. J. Simpson, R. Spahni, L. P. Steele, S. A. Strode, K. Sudo, S. Szopa, G. R. van der Werf, A. Voulgarakis, M. van Weele, R. F. Weiss, J. E. Williams, and G. Zeng (2013). Three decades of global methane sources and sinks. *Nature Geoscience* 6, 813–823.

Klemedtsson, Å. and L. Klemedtsson (1997). Methane uptake in Swedish forest soil in relation to liming and extra N-deposition. *Biology and fertility of soils* 25 (3), 296–301.

Kljun, N., T. A. Black, T. J. Griffis, A. Barr, D. Gaumont-Guay, K. Morgenstern, J. McCaughey, and Z. Nesic (2007). Response of net ecosystem productivity of three boreal forest stands to drought. *Ecosystems* 10 (6), 1039–1055.

Korkiakoski, M. (2014). Water vapor correction functions for CO2 and CH4 in cavity ringdown spectroscopy. MA thesis. Department of physics, University of Helsinki, 45 pp.

Korkiakoski, M., J.-P. Tuovinen, M. Aurela, M. Koskinen, K. Minkkinen, P. Ojanen, T. Penttilä, J. Rainne, T. Laurila, and A. Lohila (2017). Methane exchange at the peatland forest floor–automatic chamber system exposes the dynamics of small fluxes. *Biogeosciences* 14 (7), 1947–1967.

Kähkönen, M. A., C. Wittmann, H. Ilvesniemi, C. J. Westman, and M. S. Salkinoja-Salonen (2002). Mineralization of detritus and oxidation of methane in acid boreal coniferous forest soils: seasonal and vertical distribution and effects of clear-cut. *Soil Biology and Biochemistry* 34 (8), 1191–1200.

Lai, D. Y. F. (2009). Methane dynamics in northern peatlands: a review. *Pedosphere* 19 (4), 409–421.

Langsrud, Ø. (2003). ANOVA for unbalanced data: Use Type II instead of Type III sums of squares. *Statistics and Computing* 13 (2), 163–167.

Le Mer, J., S. Escoffier, C. Chessel, and P.-A. Roger (1996). Microbiological aspects of methane emission in a rice field soil from the Camargue (France): 2. Methanotrophy and related microflora. *European journal of soil biology* 32 (2), 71–80.

Le Mer, J. and P. Roger (2001). Production, oxidation, emission and consumption of methane by soils: A review. *European Journal of Soil Biology* 37, 25–50.

Lehtonen, I., K. Ruosteenoja, and K. Jylhä (2014). Projected changes in European extreme precipitation indices on the basis of global and regional climate model ensembles. *International journal of climatology* 34 (4), 1208–1222.

Liebner, S. (2007). Adaptation, spatial variability, and phylogenetic characterization of methanotrophic communities in permafrost soils of the Lena Delta, Siberia. PhD thesis. Fachbereich Biologie/Chemie.

Littell, R. C., J. Pendergast, and R. Natarajan (2000). Modelling covariance structure in the analysis of repeated measures data. *Statistics in medicine* 19 (13), 1793–1819.

Logan, M. (2010). *Biostatistical design and analysis using R : a practical guide*. Ed. by M. Logan. Hoboken, N.J.: Wiley-Blackwell, 546 pp.

Lohila, A., T. Aalto, M. Aurela, J. Hatakka, J.-P. Tuovinen, J. Kilkki, T. Penttilä, J. Vuorenmaa, P. Hänninen, R. Sutinen, Y. Viisanen, and T. Laurila (2016). Large contribution of boreal upland forest soils to a catchment-scale CH4 balance in a wet year. *Geophysical Research Letters* 43 (6), 2946–2953.

Lohila, A., T. Penttilä, S. Jortikka, T. Aalto, P. Anttila, E. Asmi, M. Aurela, J. Hatakka, H. Hellén, H. Henttonen, P. Hänninen, J. Kilkki, K. Kyllönen, T. Laurila, A. Lepistö, H. Lihavainen, U. Makkonen, J. Paatero, M. Rask, R. Sutinen, J.-P. Tuovinen, J. Vuorenmaa, and Y. Viisanen (2015a). Preface to the special issue on integrated research of atmosphere, ecosystems and environment at Pallas. *Boreal Environment Research* 20 (4), 431–454.

Lohila, A., J.-P. Tuovinen, J. Hatakka, M. Aurela, J. Vuorenmaa, M. Haakana, and T. Laurila (2015b). Carbon dioxide and energy fluxes over a northern boreal lake. *Boreal Environment Research* 20 (4), 474–488.

Marion, G. (1996). Temperature enhancement experiments. *International Tundra Experiment: ITEX Manual*. Ed. by U. Molau and P. Mølgaard. Copenhagen: Danish Polar Center, pp. 17–22.

McBride, M. B. (1994). *Environmental Chemistry of Soils*. New York: Oxford University Press Inc, 406 pp.

McGuire, A. D., L. G. Anderson, T. R. Christensen, S. Dallimore, L. Guo, D. J. Hayes, M. Heimann, T. D. Lorenson, R. W. Macdonald, and N. Roulet (2009). Sensitivity of the carbon cycle in the Arctic to climate change. *Ecological Monographs* 79 (4), 523–555.

McKinney, W. (2011). pandas: a foundational Python library for data analysis and statistics. *Python for High Performance and Scientific Computing* 14.

Megonigal, J. P., M. E. Hines, and P. T. Visscher (2003). Anaerobic Metabolism: Linkages to Trace Gases and Aerobic Processes. *Treatise on Geochemistry* 8, 317–424.

Megonigal, J. P. and A. B. Guenther (2008). Methane emissions from upland forest soils and vegetation. *Tree Physiology* 28, 491–498.

Minkkinen, K., R. Korhonen, I. Savolainen, and J. Laine (2002). Carbon balance and radiative forcing of Finnish peatlands 1900–2100–the impact of forestry drainage. *Global Change Biology* 8 (8), 785–799.

Minkkinen, K., J. Laine, N. J. Shurpali, P. Mäkiranta, J. Alm, and T. Penttilä (2007). Heterotrophic soil respiration in forestry-drained peatlands. *Boreal Environment Research* 12, 115–126.

Moor, H., H. Rydin, K. Hylander, M. B. Nilsson, R. Lindborg, and J. Norberg (2017). Towards a trait-based ecology of wetland vegetation. *Journal of Ecology* 105 (6), 1623–1635.

Mäkiranta, P., T. Riutta, T. Penttilä, and K. Minkkinen (2010). Dynamics of net ecosystem CO_2 exchange and heterotrophic soil respiration following clearfelling in a drained peatland forest. *Agricultural and Forest Meteorology* 150 (12), 1585–1596.

National Land Survey of Finland (2020). National Land Survey of Finland: Topographic Database. https://tiedostopalvelu.maanmittauslaitos.fi/tp/kartta.

Neef, L., M. van Weele, and P. van Velthoven (2010). Optimal estimation of the present-day global methane budget. *Global Biogeochemical Cycles* 24 (GB4024), 1–10.

Niinistö, S. M., J. Silvola, and S. Kellomäki (2004). Soil CO2 efflux in a boreal pine forest under atmospheric CO2 enrichment and air warming. *Global Change Biology* 10 (8), 1363–1376.

Olefeldt, D., M. R. Turetsky, P. M. Crill, and A. D. McGuire (2013). Environmental and physical controls on northernterrestrial methane emissions across permafrost zones. *Global Change Biology* 19, 589–603.

Peterson, B. G. and P. Carl (2020). *PerformanceAnalytics: Econometric Tools for Performance and Risk Analysis*. R package version 2.0.4. URL: https://CRAN.R-project.org/package=PerformanceAnalytics.

Pihlatie, M., J. R. Christiansen, H. Aaltonen, J. F. Korhonen, A. Nordbo, T. Rasilo, G. Benanti, M. Giebels, M. Helmy, J. Sheehy, S. Jones, R. Juszczakk, R. Klefothl, R. Lobo-do-Valem, A. P. Rosa, P. Schreiber, D. Serc, S. Vicca, B. Wolf, and J. Pumpanen (2013). Comparison of static chambers to measure CH4 emissions from soils. *Agricultural and forest meteorology* 171, 124–136.

Pihlatie, M., A. Simojoki, J. Pumpanen, and P. Hari (2008). Chapter 7.6.5: Methane fluxes in boreal forest soil. *Boreal forest and climate change*. Ed. by P. Hari and L. Kulmala. Advances in global change research. Dordrecht: Springer, pp. 393–398.

Pinheiro, J., D. Bates, S. DebRoy, D. Sarkar, and R Core Team (2019). *nlme: Linear and Nonlinear Mixed Effects Models*. R package version 3.1-142. URL: https://CRAN.R-project.org/package=nlme.

Pirinen, P., H. Simola, J. Aalto, J.-P. Kaukoranta, P. Karlsson, and R. Ruuhela (2012). *Tilastoja Suomen ilmastosta 1981-2010*. Raportteja / Ilmatieteen laitos. Helsinki: Finnish Meteorological Institute.

Post, W. M., J. Pastor, P. J. Zinke, and A. G. Stangenberger (1985). Global patterns of soil nitrogen storage. *Nature* 317 (6038), 613.

Potter, C. S., E. A. Davidson, and L. V. Verchot (1996). Estimation of global biogeochemical controls and seasonality in soil methane consumption. *Chemosphere* 32 (11), 2219–2246.

Python Core Team (2019). *Python: A dynamic, open source programming language*. Python Software Foundation. Delaware, United States. URL: https://www.python.org/.

R Core Team (2019). *R: A Language and Environment for Statistical Computing*. R Foundation for Statistical Computing. Vienna, Austria. URL: https://www.R-project.org/.

Regina, K., M. Pihlatie, M. Esala, and L. Alakukku (2007). Methane fluxes on boreal arable soils. *Agriculture, ecosystems & environment* 119 (3-4), 346–352.

Rella, C., H. Chen, A. Andrews, A. Filges, C. Gerbig, J. Hatakka, A. Karion, N. L. Miles, S. J. Richardson, M. Steinbacher, C. Sweeney, B. Wastine, and C. Zellweger (2013). High accuracy measurements of dry mole fractions of carbon dioxide and methane in humid air. *Atmospheric Measurement Techniques* 6 (3), 837–860.

Rustad, L. E. and I. J. Fernandez (1998). Experimental soil warming effects on CO2 and CH4 flux from a low elevation spruce–fir forest soil in Maine, USA. *Global Change Biology* 4 (6), 597–605.

Rutherford, A. (2001). *Introducing ANOVA and ANCOVA : a GLM approach*. ISM (London, England). London ; Thousand Oaks, Calif.: SAGE, 182 pp.

Saari, A., P. J. Martikainen, A. Ferm, J. Ruuskanen, W. De Boer, S. R. Troelstra, and H. J. Laanbroek (1997). Methane oxidation in soil profiles of Dutch and Finnish coniferous forests with different soil texture and atmospheric nitrogen deposition. *Soil Biology and Biochemistry* 29 (11-12), 1625–1632.

Saari, A., P. J. Martikainen, and J. Heiskanen (1998). Effect of the organic horizon on methane oxidation and uptake in soil of a boreal Scots pine forest. *FEMS Microbiology Ecology* 26 (3), 245–255.

Savage, K., T. R. Moore, and P. M. Crill (1997). Methane and carbon dioxide exchanges between the atmosphere and northern boreal forest soils. *Journal of Geophysical Research: Atmospheres* 102 (D24), 29279–29288.

Schlesinger, W. H. and E. S. Bernhardt (2013). *Biogeochemistry : an analysis of global change*. Third edition. Amsterdam: Academic Press, 672 p.

Seneviratne, S. I., T. Corti, E. L. Davin, M. Hirschi, E. B. Jaeger, I. Lehner, B. Orlowsky, and A. J. Teuling (2010). Investigating soil moisture–climate interactions in a changing climate: A review. *Earth-Science Reviews* 99 (3-4), 125–161.

Serrano-Silva, N., Y. Sarria-Guzmán, L. Dendooven, and M. Luna-Guido (2014). Methanogenesis and methanotrophy in soil: a review. *Pedosphere* 24 (3), 291–307.

Simojoki, A., H. Garcia, M. Pihlatie, J. Pumpanen, J. Kurola, M. Salkinoja-Salonen, and P. Hari (2008a). Chapter 5.4: Soil. *Boreal forest and climate change*. Ed. by P. Hari and L. Kulmala. Advances in global change research. Dordrecht: Springer, pp. 132–142.

Simojoki, A., H. Garcia, M. Pihlatie, J. Pumpanen, J. Kurola, M. Salkinoja-Salonen, and P. Hari (2008b). Chapter 7.4: Environmental factors in soil. *Boreal forest and climate change*. Ed. by P. Hari and L. Kulmala. Advances in global change research. Dordrecht: Springer, pp. 306–312.

Sjögersten, S. and P. A. Wookey (2002). Spatio-temporal variability and environmental controls of methane fluxes at the forest–tundra ecotone in the Fennoscandian mountains. *Global Change Biology* 8 (9), 885–894.

Smith, K. A., T. Ball, F. Conen, K. E. Dobbie, J. Massheder, and A. Rey (2003). Exchange of greenhouse gases between soil and atmosphere: interactions of soil physical factors and biological processes. *European Journal of Soil Science* 54 (4), 779–791.

Smith, K., K. Dobbie, B. Ball, L. Bakken, B. Sitaula, S. Hansen, R. Brumme, W. Borken, S. Christensen, A. Priemé, D. Fowler, J. MacDonald, U. Skiba, L. Klemdtsson, A. Kasimir-Klemedtsson, A. Degoarska, and P. Orlanski (2000). Oxidation of atmospheric methane in Northern European soils, comparison with other ecosystems, and uncertainties in the global terrestrial sink. *Global Change Biology* 6 (7), 791–803.

Ström, L. and T. R. Christensen (2007). Below ground carbon turnover and greenhouse gas exchanges in a sub-arctic wetland. *Soil Biology and Biochemistry* 39 (7), 1689–1698.

Ström, L., M. Mastepanov, and T. R. Christensen (2005). Species-specific effects of vascular plants on carbon turnover and methane emissions from wetlands. *Biogeochemistry* 75, 65–82.

Tabachnick, B. G. (2014). *Using multivariate statistics*. 6. ed., Pearson new international edition. Always learning. Harlow: Pearson, 1056 pp.

Tierney, N., D. Cook, M. McBain, and C. Fay (2020). *naniar: Data Structures, Summaries, and Visualisations for Missing Data*. R package version 0.5.0. URL: https://CRAN.R-project.org/package=naniar.

Ueki, A., K. Ono, A. Tsuchiya, and K. Ueki (1997). Survival of methanogens in air-dried paddy field soil and their heat tolerance. *Water Science and Technology* 36 (6-7), 517–522.

van den Gon, H. D. and H.-U. Neue (1995). Methane emission from a wetland rice field as affected by salinity. *Plant and Soil* 170, 307–313.

Vesala, T., U. Rannik, and P. Hari (2008). Chapter 4: Transport. *Boreal forest and climate change*. Ed. by P. Hari and L. Kulmala. Advances in global change research. Dordrecht: Springer, pp. 75–88.

Vincent, A., B. Turner, and E. Tanner (2010). Soil organic phosphorus dynamics following perturbation of litter cycling in a tropical moist forest. *European Journal of Soil Science* 61, 48–57.

von Fischer, J. C. and L. O. Hedin (2002). Separating methane production and consumption with a field-based isotope pool dilution technique. *Global Biogeochemical Cycles* 16 (3), 8–1.

von Fischer, J., R. C. Rhew, G. M. Ames, B. K. Fosdick, and P. E. von Fischer (2010). Vegetation height and other controls of spatial variability in methane emissions from the Arctic coastal tundra at Barrow, Alaska. *Journal of Geophysical Research: Biogeosciences* 115 (G4).

Wagner, D., E. M. Pfeiffer, and E. Bock (1999). Methane production in aerated marshland and model soils: effects of microflora and soil texture. *Soil Biology and Biochemistry* 31 (7), 999–1006.

Wang, F. L. and J. R. Bettany (1997). Methane emission from Canadian prairie and forest soils under short term flooding conditions. *Nutrient Cycling in Agroecosystems* 49 (1-3), 197–202.

Whalen, S. C. (2005). Biogeochemistry of methane exchange between natural wetlands and the atmosphere. *Environmental Engineering Science* 22 (1), 73–94.

Whalen, S. C. and W. S. Reeburgh (1996). Moisture and temperature sensitivity of CH4 oxidation in boreal soils. *Soil Biology and Biochemistry* 28 (10-11), 1271–1281.

Whalen, S. C., W. S. Reeburgh, and K. S. Kizer (1991). Methane consumption and emission by taiga. *Global Biogeochemical cycles* 5 (3), 261–273.

Wickham, H. (2011). The Split-Apply-Combine Strategy for Data Analysis. *Journal of Statistical Software* 40 (1), 1–29. URL: http://www.jstatsoft.org/v40/i01/.

Wickham, H. (2016). *ggplot2: Elegant Graphics for Data Analysis*. Springer-Verlag New York. ISBN: 978-3-319-24277-4. URL: https://ggplot2.tidyverse.org.

Wickham, H., R. François, L. Henry, and K. Muller (2020). *dplyr: A Grammar of Data Manipulation*. R package version 0.8.5. URL: https://CRAN.R-project.org/package=dplyr.

Wickham, H. and L. Henry (2020). *tidyr: Tidy Messy Data*. R package version 1.0.2. URL: https://CRAN.R-project.org/package=tidyr.

Wu, Z., P. Dijkstra, G. W. Koch, J. Peñuelas, and B. A. Hungate (2011). Responses of terrestrial ecosystems to temperature and precipitation change: A meta-analysis of experimental manipulation. *Global Change Biology* 17 (2), 927–942.

Wuebbles, D. J. and K. Hayhoe (2002). Atmospheric methane and global change. *Earth-Science Reviews* 57, 177–210.

Xu, S., L. Liu, and E. J. Sayer (2013). Variability of above-ground litter inputs alters soil physicochemical and biological processes: a meta-analysis of litterfall-manipulation experiments. *Biogeosciences* 10 (11), 7423–7433.

Xu, X., W. J. Riley, C. D. Koven, D. P. Billesbach, R. Y.-W. Chang, R. Commane, E. S. Euskirchen, S. Hartery, Y. Harazono, H. Iwata, K. C. McDonald, C. E. Miller, W. C. Oechel, B. Poulter, N. Raz-Yaseef, C. Sweeny, M. Torn, S. C. Wofsy, Z. Zhang, and D. Zona (2016). A multi-scale comparison of modeled and observed seasonal methane emissions in northern wetlands. *Biogeosciences* 13, 5043–5056.

Yavitt, J. B., D. M. Downey, G. E. Lang, and A. J. Sexstone (1990). Methane consumption in two temperate forest soils. *Biogeochemistry* 9 (1), 39–52.

Yavitt, J. B., T. J. Fahey, and J. A. Simmons (1995). Methane and carbon dioxide dynamics in a northern hardwood ecosystem. *Soil Science Society of America Journal* 59 (3), 796–804.

Ylläsjärvi, I. and T. Kuuluvainen (2009). How homogeneous is the boreal forest? Characteristics and variability of old-growth forest on a Hylocomium—Myrtillus site type in the Pallas-Yllästunturi National Park, northern Finland. *Annales Botanici Fennici*. Vol. 46. 4, pp. 263–280.

Zeileis, A. and G. Grothendieck (2005). zoo: S3 Infrastructure for Regular and Irregular Time Series. *Journal of Statistical Software* 14 (6), 1–27. DOI: 10.18637/jss.v014.i06.

Zhuang, Q., J. M. Melillo, D. W. Kicklighter, R. G. Prinn, A. D. McGuire, P. A. Steudler, B. S. Felzer, and S. Hu (2004). Methane fluxes between terrestrial ecosystems and the atmosphere at northern high latitudes during the past century: A retrospective analysis with a process-based biogeochemistry model. *Global Biogeochemical Cycles* 18 (3).

Appendices

A Organic litter and root exclusion

Table 8: Details of the dimensions of the extraction subplots. Mean depth was calculated from the four sides of the extracted area and root depth was the approximate depth at which the visible roots of vegetation ended. O horizon is the topmost soil layer with live vegetation and organic matter and approximately corresponds to the extracted organic layer used in the soil layer analyses. The extraction pit refers to the total area of the pit dug around the excluded subplot and collar and the last column refers to the total area of the extracted plot (figure 18). The last row ("All") contains the averaged values of the measured dimensions.

Plot	**Mean depth (cm)**	**Mean root depth (cm)**	**Mean O thickness (cm)**	**Extraction pit** (m^2)	**Extracted** (m^2)
IE1	32.0	6.92	24.75	1.27	1.05
IE2	35.25	8.71	29.42	1.34	1.29
IE3	29.83	3.42	24.42	1.24	1.11
CE1	31.67	4.83	25.83	1.12	1.19
CE2	30.42	4.38	25.17	1.49	1.15
CE3	35.08	6.0	30.42	1.29	1.19
All	32.38	5.71	26.97	1.29	1.16

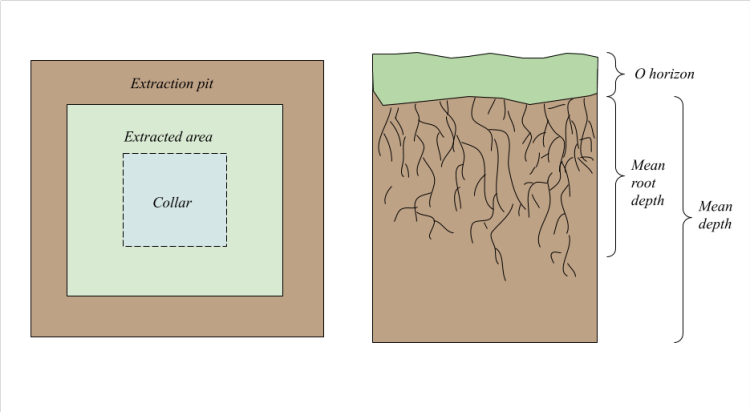

Figure 18: An example figure of the extraction subplots (IE and CE) and the dimensions which the calculations of table 8 are based on.

B Organic litter additions

Table 9: Added organic litter with dates. "Weight" refers to the weight of the collected litter per site or subplot, "total" to the total sum of the collected litter, "sample" to the fresh weight of the sample and "added" to the amount of litter added to each IA and CA subplot. In 5.7.2018 both the weekly organic litter from the exclusion nets and old accumulated organic litter were collected from the exclusion subplots and added to IA and CA subplots.

Date	Site/plot	Weight (g)	Total (g)	Sample (g)	Added (g)
28.6.2018	Irrigation	0.58			
	Control	1.1	1.68	0.25	0.24
5.7.2018	Irrigation	1.35			
	Control	0.13	1.48	0.15	0.22
	IE1	55.39			
	IE2	176.55			
	IE3	38.94			
	CE1	361.14			
	CE2	108.77			
	CE3	171.23	912.02	91.21	136.80
12.7.2018	Irrigation	0.62			
	Control	2.01	2.63	0.26	0.40
18.7.2018	Irrigation	0.34			
	Control	0.13	0.47	0.04	0.07
2.8.2018	Irrigation	0.45			
	Control	1.22	1.67	0.17	0.25
8.8.2018	Irrigation	0.2			
	Control	1.18	1.38	0.13	0.21
15.8.2018	Irrigation	1.96			
	Control	0.33	2.29	0.23	0.34
21.8.2018	Irrigation	0.08			
	Control	0.34	0.42	0.04	0.06
4.9.2018	Irrigation	0.32			
	Control	0.14	0.46	0.04	0.07

C Field measurement details

Table 10: Details of the field measurement instruments per subplot and sensor installment dates. [a] The sensor malfunctioned and no soil temperature data was obtained from that sensor.

Plot	Temperature sensor	Date of installment	Moisture sensor	Date of installment
IO1	HydraProbe	5.6.2018	HydraProbe	5.6.2018
IO2	HOBO & HydraProbe	6.6.2018 & 5.6.2018	HydraProbe	5.6.2018
IO3	HOBO & HydraProbe	6.6.2018 & 5.6.2018	HydraProbe	5.6.2018
IO4	Soil Scout	5.6.2018	Soil Scout	5.6.2018
IA1	Soil Scout	5.6.2018	Soil Scout	5.6.2018
IA2	Soil Scout	28.5.2018	Soil Scout	28.5.2018
IA3	Soil Scout	6.6.2018	Soil Scout	6.6.2018
IE1	HydraProbe	27.5.2018	HydraProbe	27.5.2018
IE2	HOBO & HydraProbe	27.5.2018	HydraProbe	27.5.2018
IE3	Soil Scout	28.5.2018	Soil Scout	28.5.2018
IT1	HydraProbe	5.6.2018	HydraProbe	5.6.2018
IT2	Soil Scout	5.6.2018	Soil Scout	5.6.2018
IT3	Soil Scout	5.6.2018	Soil Scout	5.6.2018
CO1	HOBO	5.6.2018	HOBO	5.6.2018
CO2	HOBO	6.6.2018	HOBO	6.6.2018
CO3	HOBO	6.6.2018	HOBO	6.6.2018
CO4	HOBO	6.6.2018	HOBO	6.6.2018
CA1	Soil Scout	28.5.2018	Soil Scout	28.5.2018
CA2	HOBO	6.6.2018	HOBO	6.6.2018
CA3	HOBO	6.6.2018	HOBO	6.6.2018
CE1	HOBO	27.5.2018	HOBO	27.5.2018
CE2	Soil Scout	27.5.2018	Soil Scout	27.5.2018
CE3	Soil Scout	27.5.2018	Soil Scout	27.5.2018
CT1	HOBO	6.6.2018	HOBO	6.6.2018
CT2	HOBO[a]	6.6.2018	HOBO	6.6.2018
CT3	HOBO	6.6.2018	HOBO	6.6.2018

D Irrigation measures

Table 11: Details of the irrigation measures by each irrigation event. The pumped water is the amount of water pumped to the irrigation site without calculating its even distribution into the site in millimetres and the gauge mean refers to the average of the water amounts measured by the 22 rain gauges. Water collected by the gauges was not measured every time due to calm weather and seemingly even distribution of irrigated water.

Date	Time	Pumped water (l)	Gauge mean (mm)
28.5.2018	17:20-18:00	1000	9.7
1.6.2018	16:50-17:20	1000	9.5
5.6.2018	10:25-12:00	2000	16.8
7.6.2018	18:40-19:20	1000	10.4
8.6.2018	14:35-15:30	1000	11.3
11.6.2018	15:55-16:45	1000	11.3
13.6.2018	15:25-16:15	1000	10.7
15.6.2018	13:35-15:25	2000	18.4
18.6.2018	17:00	1000	10.9
20.6.2018	16:00-17:35	2000	21.4
21.6.2018	13:40-15:20	2000	-
22.6.2018	-	2000	-
25.6.2018	-	1000	-
28.6.2018	16:50-18:30	2000	-
29.6.2018	14:15	1900	-
2.7.2018	20:50-22:40	2000	-
3.7.2018	17:45-19:20	2000	-
4.7.2018	18:30-21:00	2000	-
5.7.2018	15:05-17:40	2000	19.8
6.7.2018	14:05-15:40	2000	22.5
9.7.2018	16:05-18:00	2000	-
10.7.2018	15:30-17:00	2000	-
11.7.2018	17:20-19:00	2000	-
12.7.2018	18:40-20:20	2000	-
13.7.2018	17:05-18:55	2000	-
16.7.2018	18:00-19:30	2000	-
17.7.2018	15:45-17:30	2000	20.4
18.7.2018	17:30-19:00	2000	18.7
19.7.2018	19:10-20:50	2000	19.6
23.7.2018	16:30-19:20	2000	21.2
24.7.2018	16:45-19:35	2000	20.0
25.7.2018	16:40-19:30	2000	-
26.7.2018	16:30-19:10	2000	-
27.7.2018	13:40-16:50	2000	-
30.7.2018	15:50-16:40	1000	-
31.7.2018	17:30-18:20	1000	-
2.8.2018	15.10-16:40	1600	18.8
6.8.2018	15:30-16:30	1000	-
7.8.2018	17:55-19:30	2000	-
8.8.2018	15:20	2000	-
10.8.2018	15:45-17:45	2000	-
13.8.2018	17:10-18:00	1000	-
14.8.2018	15:45-17:45	2000	-
15.8.2018	14:25-16:05	2000	-
17.8.2018	14:00-16:00	2000	18.8
21.8.2018	16:05-17:55	2000	24.3
22.8.2018	-	2000	-
23.8.2018	-	2000	20.5
24.8.2018	15:30-17:30	2000	22.8
27.8.2018	15:15-16:55	2000	20.2
28.8.2018	-	2000	-
29.8.2018	17:05-18:45	2000	24.2
30.8.2018	13:50-15:40	2000	19.8
31.8.2018	-	2000	-
3.9.2018	17:00-19:40	2000	23.3
4.9.2018	15:15-18:00	2000	21.9
5.9.2018	10:30-13:00	2000	-
6.9.2018	10:30-13:10	2000	-
7.9.2018	10:40-11:30	1000	-

E Descriptive statistics of the variables

Table 12: Descriptive statistics of soil temperature, soil moisture and CH_4 flux (linear fit, uptake rate) by month for the whole study site.

variable	month	max	min	mean	median	SD	NAs
Soil temperature (°C)	June	15.247	4.212	8.948	8.818	2.367	0
	July	21.231	7.386	14.223	14.144	2.921	0
	August	21.758	8.141	12.731	12.174	2.685	0
	September	15.708	7.550	10.180	9.310	2.069	0
Soil moisture (%VWC)	June	39.695	2.859	21.476	22.242	9.957	0
	July	41.630	1.568	22.347	23.648	10.400	0
	August	44.290	1.779	24.895	28.135	10.734	0
	September	43.094	8.179	24.021	26.211	10.704	0
CH_4 flux ($\mu g\ m^{-2}\ h^{-1}$)	June	-48.021	-460.371	-201.790	-202.346	75.912	1
	July	-45.477	-643.889	-218.208	-201.396	115.624	4
	August	-38.554	-588.308	-190.313	-168.417	101.255	2
	September	-46.416	-442.534	-191.401	-184.596	85.648	1

Table 13: Descriptive statistics of soil temperature, soil moisture and CH_4 flux (linear fit, uptake rate) by month for the main plots (C= control and I= irrigation).

variable	month	plot	max	min	mean	median	SD	NAs
Soil temperature (°C)	June	C	11.824	4.212	7.802	8.069	1.599	0
		I	15.247	5.135	10.007	9.540	2.468	0
	July	C	17.971	7.386	12.690	12.800	2.070	0
		I	21.231	9.041	15.638	15.714	2.879	0
	August	C	18.557	8.141	11.457	11.212	1.740	0
		I	21.758	8.286	13.907	13.489	2.863	0
	September	C	11.182	7.550	9.015	8.976	0.639	0
		I	15.708	7.756	11.255	10.127	2.335	0
Soil moisture (%VWC)	June	C	26.016	2.859	12.606	11.689	5.106	0
		I	39.695	22.000	30.347	29.709	3.829	0
	July	C	21.258	1.568	12.784	11.355	4.458	0
		I	41.630	26.038	31.910	30.910	3.658	0
	August	C	33.341	1.779	15.581	13.560	6.171	0
		I	44.290	26.305	34.209	33.503	4.327	0
	September	C	30.668	8.179	14.528	12.975	5.398	0
		I	43.094	25.910	33.514	32.213	4.396	0
CH_4 flux ($\mu g\ m^{-2}\ h^{-1}$)	June	C	-101.059	-460.371	-223.014	-221.163	74.031	0
		I	-48.021	-328.763	-180.116	-190.062	72.290	1
	July	C	-107.098	-643.889	-285.911	-274.254	110.942	0
		I	-45.477	-307.014	-143.501	-145.675	62.716	4
	August	C	-105.649	-588.308	-248.413	-221.501	104.586	0
		I	-38.554	-247.117	-130.723	-126.575	50.772	2
	September	C	-121.636	-442.534	-239.174	-222.364	78.599	0
		I	-46.416	-320.709	-143.629	-145.080	63.412	1

Table 14: Descriptive statistics of soil temperature (°C) by month for the subtreatment groups (C=control, I=irrigation, E=root and organic litter exclusion, A=organic litter addition, O=no subtreatment, T=warming).

month	treatment	max	min	mean	median	SD	NAs
June	CE	9.652	4.738	7.475	8.016	1.435	0
	CA	11.322	4.949	8.227	8.375	1.553	0
	CO	11.824	4.212	7.680	7.719	1.783	0
	CT	10.101	5.140	7.899	8.332	1.398	0
	IE	14.885	5.246	10.687	10.885	2.428	0
	IA	10.482	5.135	8.218	8.739	1.479	0
	IO	15.247	5.884	11.081	11.366	2.200	0
	IT	14.855	5.480	9.683	9.270	2.595	0
July	CE	15.183	8.552	12.566	12.863	1.791	0
	CA	17.126	8.362	12.853	12.777	2.016	0
	CO	17.971	7.386	12.647	12.631	2.410	0
	CT	15.842	8.797	12.719	13.061	1.818	0
	IE	21.061	9.460	16.325	16.456	2.774	0
	IA	17.359	9.041	13.855	14.306	2.170	0
	IO	21.231	9.775	16.739	16.765	2.629	0
	IT	21.088	9.349	15.267	15.365	3.017	0
August	CE	15.603	8.165	11.146	10.923	1.736	0
	CA	17.232	8.141	11.484	11.255	1.818	0
	CO	18.557	8.875	11.495	11.148	1.758	0
	CT	16.411	9.116	11.451	11.218	1.614	0
	IE	21.653	8.664	14.687	15.004	2.889	0
	IA	17.720	8.286	11.947	11.876	2.139	0
	IO	21.758	8.744	14.787	14.597	2.677	0
	IT	21.719	9.258	13.763	13.281	2.863	0
September	CE	10.077	7.652	8.723	8.747	0.599	0
	CA	10.438	7.550	8.820	8.734	0.690	0
	CO	11.182	8.506	9.264	9.171	0.577	0
	CT	10.316	8.711	9.247	9.079	0.458	0
	IE	15.708	8.347	12.123	12.303	2.346	0
	IA	10.287	7.756	9.084	9.094	0.678	0
	IO	15.482	8.105	12.192	12.324	2.034	0
	IT	15.521	8.922	11.308	9.996	2.410	0

Table 15: Descriptive statistics of soil moisture (%VWC) by month for the subtreatment groups (C=control, I=irrigation, E=root and organic litter exclusion, A=organic litter addition, O=no subtreatment, T=warming).

month	treatment	max	min	mean	median	SD	NAs
June	CE	21.000	8.037	15.257	15.000	4.419	0
	CA	26.016	9.917	14.465	13.261	3.899	0
	CO	23.364	2.859	11.292	10.175	6.285	0
	CT	14.041	6.049	9.848	10.603	2.435	0
	IE	31.278	22.000	27.100	26.961	2.777	0
	IA	34.432	26.482	30.372	30.449	2.061	0
	IO	39.695	26.225	32.524	32.755	4.698	0
	IT	35.212	27.273	30.666	30.015	2.351	0
July	CE	20.964	10.698	16.290	18.000	3.812	0
	CA	21.258	10.765	13.640	12.699	2.647	0
	CO	20.783	1.568	11.127	9.569	5.614	0
	CT	12.951	7.931	10.632	10.719	1.270	0
	IE	32.190	26.038	28.855	29.059	1.748	0
	IA	36.229	27.258	32.918	32.967	2.025	0
	IO	41.630	26.434	33.160	32.460	4.708	0
	IT	38.232	28.063	32.290	31.453	2.994	0
August	CE	29.386	10.791	19.454	21.173	5.704	0
	CA	33.341	11.503	18.829	14.836	6.922	0
	CO	21.809	1.779	13.936	12.851	4.618	0
	CT	14.285	7.425	10.655	9.808	1.847	0
	IE	32.927	26.305	29.941	30.506	1.699	0
	IA	41.714	31.291	35.362	34.709	2.082	0
	IO	44.290	27.913	34.767	34.688	4.312	0
	IT	43.630	29.170	36.579	37.643	4.888	0
September	CE	25.882	11.157	17.788	19.997	4.563	0
	CA	30.668	12.811	17.510	13.627	5.810	0
	CO	20.925	9.232	13.089	10.705	4.541	0
	CT	15.021	8.179	10.205	8.919	2.156	0
	IE	32.050	25.910	29.216	29.324	1.828	0
	IA	38.892	30.025	34.110	34.067	2.347	0
	IO	41.637	28.045	33.939	33.245	4.142	0
	IT	43.094	28.691	36.652	37.286	4.895	0

Table 16: Descriptive statistics of CH_4 flux ($\mu g\ m^{-2}\ h^{-1}$, linear fit, uptake rate) by month for the subtreatment groups (C=control, I=irrigation, E=root and organic litter exclusion, A=organic litter addition, O=no subtreatment, T=warming).

month	treatment	max	min	mean	median	SD	NAs
June	CE	-101.059	-303.100	-195.495	-183.140	61.573	0
	CA	-112.662	-295.073	-202.351	-205.049	60.724	0
	CO	-189.610	-460.371	-297.439	-283.889	71.442	0
	CT	-130.613	-285.786	-199.478	-193.500	48.177	0
	IE	-108.943	-328.763	-207.799	-192.963	65.567	1
	IA	-56.453	-250.914	-112.352	-90.435	58.043	0
	IO	-48.021	-309.583	-196.893	-216.018	76.635	0
	IT	-67.866	-223.540	-173.219	-195.946	52.308	0
July	CE	-107.098	-348.363	-217.054	-200.348	69.335	0
	CA	-129.125	-526.228	-296.840	-259.008	119.584	0
	CO	-208.219	-643.889	-363.229	-338.921	112.917	0
	CT	-153.237	-468.185	-309.606	-291.396	90.176	0
	IE	-47.501	-307.014	-168.434	-167.058	69.958	4
	IA	-53.611	-142.899	-86.848	-89.574	25.551	0
	IO	-68.619	-261.905	-168.731	-164.567	43.595	0
	IT	-45.477	-214.259	-126.836	-145.675	56.005	0
August	CE	-105.649	-360.721	-196.200	-176.181	67.333	0
	CA	-129.332	-475.370	-247.914	-221.602	101.196	0
	CO	-154.447	-588.308	-318.519	-301.431	120.579	0
	CT	-152.711	-511.782	-259.865	-262.151	96.726	0
	IE	-92.115	-247.117	-153.017	-135.991	51.946	2
	IA	-47.614	-95.468	-71.080	-75.108	14.504	0
	IO	-104.000	-199.072	-152.815	-150.784	29.934	0
	IT	-38.554	-166.663	-119.291	-140.251	43.643	0
September	CE	-148.029	-306.451	-217.362	-192.783	63.541	0
	CA	-153.069	-326.188	-237.510	-235.363	75.126	0
	CO	-133.860	-442.534	-283.909	-268.222	98.599	0
	CT	-121.636	-312.589	-221.180	-207.942	71.394	0
	IE	-91.322	-320.709	-175.515	-179.430	65.143	1
	IA	-50.679	-119.673	-72.617	-64.144	26.568	0
	IO	-110.550	-221.863	-170.199	-184.009	37.146	0
	IT	-46.416	-184.962	-120.757	-142.679	54.375	0

Table 17: Descriptive statistics of CH_4 flux ($\mu g\ m^{-2}\ h^{-1}$, linear fit, uptake rate) by week for the whole study site starting from 15.6.2018. The weeks correspond to the dates of flux measurements starting from 15.6.2018 (week 01) and ending on 11.9.2018 (week 14). Week 07 contains the average of measurements executed in 23., 25. and 26.7.2018.

week	max	min	mean	median	SD	NAs
01	-67.866	-460.371	-220.035	-207.197	82.925	0
02	-48.021	-356.578	-179.611	-165.371	75.415	0
03	-87.906	-354.419	-205.852	-217.350	64.625	1
04	-49.782	-499.807	-212.487	-208.367	90.571	0
05	-45.477	-436.481	-183.074	-153.237	100.553	1
06	-47.501	-471.214	-199.087	-169.782	119.811	1
07	-45.897	-643.889	-237.744	-208.027	122.673	2
08	-49.122	-588.308	-241.368	-178.101	148.390	1
09	-38.554	-519.278	-205.030	-192.593	101.376	0
10	-48.575	-348.705	-168.668	-154.742	68.058	1
11	-61.662	-373.187	-172.248	-160.555	74.200	0
12	-47.614	-405.844	-165.169	-149.448	77.856	0
13	-46.416	-442.534	-199.803	-187.802	95.296	0
14	-50.679	-320.709	-182.439	-183.134	74.574	1

Table 18: Descriptive statistics of CH_4 flux ($\mu g\ m^{-2}\ h^{-1}$, linear fit, uptake rate) by week for the main plots (C=control, I=irrigation). The weeks correspond to the dates of flux measurements starting from 15.6.2018 (week 01) and ending on 11.9.2018 (week 14). Week 07 contains the average of measurements executed in 23., 25. and 26.7.2018.

week	plot	max	min	mean	median	SD	NAs
01	C	-117.672	-460.371	-248.842	-253.842	83.640	0
	I	-67.866	-317.497	-191.229	-194.454	73.795	0
02	C	-101.059	-356.578	-211.857	-220.928	72.062	0
	I	-48.021	-265.499	-147.365	-137.989	65.900	0
03	C	-112.662	-354.419	-208.342	-199.275	62.532	0
	I	-87.906	-328.763	-203.196	-220.894	68.885	1
04	C	-129.125	-499.807	-246.503	-238.954	86.523	0
	I	-49.782	-261.905	-163.010	-178.765	74.531	0
05	C	-107.098	-436.481	-240.517	-226.263	98.985	0
	I	-45.477	-264.579	-121.800	-111.008	58.089	1
06	C	-159.004	-471.214	-288.228	-277.361	96.007	0
	I	-47.501	-205.531	-104.004	-108.918	46.003	1
07	C	-120.140	-643.889	-313.407	-290.128	120.067	0
	I	-45.897	-307.014	-158.792	-163.123	59.712	2
08	C	-154.564	-588.308	-345.954	-341.467	132.001	0
	I	-49.122	-246.551	-129.810	-130.329	51.775	1
09	C	-121.512	-519.278	-266.586	-265.649	98.398	0
	I	-38.554	-247.117	-143.474	-146.949	58.938	0
10	C	-105.649	-348.705	-203.522	-199.161	65.365	0
	I	-48.575	-232.010	-131.489	-119.665	49.784	1
11	C	-119.985	-373.187	-213.421	-201.011	72.965	0
	I	-61.662	-226.792	-131.076	-131.858	49.378	0
12	C	-118.149	-405.844	-212.583	-202.457	74.699	0
	I	-47.614	-219.650	-117.755	-119.685	46.382	0
13	C	-154.335	-442.534	-262.100	-266.009	83.992	0
	I	-46.416	-224.181	-137.507	-140.170	58.602	0
14	C	-121.636	-308.933	-214.719	-196.491	66.620	0
	I	-50.679	-320.709	-150.160	-146.001	69.633	1

Table 19: Descriptive statistics of soil CH_4 flux ($\mu g\ m^{-2}\ h^{-1}$, linear fit, uptake rate) in organic (O) and mineral (M) layers in the whole study site and main plots during the whole study period.

treatment level	plot	layer	max	min	mean	median	SD	NAs
Whole study site	-	O	–47.501	-310.085	-172.372	-164.411	59.476	0
	-	M	-78.880	-360.721	-209.713	-205.357	71.236	7
Main plot	C	O	-101.059	-310.085	-189.841	-180.210	59.010	0
		M	-121.623	-360.721	-223.351	-209.257	69.923	0
	I	O	-47.501	-274.494	-154.531	-157.423	55.019	0
		M	-78.880	-328.763	-193.277	-197.185	70.179	7

Table 20: Descriptive statistics of soil CH_4 flux ($\mu g\ m^{-2}\ h^{-1}$, linear fit, uptake rate) in organic (O) and mineral (M) layers in the whole study site and main plots, divided into four months from June to September.

treatment level	month	plot	layer	max	min	mean	median	SD	NAs
Whole study site	June	-	O	-101.059	-287.319	-190.933	-183.510	57.887	0
		-	M	-108.943	-328.763	-212.629	-192.963	67.768	1
	July	-	O	-47.501	-310.085	-175.390	-172.183	64.600	0
		-	M	-78.880	-348.363	-217.043	-220.732	77.128	4
	August	-	O	-92.115	-303.058	-157.024	-152.890	52.236	0
		-	M	-99.554	-360.721	-194.992	-185.348	69.744	2
	September	-	O	-91.322	-295.614	-174.094	-166.883	60.986	0
		-	M	-140.062	-320.709	-223.251	-209.774	65.278	0
Main plot	June	C	O	-101.059	-287.319	-188.259	-185.955	62.009	0
			M	-131.590	-303.100	-202.732	-180.325	63.981	0
		I	O	-109.139	-272.246	-193.607	-181.065	57.092	0
			M	-108.943	-328.763	-223.764	-197.654	74.505	1
	July	C	O	-107.098	-310.085	-197.563	-187.549	61.134	0
			M	-144.987	-348.363	-236.545	-222.140	73.183	0
		I	O	-47.501	-274.494	-151.913	-162.638	61.304	0
			M	-78.880	-307.014	-190.039	-211.330	76.968	4
	August	C	O	-105.649	-303.058	-177.419	-161.851	56.715	0
			M	-121.623	-360.721	-214.981	-193.842	73.613	0
		I	O	-92.115	-203.682	-136.628	-119.665	39.296	0
			M	-99.554	-247.117	-171.927	-159.260	59.554	2
	September	C	O	-148.029	-295.614	-200.101	-172.855	63.704	0
			M	-166.748	-306.451	-238.075	-222.364	63.544	0
		I	O	-91.322	-214.533	-148.088	-147.040	50.011	0
			M	-140.062	-320.709	-208.426	-197.185	70.713	0

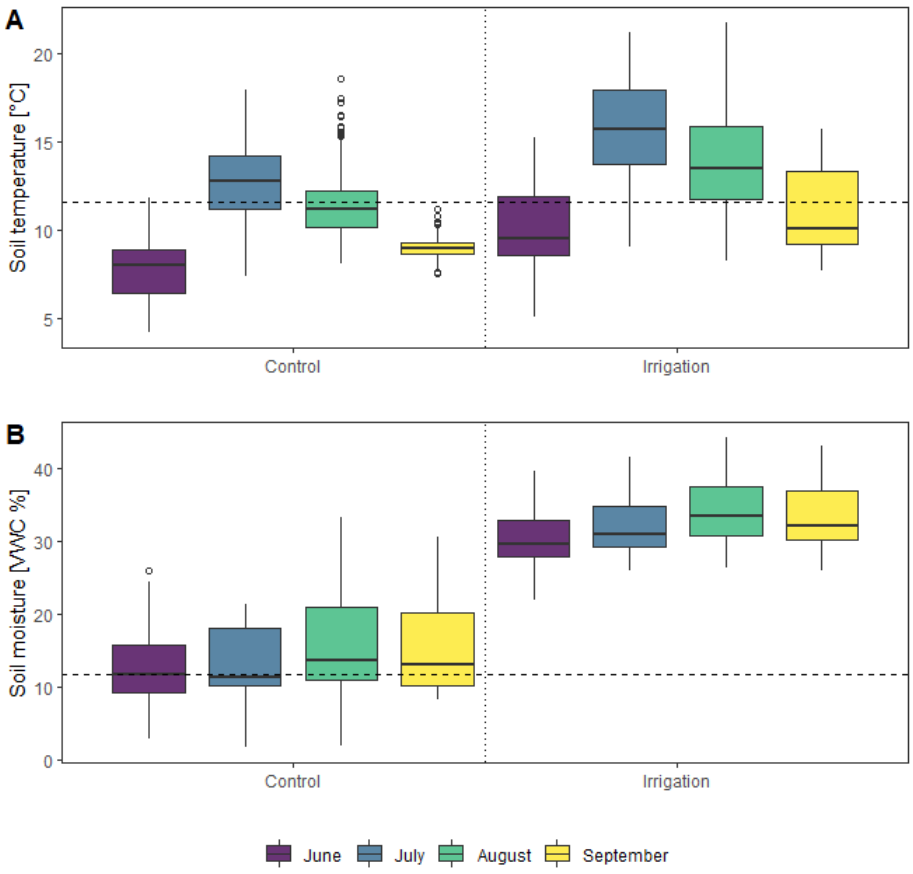

Figure 19: Boxplots of soil temperature and soil moisture by main plots, divided by months. The horizontal dashed line represents the median of the whole study period in both main plots together.

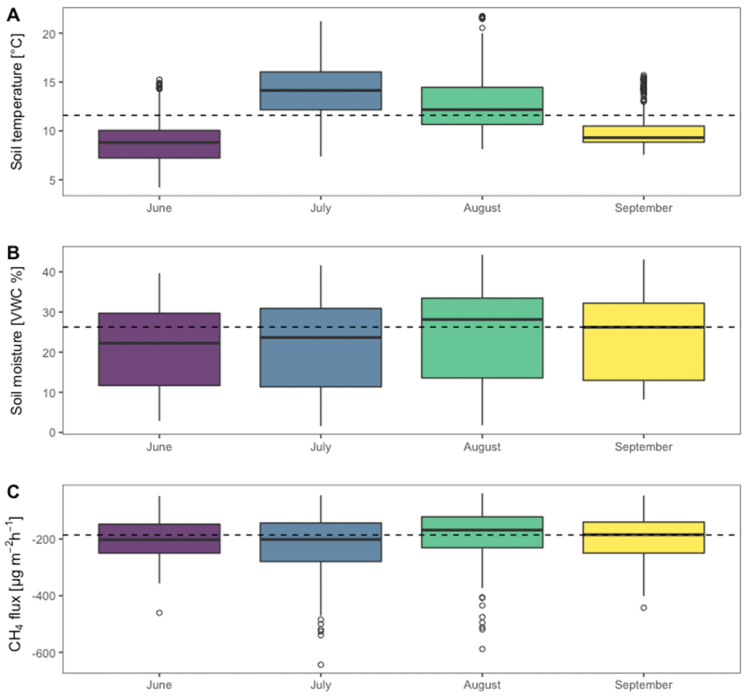

Figure 20: Boxplots of soil temperature (A, °C), soil moisture (B, %VWC) and CH_4 flux (C, $\mu g\ m^{-2}\ h^{-1}$, linear fit, uptake rate) in the whole study site, divided by months. The horizontal dashed line represents the median of the whole study period.

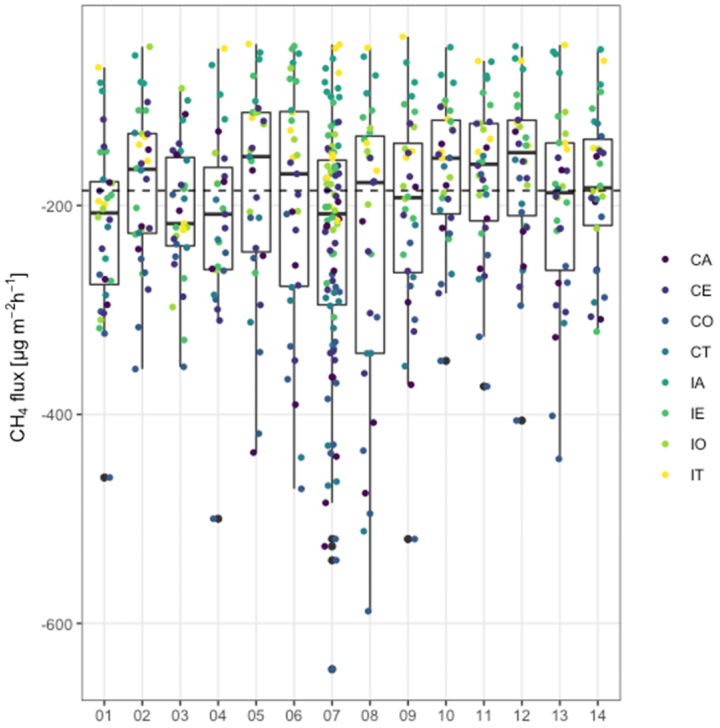

Figure 21: CH_4 flux ($\mu g\ m^{-2}\ h^{-1}$, linear fit, uptake rate) along subtreatments by week. Each week contained one CH_4 flux measurement campaign, with the exception of week 07 which included three measurement campaigns in one week (23., 25. and 26.7.2018).

F Variable frequencies

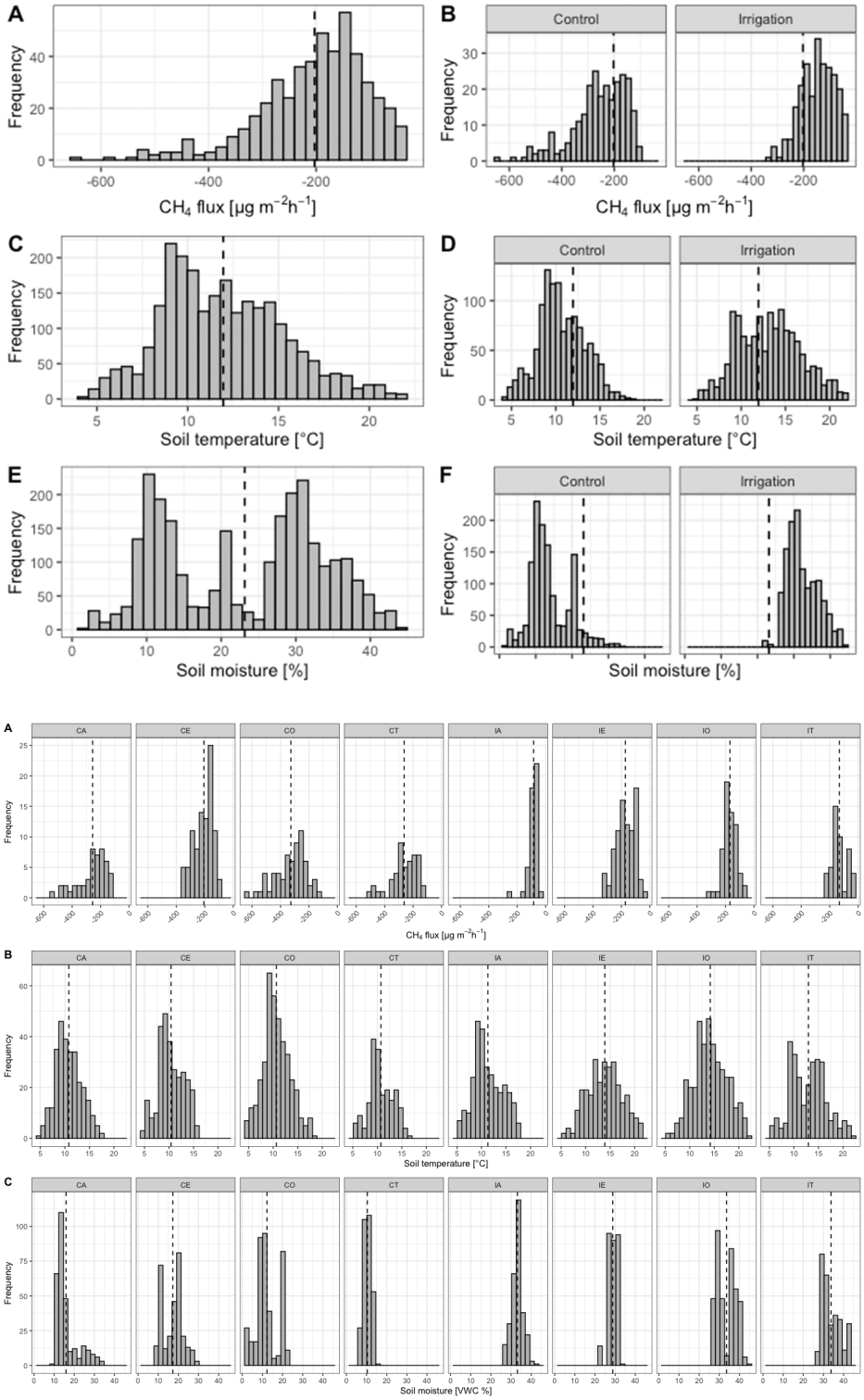

Figure 22: Frequency histograms of CH_4 flux ($\mu g\ m^{-2}\ h^{-1}$, linear fit, uptake rate) in 1: the whole study site (A) and in the control and irrigation sites (B), soil temperature in the whole study site (C) and in the control and irrigation sites (D) and soil moisture in the whole study site (E) and in the control and irrigation sites (F). 2: CH_4 flux (A), soil temperature (B) and soil moisture (C), divided into subtreatment groups. All histograms include the whole study period from 15.6.2018 (CH_4 flux) and 7.6.2018 (soil temperature and moisture) to 11.9.2018 (CH_4 flux) and 12.9.2018 (soil temperature and moisture). Vertical dashed lines represent the means of the data over the whole study period.

G TukeyHSD outputs

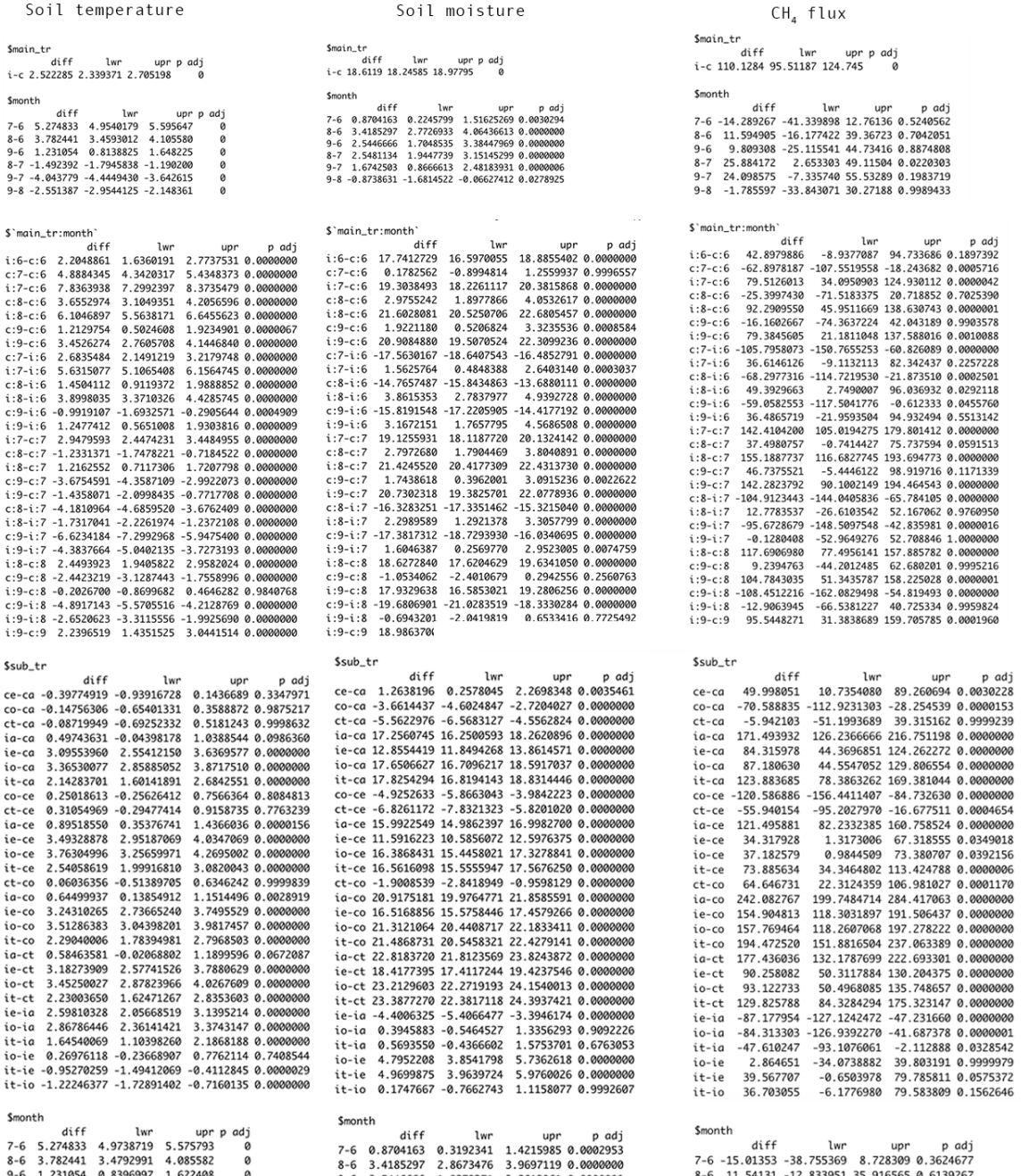

Figure 23: TukeyHSD outputs at 95% confidence level for the significance of differences in the means of soil temperature (°C)l, soil moisture (%VWC) and CH_4 flux ($\mu g\ m^{-2}\ h^{-1}$, uptake rate) between main plots (main_tr) and subtreatment (sub_tr) groups (C=control, I=irrigation, E=root and organic litter exclusion, A=organic litter addition, O=no subtreatment, T=warming) and between months (6=June, 7=July, 8=August and 9=September). The results are based on two-way ANOVAs computed separately for main plots and subtreatments. Main treatment analysis shows both separate pairwise comparisons for main treatments and subtreatments and months, and in the case of main treatments, the interaction comparisons (main_tr:month). Despite high significance (soil moisture: p<0.001 ***, CH_4 flux: p<0.01 **) the pairwise interaction comparisons between months and subtreatments in soil moisture and CH_4 flux analyses are not shown due to lack of space.

CH_4 flux - exclusion soil layers

A

```
$measlayer
        diff      lwr      upr     p adj
o-m 37.34118 18.24597 56.43639 0.0001595

$month
          diff       lwr      upr     p adj
7-6   5.918854 -29.33718 41.17489 0.9722798
8-6  26.007462 -10.08132 62.09624 0.2451144
9-6   3.869120 -42.00533 49.74357 0.9962920
8-7  20.088608 -10.25755 50.43476 0.3179282
9-7  -2.049734 -43.55821 39.45874 0.9992468
9-8 -22.138342 -64.35642 20.07973 0.5260715

$`measlayer:month`
              diff         lwr        upr     p adj
o:6-m:6  21.696462  -46.197355  89.590280 0.9766471
m:7-m:6  -4.413154  -64.999147  56.172839 0.9999985
o:7-m:6  37.239057  -22.108126  96.586240 0.5355018
m:8-m:6  17.637343  -44.087458  79.362145 0.9877652
o:8-m:6  55.605433   -5.337136 116.548003 0.1018111
m:9-m:6 -10.621334  -90.625820  69.383153 0.9999111
o:9-m:6  38.534945  -37.155462 114.225351 0.7720195
m:7-o:6 -26.109616  -85.598780  33.379547 0.8794402
o:7-o:6  15.542595  -42.684427  73.769617 0.9918518
m:8-o:6  -4.059119  -64.707690  56.589451 0.9999992
o:8-o:6  33.908971  -25.943304  93.761245 0.6621614
m:9-o:6 -32.317796 -111.494913  46.859321 0.9146486
o:9-o:6  16.838482  -57.976861  91.653825 0.9971585
o:7-m:7  41.652211   -7.860194  91.164616 0.1699727
m:8-m:7  22.050497  -30.288219  74.389213 0.9005182
o:8-m:7  60.018587    8.604709 111.432465 0.0102779
m:9-m:7  -6.208180  -79.215768  66.799408 0.9999958
o:9-m:7  42.948098  -25.304577 111.200774 0.5317906
m:8-o:7 -19.601714  -70.501289  31.297861 0.9361912
o:8-o:7  18.366376  -31.581721  68.314473 0.9497737
m:9-o:7 -47.860391 -119.843260  24.122478 0.4581510
o:9-o:7   1.295887  -65.859553  68.451328 1.0000000
o:8-m:8  37.968090  -14.782980  90.719160 0.3518661
m:9-m:8 -28.258677 -102.214045  45.696691 0.9386942
o:9-m:8  20.897601  -48.367947  90.163150 0.9831910
m:9-o:8 -66.226767 -139.530533   7.076999 0.1089637
o:9-o:8 -17.070489  -85.639883  51.498906 0.9946731
o:9-m:9  49.156278  -36.800007 135.112563 0.6513146
```

B

```
$measlayer
        diff      lwr     upr     p adj
o-m 37.34118 18.67256 56.0098 0.0001139

$main_tr
        diff      lwr      upr     p adj
i-c 32.77766 14.10905 51.44628 0.0006654

$`measlayer:main_tr`
              diff        lwr       upr     p adj
o:c-m:c 33.510043  -0.316076  67.33616 0.0532050
m:i-m:c 30.073944  -5.630963  65.77885 0.1315192
o:i-m:c 68.820372  34.816687 102.82406 0.0000026
m:i-o:c -3.436099 -38.971942  32.09974 0.9944453
o:i-o:c 35.310329   1.484211  69.13645 0.0370551
o:i-m:i 38.746428   3.041521  74.45134 0.0276231
```

Figure 24: TukeyHSD outputs at 95% confidence level for the significance of differences in the means of CH_4 flux ($\mu g\ m^{-2}\ h^{-1}$, uptake rate) between exclusion soil layers (measlayer, O=organic layer, M=mineral) from CE and IE subtreatment groups and between months (A, 6=June, 7=July, 8=August and 9=September) and main plots (B, C=control and I=irrigation). The results are based on two-way ANOVAs computed separately for month and main plot analyses. Despite the interaction effect of soil layer and month (measlayer:month) and soil layer and main plot (measlayer:main_tr) being statistically insignificant ($p>0.05$) in the two-way ANOVA, they were left in the model and thus shown in the TukeyHSD output for obtaining more insight of temporal and spatial changes caused by those interactions.

Soil temperature

```
$sensor
                       diff        lwr        upr     p adj
hydraprobe-hobo   5.2305701  4.8965537  5.5645865 0.0000000
scout-hobo        0.2339309 -0.0521036  0.5199655 0.1338126
scout-hydraprobe -4.9966392 -5.3416098 -4.6516685 0.0000000
```

Soil moisture

```
$sensor
                       diff       lwr      upr    p adj
hydraprobe-hobo  18.7479986 18.080848 19.41515 0.000000
scout-hobo       18.3529979 17.775228 18.93077 0.000000
scout-hydraprobe -0.3950007 -1.062151  0.27215 0.347085
```

Figure 25: TukeyHSD outputs at 95% confidence level for the significance of differences between the means of soil temperatures (°C) and moisture (%VWC) measured by HOBO, HydraProbe and Soil Scout sensors. The results are based on one-way ANOVA computed separately for soil temperature and soil moisture.

H Correlations

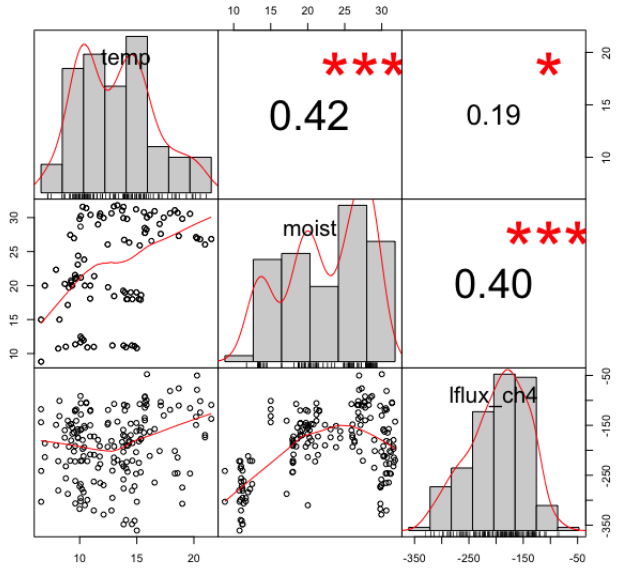

Figure 26: Correlation matrix of the measured variables in data subset for the exclusion subtreatment groups (CE and IE) with separate organic and mineral layer measurements. The soil moisture and soil temperature data used included daily means of the dates of CH_4 flux measurements. "temp"=soil temperature (°C), "moist"=soil moisture (%VWC) and "lflux_ch4"=CH_4 flux ($\mu g\ m^{-2}\ h^{-1}$).

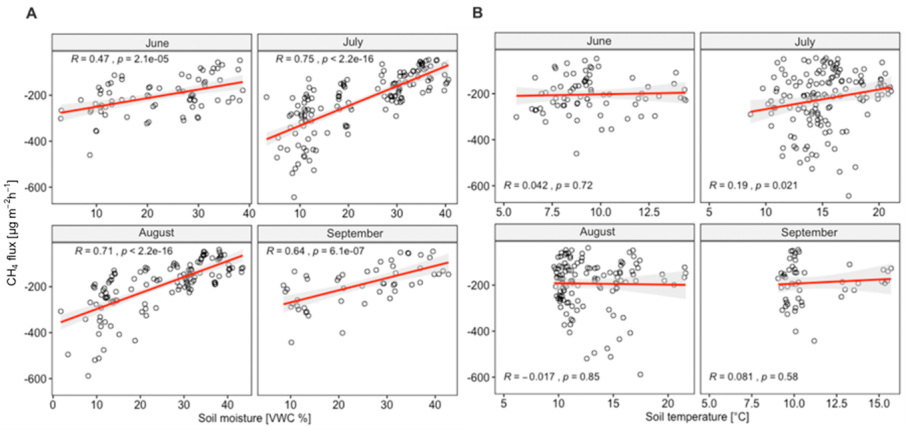

Figure 27: Correlations of the measured variables in the whole study site divided by months. The monthly data were fitted to linear regression lines with 95% confidence intervals. The used soil moisture (A) and soil temperature (B) data included daily means of the dates of CH_4 flux measurements.

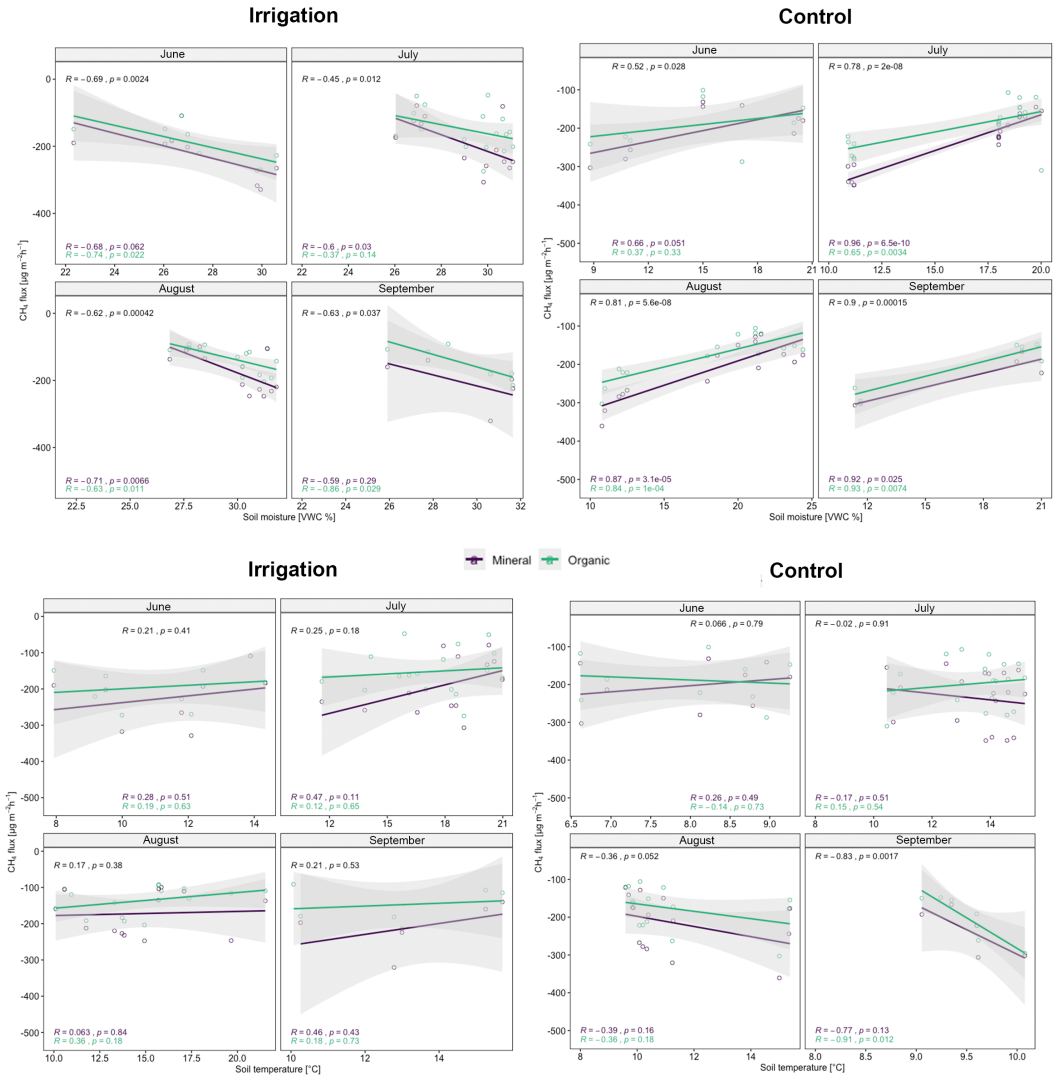

Figure 28: Correlations of the measured variables in the exclusion soil layers (organic and mineral) by month. The monthly data were fitted to linear regression lines with 95% confidence intervals. The used soil moisture and soil temperature data included daily means of the dates of CH_4 flux measurements.

I LOOCV results

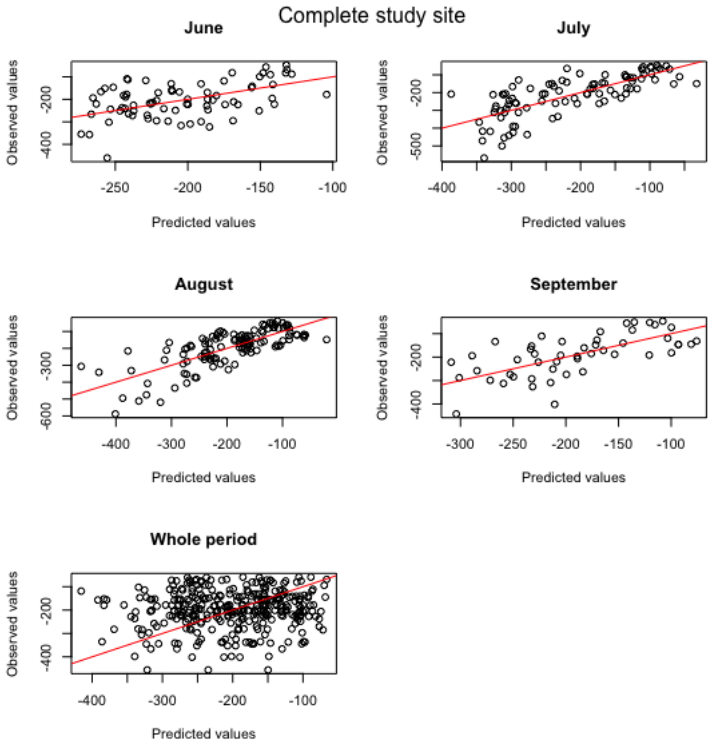

Figure 29: LOOCV-predicted values plotted against observed values with 1:1 line. 1:1 line is used when data points from two data sets are compared and shows how much they differ by the distance from the line. Ideally all points would be located along the line.

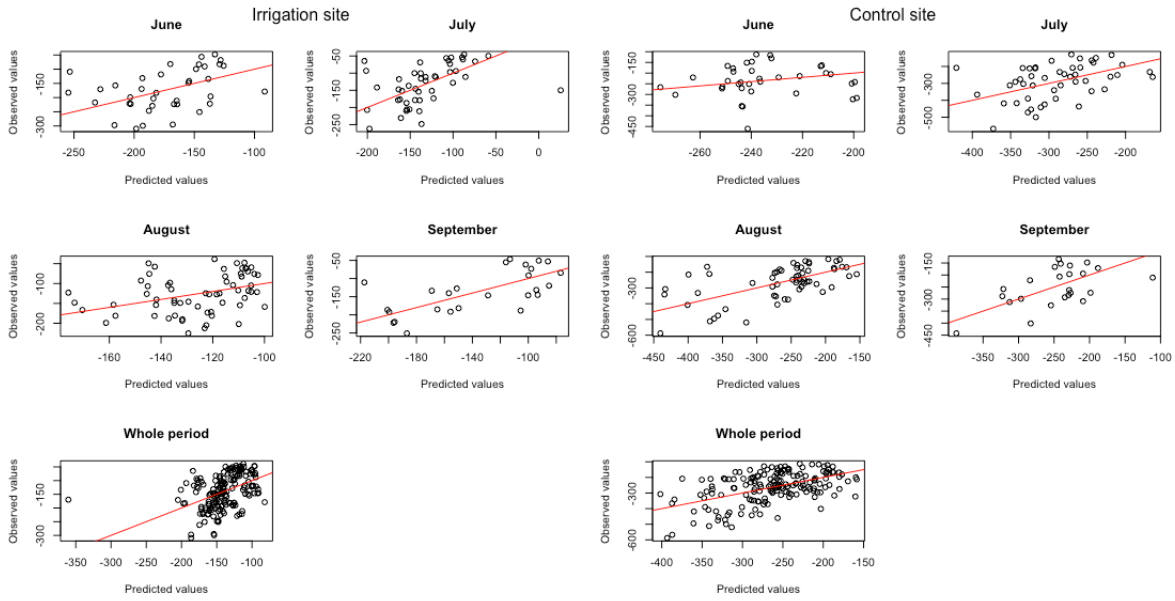

Figure 30: LOOCV-predicted values plotted against observed values for the irrigation and control sites with 1:1 line.

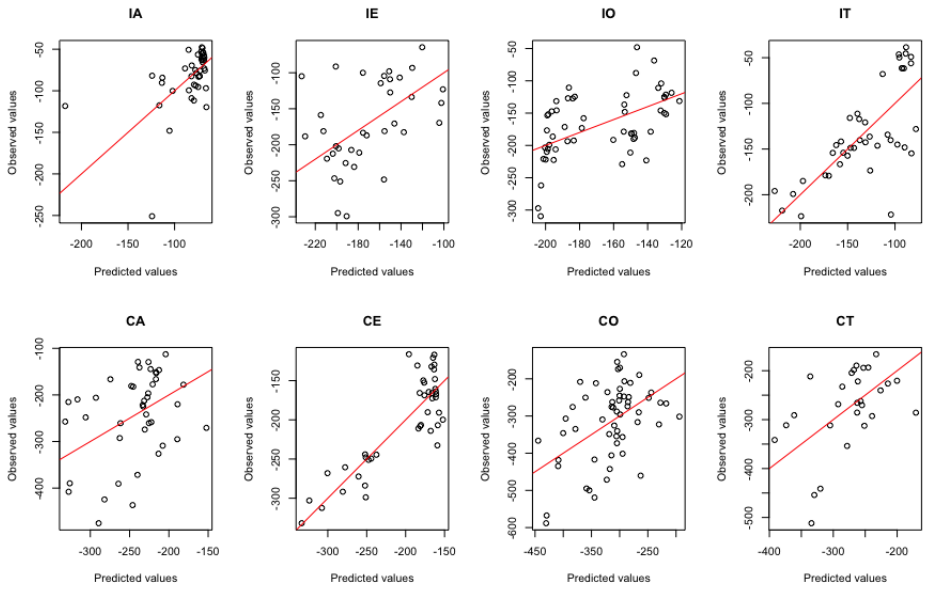

Figure 31: LOOCV-predicted values plotted against observed values for the irrigation and control sites with 1:1 line.

J R and Python packages

Table 21: R and Python packages used in the data manipulation and analyses in this study.

language	package	author(s)	usage
Python	*pandas*	McKinney (2011)	data manipulation and analysis
	matplotlib	Hunter (2007)	data exploration
R	*dplyr*	Wickham et al. (2020)	data manipulation
	plyr	Wickham (2011)	data manipulation
	lubridate	Grolemund and Wickham (2011)	timeseries data manipulation
	viridis	Garnier (2018)	graphs
	PerformanceAnalytics	Peterson and Carl (2020)	correlation matrices
	ggplot2	Wickham (2016)	graphs
	magrittr	Bache and Wickham (2014)	'pipe' coding
	mctest	Imdadullah et al. (2016)	multicollinearity tests
	rstatix	Kassambara (2020)	statistical analyses
	tidyr	Wickham and Henry (2020)	data manipulation
	zoo	Zeileis and Grothendieck (2005)	timeseries data manipulation
	naniar	Tierney et al. (2020)	data manipulation
	matrixStats	Bengtsson (2020)	statistical analyses
	nlme	Pinheiro et al. (2019)	GLS models
	effects	Fox and Hong (2009)	interaction effect plots
	ggnewscale	Campitelli (2020)	graphs